DEVELOPMENT OF A POST-TRAUMATIC OSTEOARTHRITIS MODEL TO EVALUATE THE EFFECTS OF IMPACT VELOCITY AND MAXIMUM STRAIN ON ARTICULAR CARTILAGE CELL VIABILITY, MATRIX BIOMARKERS, AND MATERIAL PROPERTIES

A Thesis
presented to
the Faculty of the Graduate School
at the University of Missouri

In Partial Fulfillment
of the Requirements for the Degree

Master of Science

---

by

NICOLE POYTHRESS WATERS

Sheila Grant, Ph.D. and James Cook, D.V.M., Ph.D., Thesis Supervisors

JULY 2009

The undersigned, appointed by the dean of the Graduate School, have examined the thesis entitled

DEVELOPMENT OF A POST-TRAUMATIC OSTEOARTHRITIS MODEL TO EVALUATE THE EFFECTS OF IMPACT VELOCITY AND MAXIMUM STRAIN ON ARTICULAR CARTILAGE CELL VIABILITY, MATRIX BIOMARKERS, AND MATERIAL PROPERTIES

presented by Nicole Poythress Waters,

a candidate for the degree of Master of Science

and hereby certify that, in their opinion, it is worthy of acceptance.

Sheila Grant, Ph.D., Department of Biological Engineering

James Cook, D.V.M., Ph.D., Department of Veterinary Pathobiology
Department of Veterinary Medicine & Surgery
Department of Orthopaedic Surgery

William Carson, Ph.D., P.E., Department of Mechanical Engineering
Professor Emeritus

Qingsong Yu, Ph.D., Department of Chemical Engineering

Shubhra Gangopadhyay, Ph.D., Department of Biological Engineering
Department of Electrical Engineering

DEDICATION

The continuation of my formal education would not have been possible without the loving support from my immediate family: Cody and Tommy. My husband, Cody, constantly reminds me to be all that I can be, and does everything in his power to make this happen. Thank you so much for understanding my passion for orthopaedic research. I realize it has been difficult at times, but I greatly appreciate your steadfast love, patience, kindness, and limitless strength. As a preschooler, Tommy has been the best distraction for me when things weren't always going according to schedule. Thank you for being so inspirational, I will always remember both personally and professionally your favorite quote from *Wonder Pets*: "What's it going to take? TEAMWORK!!!"

As always, my parents are my main driving force towards seeking novel treatments for osteoarthritis. Since both of them have endured total hip arthroplasty before the age of 50, I have seen firsthand how significant and life-impacting osteoarthritis research is for restoring people's lifestyles and getting them back to participating in the activities they love. Thank you Mom and Dad for providing such a great childhood for me and encouraging me to "always do my best!"

My personal effort as well as many others may not dramatically affect the treatment of osteoarthritis for my parents' generation, but perhaps through the synergistic, multidisciplinary efforts of teams of scientists, engineers, and physicians we will improve the lives for my three-year-old son, Tommy's, generation. Although we all wish that our children will always be healthy, I hope that the work I do today and tomorrow will

somehow help my children, my siblings' (Eric, Rachel, Ryan, and Quinn) children, and other children in the world currently or potentially afflicted with osteoarthritis.

With God all things are possible, and I truly believe that with His guidance we will someday be able to help the lame walk again.

ACKNOWLEDGEMENTS

I feel very blessed that I have had the opportunity to conduct this multidisciplinary thesis research and have many people to thank for it. Thank you so much, Dr. Cook, for reading the initial e-mail I sent you from Smith & Nephew Orthopaedics a few years ago inquiring about graduate research opportunities in the Comparative Orthopaedic Laboratory (COL). You could have easily deleted that e-mail, but I appreciate you taking the time to give me a chance. Thank you again for all the research autonomy and support that you have provided. I hope I have been able to contribute to the COL team/family through this thesis work; I'm very excited to learn more about post-traumatic osteoarthritis via this PTOA model and hopefully discover novel treatments for the disease.

Some of the undergraduate and graduate coursework that I've completed has been extremely beneficial. Dr. Yu, the information I acquired in your *Polymer Materials* class was very helpful for understanding the viscoelastic behavior of cartilage especially for cartilage tissue engineering applications. In addition, both *Biomaterials* and *Orthopaedic Biomechanics* classes that you taught Dr. Grant were excellent. I would highly recommend them to any aspiring bio-engineer.

Although I never had the privilege to formally take any of the mechanical engineering courses taught by Dr. Carson before he retired, I feel like I have learned more from him in the past few years than all of my formal education experiences combined. Professionally, you have taught me lifelong lessons to <u>never</u> underestimate the value of

fundamental classical mechanics or the significance of emphasizing *quality* of work over quantity of work. Personally, I'm not sure whether I've met anyone as selfless and caring as you. The time, energy, and resources you've devoted to helping *volunteer* with COL projects is a feat that I feel honored to have directly witnessed. Moreover, the love you demonstrate towards your wife of 46 years has been an AWESOME example for any married person who takes that vow to love and honor their spouse during times of sickness and in health, etc. You are one of the best examples of a true Christian that I've ever met and I feel so deeply humbled and fortunate to have you in my life as a mentor.

Many thanks go to Dr. Aaron Stoker, Ms. Mary Cockrell, and Dr. Chris Hanks and other COL team members for all the technical and emotional support they provided before/during/after the experiments. You guys made this journey so much easier for me and I greatly appreciate it. ***THANK YOU ALL!!!***

TABLE OF CONTENTS

LIST OF FIGURES

Figure Page

LIST OF TABLES

DEVELOPMENT OF A POST-TRAUMATIC OSTEOARTHRITIS MODEL TO EVALUATE THE EFFECTS OF IMPACT VELOCITY AND MAXIMUM STRAIN ON ARTICULAR CARTILAGE CELL VIABILITY, MATRIX BIOMARKERS, AND MATERIAL PROPERTIES

Nicole Poythress Waters

Drs. Sheila Grant and James Cook, Thesis Supervisors

ABSTRACT

Post-traumatic osteoarthritis (PTOA) is a painful and debilitating disease that is often associated with mechanical injury to articular cartilage, yet the severity of trauma required to induce the disease process and the steps involved are unknown. Therefore, the objective of this thesis work was to develop a clinically-relevant *ex vivo* PTOA model with repeatable severity of mechanical injury by delivering a single impact load with controlled combinations of velocity and maximum strain (i.e. severity of trauma categories normalized to cartilage thickness) to a radially-constrained articular cartilage explant to study their effect on articular cartilage's biomarkers: cell viability, extracellular matrix, and material properties. This is part of the Comparative Orthopaedic Laboratory's broader goal of finding post trauma biomarkers that could clinically be measured to predict the likelihood of the onset of PTOA and its progression for purposes of selecting or determining optimum treatments.

A protocol was developed using a 25 kN actuator servo-hydraulic test machine to measure canine cartilage explant thickness (0.36 to 0.75 mm) and subsequently injure 4 mm diameter radially-constrained *ex vivo* canine cartilage explants at a constant impact velocity V of 1 or 100 mm/sec to a maximum strain S of 10, 30, or 50%; resulting in six

(velocity:strain) test groups, for example high velocity:low strain (100V:10S). (0V:0S) and sham (tissue thickness and material moduli only measured after 12 days in media) test groups were used as controls. Thereafter, explants were cultured in supplemented media for twelve days. Cell viability was analyzed post-injury at day 0 and 12 as was cartilage matrix for collagen (hydroxyproline (HP)) and glycosaminoglycan (GAG) content. Media were changed after day 1, 2, 3, 6, 9, and 12; and tested for GAG content, collagen II synthesis (procollagen II C-propeptide), nitric oxide (NO), and prostaglandin E_2 (PGE_2). Material testing was performed via stress-relaxation and dynamic testing at day 0 (pre-injury) and days 6 and 12 (post-injury).

Greater cell death (concentrated in the superficial zone) occurred at days 0 and 12 for both high strain (1V:50S, 100V:50S) groups, with greater propagation into the deep zone by day 12 for the higher velocity (100V:50S) group. Both high strain groups released significantly greater GAG and PGE_2 into the media at day 1 than the other impacted and non-impacted control groups, indicating that a strain threshold (in the order of 50%) may exist for significant release to occur. Significant differences in PGE_2 release continued to be observed 2, 3 and 6 days post impact for the high velocity: high strain (100V:50S) group but not for the low velocity:high strain (1V:50S) group, which implies that higher velocity impact prolongs the release of PGE_2. Release of detectable levels of nitric oxide was not observed. There were no significant differences in GAG and HP tissue biomarkers, and CPII media biomarker. Decrease in cartilage explant's radially confined compression elastic modulus and equilibrium modulus were found to correlate to greater GAG release from the explant.

The development of this model will enable further study of biomarkers involved in PTOA that could potentially be clinically measured to evaluate the etiopathogenesis of the disease as well as various treatment strategies to mitigate symptoms of the disease.

CHAPTER 1

INTRODUCTION

1.1 Articular Cartilage

1.1.1 Structure: Anatomy

Articular cartilage is a hard, translucent tissue that covers the ends of articulating bones providing a surface for diarthordial joints that reduces friction and dissipates force during movement. It is an inhomogenous material consisting of a single cell type (chondrocyte) embedded within a highly complex extracellular matrix of water (60-85% wet weight), type II collagen (15-22% wet weight), and aggrecan (4-7% wet weight) (Figure 1).

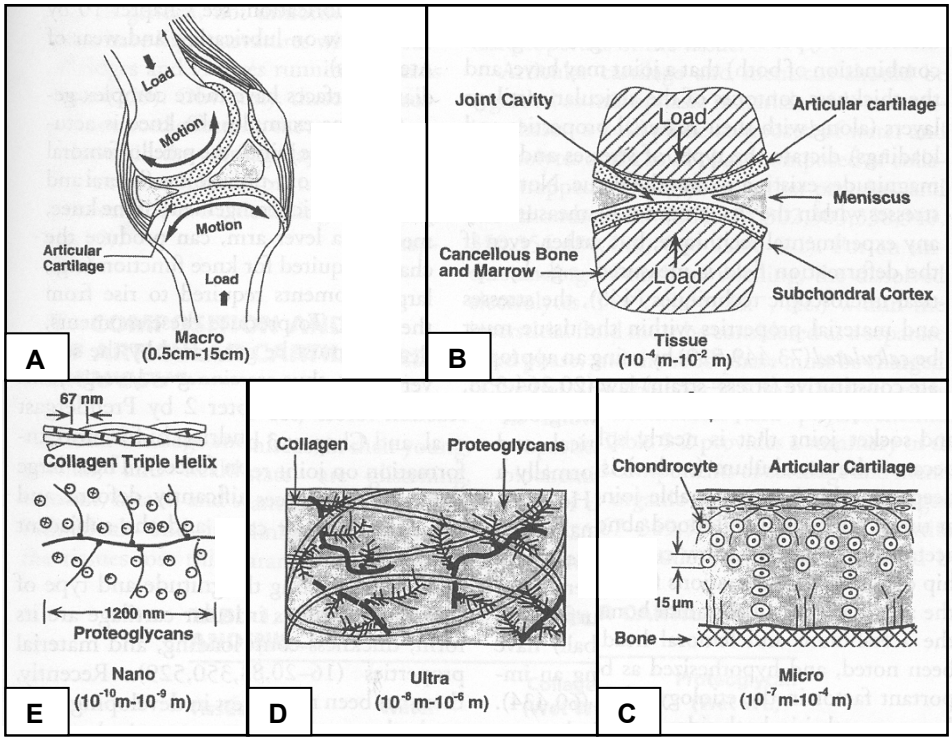

Figure 1. Views of a diarthroidal joint. Some of the important structural features of a typical diarthrodial joint at different hierarchical scale: A) macro (0.5 to 15 cm), B) tissue (10^{-4} to 10^{-2} m), C) micro (10^{-7} to 10^{-4} m), D) ultra (10^{-8} to 10^{-6} m), and E) nano (10^{-10} to 10^{-9} m) (Mow et al., 1992)

Other minor constituents include collagen type I, V, VI, IX, XI, hyaluronan, link protein, decorin, biglycan, fibromodulin, perlican, thrombospondin, and cartilage oligomeric matrix protein (Mow and Huiskes, 2005). The anisotropy of articular cartilage is indicated by three distinct zones within the tissue: superficial tangential, middle, and deep (Figure 2).

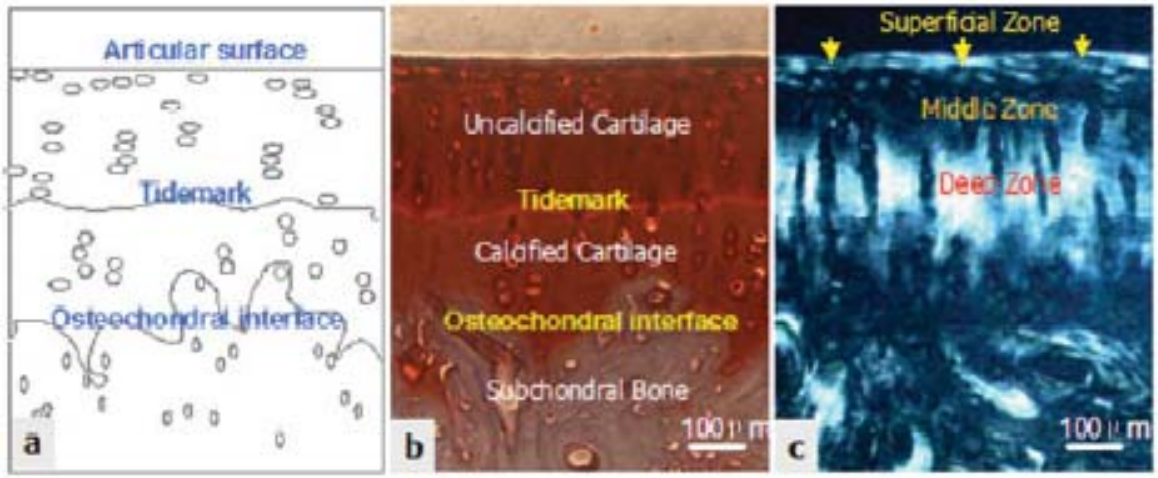

Figure 2. Ultrastructure of articular cartilage. Three distinct zones by depth of articular cartilage. (a) Schematic photomicrograph. (b) Tissue section stained by safranin O. (c) Photomicrograph of the serial section under polarized light (Li et al., 2006)

Collagen is a rod-shaped protein with three polypeptide chains that form a characteristic tight right-handed triple helix. Type II collagen contains three identical α1(II) polypeptide chains. In contrast, type I collagen contains two α1(I) and one α2(I) polypeptide chains, type V contains two α1(V) and one α2(V) polypeptide chains, type VI contains one α1(VI), α2(VI), α3(VI) polypeptide chains, type IX contains one α1(IX), α2(IX), α3(IX) polypeptide chains, and type XI contains one α1(XI), α2(XI), α3(XI). Types I, II, V, XI belong to the class of fibril-forming collagens; Type VI belong to the beaded filament-forming collagens; Type IX also contain glycosaminoglycan chains attached to the α chains. Each α chain in collagen is composed of repeating $(Gly\text{-}X\text{-}Y)_n$ triplets that form a left-handed helix, where X is usually proline, and Y is often

hydroxyproline. This orientation allows for a tight triple helical structure that provides optimal tensile strength.

Aggrecan is a large proteoglycan that consists of a core protein surrounded by the glycosaminoglycan (GAG) chains: chondroitin sulfate and keratan sulfate. The core protein consists of ~10% of its molecular mass, thus most of the surface area of aggrecan is due to the surrounding GAG chains, resulting in its bottle-brush appearance. The negatively charged sulfate and carboxyl groups of GAGs enable the high negative charge to attract counterions which gives rise to Donnan osmotic pressure that favors hydration. GAGs also tend to repel each other, which is restrained by the collagen fibril network.

Chondrocytes are highly specialized, terminally differentiated cells that are surrounded by a ~2 μm thick pericellular matrix that is mostly comprised of type VI collagen. The term chondron refers to chondrocytes surrounded by its pericellular matrix. Even though chondrocytes occupy only a small proportion of the total volume (~10%) of articular cartilage, they are responsible for maintaining homeostasis in articular cartilage: organization, synthesis, degradation, and/or repair of the extracellular matrix. Chondrocytes in the superficial zone closest to the articular surface are flattened, oriented parallel to the surface, and maintain a matrix high in collagen and low in proteoglycans. In contrast, chondrocytes in the deep zone are lined up in columns perpendicular to the surface. Chondrocytes in the middle zone are rounded and are responsible for maintaining a higher concentration of proteoglycans and larger collagen fibrils. Cell density decreases from the superficial to deep zones as well as with age (Mitrovic et al., 1983).

1.1.2 Function: Physiology and Biomechanics

Water and collagen content decrease from the surface to the deep zone. Proteoglycan content is highest in the middle zone. Dense collagen fibrils are oriented parallel to the surface in the surface tangential zone, yet change orientation to perpendicular at the tidemark, or bottom of the deep zone. Tensile strength has been shown to be highest at the superficial tangential zone, indicating that perhaps the parallel arrangement of the collagen fibrils help resist shear forces generated during joint motion. Interestingly, collagen content increases during development, whereas proteoglycan content remains constant. This unique structure of articular cartilage allows diarthrodial joints to withstand load-bearing activities, yet promotes joint flexibility.

Materials may behave like elastic solids (i.e. metal spring), viscous fluids (i.e. dashpot), or a combination of the two representing a viscoelastic material such as articular cartilage. The mechanical behavior of a purely elastic material may be characterized by a linear load-deformation, $F = kx$, where F (N) is force, k (N/m) is the slope of this curve representing structural stiffness, and x (m) is displacement of the material during loading. Likewise, a purely elastic material has a linear stress-strain relationship, $\sigma = E\varepsilon$, where σ ($N/m^2 = Pa$) is stress, E (Pa) is the Young's modulus of elasticity, and ε is strain (m/m) of the material during loading. In contrast to the Young's modulus of bone which has been reported in the literature as ranging from 0.1 to 15 GPa (Mow and Huiskes, 2005), the modulus of articular cartilage is much lower ranging from 0.3 to 1.0 MPa (Armstrong and Mow, 1982; Athanasiou et al., 1991; Athanasiou et al., 1995; Froimson et al., 1997; Mow et al., 1984; Mow et al., 1980).

A dashpot is a piston moving through a closed cylinder within a viscous fluid. Thus, the measured force, F (N), is related to the piston's velocity (or rate of displacement, $\dot{x}$, m/s) by $F = c\dot{x}$, where c is the constant of proportionality c (N-sec/m), often referred to as the frictional damping coefficient of the dashpot. A linear, purely viscous material (defined as a Newtonian fluid) has a linear shear stress-shear rate relationship, $\tau = \eta\dot{\gamma}$, where τ (Pa) is shear stress, η (Pa-sec) is the viscosity coefficient, and $\dot{\gamma}$ (sec^{-1}) is the shear rate. For example, the viscosity coefficient of water at 20°C is 1 mPa-sec. In contrast to a purely elastic solid material, a viscous fluid does not recover to its original shape after the applied stress is removed. Thus, no energy is stored in the material during loading therefore all energy undergoes heat dissipation by internal friction.

A viscoelastic material such as articular cartilage may be modeled as combinations of a Kelvin-Voigt body (spring and dashpot connected in parallel) and a Maxwell body (spring and dashpot connected in series). The equation governing the force-displacement curve for a Kelvin-Voigt body is

$$\mathbf{F = kx + c\dot{x}, \quad x = 0 \text{ at } t = 0} \tag{1-1}$$

After load is applied, its initial response is governed by that of the dashpot (i.e. x(0) = 0). Thus, its creep response (deformation produced by a sudden application of a constant F at t = 0) is

$$\mathbf{x(t) = [F/k][1-e^{-(k/c)t}], \quad t > 0} \tag{1-2}$$

The equation governing the force-displacement curve for a Maxwell body is

$$\mathbf{(F/c) + (\dot{F}/k) = \dot{x}, \quad x = F/k \text{ at } t = 0} \tag{1-3}$$

When load is applied to the Maxwell body its initial response is the sudden deformation of a spring (i.e. x(0) = F/k). Its creep response is governed by

$$\mathbf{x(t) = F[(1/k) + (t/c)], \quad t > 0} \tag{1-4}$$

Comparisons of the theoretical load-deformation response (using appropriate combinations of the Kelvin-Voigt and Maxwell bodies) to experimental load-deformation response of the material of interest (i.e. articular cartilage) enables the calculation of the elastic and viscous material coefficients based on the assumed constitutive laws.

It is important to note that the viscoelastic behavior of articular cartilage is dependent upon its composition, molecular structure, water and electrolyte contents, especially during compressive loading where the frictional drag of interstitial fluid flow through the collagen-proteoglycan matrix subsequently causes viscous dissipation. Thus, the degree of hydration and permeability of articular cartilage are key parameters since they affect viscous dissipation which in turn affects the creep and stress-relaxation behaviors. Interestingly, one of the earliest features of cartilage pathology (potentially resulting in osteoarthritis described in Section 1.2) are increases in hydration (Bollet and Nance, 1966; Froimson et al., 1997; Mankin and Thrasher, 1975; Maroudas and Venn, 1977) which subsequently affects the material properties of articular cartilage (Armstrong and Mow, 1982; Setton et al., 1993, 1994).

The classical biphasic theory was developed by Mow et al. (1980) to describe the material behavior of cartilage under a variety of conditions (Ateshian et al., 1997; Holmes and Mow, 1990; Mow et al., 1984).

"The theory may be conceptually understood by the following simplified constitutive assumptions:

1. The solid matrix may be linearly elastic or hyperelastic, and isotropic or anisotropic.
2. The solid matrix and interstitial fluid are intrinsically incompressible; that is, compression of the tissue as a whole is possible only if there is fluid exudation.
3. Viscous dissipation is a result mainly of interstitial fluid flow relative to the porous-permeable solid matrix.
4. Frictional drag is directly proportional to the relative velocity; the proportionality factor is known as the diffusive drag coefficient (K), and this may be strain dependent (Mow and Huiskes, 2005)."

Recently, a triphasic theory was developed by Mow et al. to describe all biphasic viscoelastic effects, Donnan equilibrium ion distributions (c^F, c), dimensional swelling effect (ε_s), Donnan osmotic pressures (π), kinetics of swelling, and all diffusion and streaming potentials (Lai et al., 1991; Lai et al., 2000). Essentially, the triphasic theory predicts that the total equilibrium axial stress, σ^T, at the loading platen may be characterized by $\sigma^T = \sigma^S + \pi$, where σ^S is the stress in the elastic solid matrix caused by applied uniaxial compression, and π is the Donnan osmotic swelling pressure. It has been shown previously that the swelling pressure has a significant effect on tissue stiffness, other equilibrium material properties, and ultimately the stress-relaxation behavior of cartilage (Lai et al., 1991; Lu et al., 2004; Wan et al., 2004).

1.2 Osteoarthritis

1.2.1 Etiopathogenesis

Osteoarthritis (OA) is a debilitating disease that affects musculoskeletal joints (Figure 3) which is anticipated to affect 59 million Americans by 2020 (Lawrence et al., 1998). A classic hallmark of OA is cartilage degradation; however, hypertrophy and spurring of bone (osteophyte formation), and synovitis are additional features of late-stage OA. These joint conditions cause pain and stiffness in the affected joint, leading to decreases

in range of motion. The common treatment for late-stage OA is total joint replacement. There are major risks involved with this surgery including implant loosening and/or infection which may lead to implant failure requiring revisional surgery (Parratte and Pagnano, 2008). The intense rehabilitation process after total joint replacement surgery may be physically painful, and/or psychologically taxing for the individual (Wylde et al., 2007). Currently, there is no cure for OA.

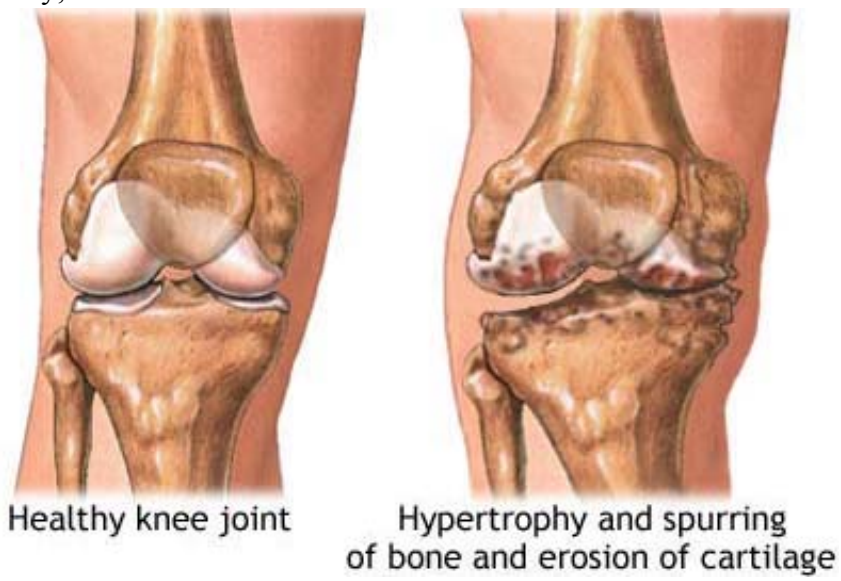

Figure 3. Comparison of healthy and osteoarthritic knee joints (http://www.nlm.nih.gov/medlineplus/ency/imagepages/17103.htm)

1.2.2 Post-Traumatic Osteoarthritis

Despite the fact that the exact pathogenesis of OA is unknown, acute traumatic mechanical injury to articular cartilage (e.g. during sports injury, vehicular accident, falling, etc.) has been shown to significantly increase the risk of developing post-traumatic osteoarthritis with 12% (5.6 million Americans) of all OA cases being post-traumatic in origin, resulting in annual costs of 3.06 billion dollars (Brown et al., 2006). Although the exact etiology and pathogenesis of OA is often unknown, acute joint trauma from sports injuries, vehicular accidents, or falls may initiate a common series of

events culminating in post-traumatic osteoarthritis (PTOA) (Buckwalter and Brown, 2004). The amount of cartilage damaged during injury is dependent on the rate and magnitude of impact loads (Ewers et al., 2001; Milentijevic and Torzilli, 2005; Milentijevic et al., 2003; Quinn et al., 2001) and may elicit immediate cell (chondrocyte) death (Borrelli et al., 2003; D'Lima et al., 2001a, 2001b; Ewers et al., 2001; Huser and Davies, 2006; Krueger et al., 2003; Loening et al., 2000; Milentijevic and Torzilli, 2005; Milentijevic et al., 2003; Natoli et al., 2008; Patwari et al., 2004) breakdown of cell membrane phospholipids into arachidonic acid ultimately resulting in inflammation (Chrisman et al., 1981) and physical disruption of the extracellular matrix (ECM) of the cartilage (Borrelli et al., 2004; D'Lima et al., 2001b; Ewers et al., 2001; Jeffrey and Aspden, 2006; Jeffrey et al., 1995; Krueger et al., 2003; Lewis et al., 2003; Morel and Quinn, 2004; Morel et al., 2006; Quinn et al., 2001; Repo and Finlay, 1977; Thompson et al., 1993). Destruction of the ECM correlates to glycosaminoglyan (GAG) release (D'Lima et al., 2001a; DiMicco et al., 2004; Huser and Davies, 2006; Jeffrey and Aspden, 2006, 2007; Jeffrey et al., 1997; Otsuki et al., 2008; Patwari et al., 2007; Patwari et al., 2003) from the tissue consequently leading to increases in tissue water content (swelling) (Jeffrey et al., 1995; Loening et al., 2000). Delayed pathologic effects of mechanical injury to articular cartilage include additional cell death and decreased tissue mechanical stiffness (Natoli et al., 2008).

1.3 Literature Review

1.3.1 Effect of Impact

Some of the pathologic responses typically reported for PTOA include chondrocyte cell death (viability), (Huser and Davies, 2006; Jeffrey et al., 1995; Kurz et al., 2001;

Loening et al., 2000; Milentijevic and Torzilli, 2005; Milentijevic et al., 2003; Torzilli et al., 2006; Torzilli et al., 1999) direct tissue disruption with cartilage GAG (aggrecan), (Borrelli et al., 2009; DiMicco et al., 2004; Huser and Davies, 2006; Natoli et al., 2008) and collagen II loss, (Borrelli et al., 2009; Mrosek et al., 2006) and increased release of prostaglandin E_2 (PGE_2) (Jeffrey and Aspden, 2007) and nitric oxide (Green et al., 2006; Loening et al., 2000) as well as other inflammatory and catabolic mediators.

Chondrocyte death has been associated with PTOA (Borrelli, 2006) and degree of cell death is reportedly dependent on impact energy, (Jeffrey et al., 1995) peak stress, (Milentijevic et al., 2003) stress rate, (Milentijevic and Torzilli, 2005) and compressive strain (Torzilli et al., 2006). Chondrocyte death after impact injury occurs via necrotic and apoptotic pathways with the latter predominantly occurring via the caspase-9/3 pathway (Huser and Davies, 2008; Huser et al., 2006).

Jeffrey et al. (1995) provided evidence that chondrocyte viability reduces linearly with increasing impact energy from 0.2-0.98 J in calf articular cartilage explants. Recent studies by Huser and Davies (2006) suggest that chondrocyte death is primarily a result of calcium released from the endoplasmic reticulum via the ryanodine receptor and is subsequently processed into the mitochondria by the uniport transporter, initiating mitochondrial depolarization and subsequent caspase-9-activation (Huser and Davies, 2007; Huser et al., 2006) and may be reduced in explants by treatment of a glucosamine derivative, Glu5, prior to impact load (Huser and Davies, 2008).

Similarly, Loening et al. (2000) reported that chondrocyte apoptosis occurred at peak stresses as low as 4.5 MPa and increased with peak stress to >20 MPa with more than 50% cell death and maximal apoptosis occurring by 24 hours post-injury in calf articular

cartilage explants. Duda et al. (2001) used a drop-tower to deliver an impact load energy of 0.06, 0.1, or 0.2 J to *ex vivo* porcine patellas that produced no gross structural damage, but significantly reduced cell viability in the tangential and middle zones with increasing impact energy. In a series of studies, D'Lima et al. (2001) evaluated the effect of mechanical injury on chondrocyte apoptosis in full-thickness human cartilage explants (5mm dia) (D'Lima et al., 2001a) and bovine explants (D'Lima et al., 2001c) as well as *in vivo* rabbit patella (D'Lima et al., 2001b) loaded to 14 MPa for 500 ms, 23 MPa for 500 ms or 30% strain for 500 ms, respectively. The authors concluded that the pan-caspase inhibitor, z-VAD.fmk [benzyloxycarbonyl-Val-Ala-Asp (OMe) fluoromethylketone], and IGF-1 (insulin growth factor-1) are effective in preventing chondrocyte apoptosis due to mechanical injury.

It has been shown in an *ex vivo* cartilage injury model that impact initiates immediate release of GAGs for up to 24 hours post-injury with the maximal amount occurring 4 hours post-injury (DiMicco et al., 2004). Aggrecan contributes to the mechanical properties of cartilage such as compressive stiffness, thus it is expected that impact injury that releases GAG will likewise affect cartilage stiffness. Supportive of this concept, Natoli et al. (2008) reported a reduction in stiffness as early as 24 hours post-impact for the high energy insult (2.8 J) with a reduction by 4 weeks after low-energy impact (1.1 J). While treatment with insulin-like growth factor 1 (IGF-1) reduced the amount of GAG released after low-energy impact, it had no effects in ameliorating the reduction in tissue stiffness (Natoli and Athanasiou, 2008) suggesting that quality as well as quantity (normal vs. pathologic state) of tissue GAG (aggrecan) is important to tissue mechanical properties.

Type II collagen (Col II) is instrumental for normal articular cartilage function by providing tensile stiffness/strength to the tissue as well as restraining the swelling pressure of negatively charged proteoglycans is susceptible to mechanical injury. For example, immunohistochemistry has revealed decreases in collagen II expression with increases in collagen I expression from articular cartilage in an *in vivo* canine impact model 6 months post-injury (Mrosek et al., 2006). Moreover, minimal changes in type II procollagen mRNA were noted immediately post-impact compared to the sham-operated control in an *in vivo* rabbit model, whereas by 1 month post-impact there was a complete absence of type II procollagen mRNA in insulted cartilage (Borrelli et al., 2009). The data suggest that reduction in Col II is a consistent consequence of impact injury but may occur as a secondary effect involving intermediate factors based on the delayed nature of the changes.

One of the inflammatory mediators involved in OA is prostaglandin E_2 (PGE_2). Increased PGE_2 after cartilage injury is most likely due to cell membrane rupture during impact which has been shown to cause release of arachidonic acid effectively activating the cyclooxygenase-2 (COX-2) pathway (Chrisman et al., 1981). Recently, Jeffrey and Aspden (2007) provided evidence that cyclooxygenase inhibition lowers prostaglandin E_2 release from articular cartilage and reduces apoptosis but not proteoglycan degradation following an *in vitro* impact load. Providing further support that PGE_2 production increases significantly during impact injury due to generation of mechanical forces, Gosset el al. (2008) demonstrated that microsomal prostaglandin E synthase-1 (mPGES-1), a key enzyme required for PGE_2 formation, is a mechanosensitive gene.

Yet, the role of PGE_2 in osteoarthritis remains vague and is considered to have both anabolic and catabolic effects on joint tissues (Guilak et al., 2004).

Another important inflammatory mediator involved in OA is nitric oxide (NO) (Abramson, 2008; Green et al., 2006). The production of NO is dependent on nitric oxide synthase 2 (NOS2) and is associated with inflammation in arthritic disorders (Grabowski et al., 1997). There appear to be feedback-control mechanisms between PGE_2 and NO in cartilage physiology. For example, specific inhibition of NOS2 (1400W) created an additional increase in PGE_2 production whereas the selective COX2 inhibitor (NS398) blocked both compression-induced NO and PGE_2 production during intermittent compressive loading at 0.5 Hz at 0.05, 0.1, 0.5, or 1.0 MPa (Fermor et al., 2002). The COX and NOS pathways are intricately linked, (Guilak et al., 2004) thus more studies are needed to further establish their relationship especially if therapeutic strategies are targeted on these pathways.

1.3.2 Application of Impact

Various devices such as drop-tower, (Burgin and Aspden, 2007; Duda et al., 2001; Haut et al., 1995; Huser and Davies, 2006; Jeffrey et al., 1995; Lahm et al., 2004; Radin et al., 1970; Repo and Finlay, 1977; Scott and Athanasiou, 2006; Thompson et al., 1991; Vrahas et al., 1997) pendulum, (Borrelli et al., 2002; Chrisman et al., 1981) servo-electrodynamic, (Frank et al., 2000; Furman et al., 2007; Milentijevic et al., 2003; Quinn et al., 2001; Torzilli et al., 2006) and servo-hydraulic, (Ashwell et al., 2008; Borrelli et al., 1997; D'Lima et al., 2001b; Ewers et al., 2001) and screw (Jeffrey et al., 1997)

devices have been developed to deliver a single impact (rapid, compressive load) to articular cartilage.

Drop-tower devices control the impact energy, E (Joules), delivered to the specimen by

$$E = mgh \tag{1-5}$$

where m is the mass of the impactor (kg), g is the gravitational acceleration constant (m/s^2), and h is the height (m) from which the impactor falls. An accelerometer is used to measure the acceleration of the impactor while in contact with the specimen. The impact velocity of the impactor is determined through integration of the acceleration-time graph and cartilage displacement is determined through integration of the velocity-time graph. Strain is measured by dividing the displacement data by the original thickness of the specimen. A force transducer is used to measure the force during impact and stress is measured by dividing the force data by the original cross-sectional area of the specimen. Jeffrey and Aspden (2006) reported that impact energy of 0.12 J to cartilage explants results in the following: peak forces (294-580 N), maximum stresses (21.7-45.8 MPa), stress rates (15,400-35,500 MPa/sec), maximum strain (0.55-0.80 mm/mm), and strain rates (303-523 s^{-1}). Recently, a drop-tower apparatus was used by Mrosek et al. to recreate a pathologic transarticular load by dropping a mass of 2.1 kg to the patellofemoral joint of an anaesthetized dog resulting in a peak force between 2010 and 2170 N with a time to peak force of ~1.5 ms (Mrosek et al., 2006).

Similar to drop-tower apparatuses, pendulum devices control impact energy, E, with the height of the pendulum arm related to its length L by

$$h = L - L\cos(\theta) \tag{1-6}$$

where θ is the angle between L and the vertical. Force is measured during impact with a piezoelectric load cell and super low pressure-sensitive film is used to measure contact surface area. Borrelli et al. (2002) used a mass of 2400 g attached to a pendulum arm to impact the posterior aspect of the medial femoral condyle of in vivo rabbits that resulted in a maximum force of 345.5 N (corresponding to a maximum stress of 54.8 MPa with a measured contact area of 6.38 mm^2) and time to peak force of 0.021 sec. To the author's knowledge, maximum strain during impact using pendulum devices has not been reported.

Milentijevic et al. (2003) developed a servo-controlled double-acting pneumatic cylinder to impact cartilage explants by controlling peak stress (ranging from 10 to 60 MPa) and stress rate (ranging from 25 to 1000 MPa/s) (Milentijevic and Torzilli, 2005) resulting in: peak forces (31.7-399 N), maximum strain (0.137-0.227 mm/mm), and time to peak force (10-1600 ms). In a follow-up study, Milentijevic et al. (2005) used the same device to apply a known stress magnitude (15-50 MPa) at a stress rate of 420 MPa/sec to the articular surface of the lateral femoral condyle of cadaveric and live anesthetized rabbits. Cell death and matrix damage was observed in explants at stress magnitudes >20 and 30 MPa, respectively. The articular cartilage in the live rabbit knees was analyzed at 0 and 3 weeks post-injury with visible surface damage observed immediately post-injury, but no gross changes present by 3 weeks post-injury. The system used was able to generate signs of late-stage osteoarthritis (e.g. matrix damage, chondrocyte death, and proteoglycan loss) by delivering an impact load to 35 MPa.

Frank et al. (2000) developed a custom-made servo electro-dynamic device with an axial motor capable of applying compressive ramps at rates up to 1 mm/sec

(corresponding to a strain rate of 1 s^{-1}) with a maximum force of 400 N. Kurz et al. (2001) used the device developed by Frank et al. (2000) to impact calf cartilage explants to 50% strain of 1 mm thick cartilage for strain rates of 0.01, 0.1, and 1s^{-1} resulted in peak stresses of 12, 18, and 24 MPa, respectively. Quinn et al. (2001) developed a similar electro-dynamic device to impact cartilage explants to maximum stresses of 3.5, 7.0, or 14 MPa at strain rates of 3 x 10^{-5}, 0.3, 0.5, or 0.7 s^{-1} that resulted in more tissue damage present with higher strain rates. The maximum strain incurred by the tissue was not reported. Recently, Furman et al. (2007) and Ward et al. (2008) used a materials testing system (BOSE, ElectroForce 3200) to apply an impact force of 55 N at a rate of 20 N/sec to produce intra-articular tibial plateau fractures in anesthetized mice.

D'Lima et al. (2001b) used a servo-hydraulic test machine (Instron 8511) to impact cartilage explants to either a maximum stress of 14 MPa or 30% strain at a rate of 3 s^{-1} lasting for 500 ms. Ewers et al. (2001) used a smaller servo-hydraulic test machine (Instron 1331) to impact cartilage explants to a maximum force of 1247 N, resulting in ~40 MPa at a rate of ~900 MPa/sec with a time to peak force of 45 ms and 1 sec, respectively. Ashwell et al. (2008) used a servo-hydraulic test machine (MTS 858 Mini Bionix II) to impact *ex vivo* porcine patella to 2000 N at a rate of 25 mm/sec.

One of the primary challenges of creating an effective PTOA model is that of mimicking clinically-relevant cartilage injury in a reproducible manner, thus devices have been used to control various impact parameter magnitudes and rate or duration (Table 1) which have been shown to affect cartilage physiology, i.e. with findings that supra- and sub-physiologic loading conditions can be detrimental.

Table 1. Previous work by others studying the effect of impact load conditions on cartilage

Author	Device	Type of Impact		Magnitude	Rate/Duration	Results
Ewers et al., 2001	Servo-hydraulic	*in vitro*	unconfined	40 MPa	*Low* (40 MPa/s)	↑↑ cell death (more distribution) ↑ matrix damage
					High (900 MPa/s)	↑ cell death (near fissures) ↑↑ matrix damage
Ewers et al., 2002	Servo-hydraulic	*in vivo*	confined		*Low* (50 ms)	↑ cartilage softening ↑ bone thickening
	Drop-tower	*in vivo*	confined		*High* (5 ms)	↑ cartilage softening ↑↑ bone thickening
Quinn et al., 2001	Electro-dynamic	*in vitro*	unconfined	3.5,7,14 MPa	*Low* (3×10^{-5} strain/sec)	↑ cell death (more distribution)
					Medium-High (0.3,0.5, 0.7 strain/sec)	↑ cell death (near fissures) ↑ matrix damage ↑ GAG release (up to 24 hrs)
Jeffrey et al., 2006	Screw	*in vitro*	unconfined	Same max strain (%) = average from drop-tower	*Low* (40 mm/s) cross-head speed	↑ cell death (immediate) ↑↑ matrix damage ↑ peak stress (0.8 MPa) ↑↑ time duration (42 ms) ↑ dynamic modulus (4.5 MPa)
	Drop-tower	*in vitro*	unconfined	0.12 J Average max strain (%) determined but values not reported	*High*	↑ cell death (delayed ~72 hrs) ↑ matrix damage ↑↑ peak stress (21.7 MPa) ↑ time duration (1.5 ms) ↑↑ dynamic modulus (87.8 MPa)
Milentijevic et al., 2003	Servo-controlled pneumatic	*in vitro*	confined	10-60 MPa	*Medium* (350 MPa/s)	↑ compressive strains in the superficial compared to deep zones
Milentijevic and Torzilli, 2005	Servo-controlled pneumatic	*in vitro*	confined	10,20,30,40 MPa	*Low-High* (25,50,130,1000 MPa/s)	↑ cell death with higher stress and lower stress rate

↑ or ↑↑ indicates increased minor or major differences compared to control

For example, Ewers et al. (2000, 2001, 2002) reported that the rate of loading affects the degree of acute and chronic injury, matrix damage, chondrocyte death, changes in retropatellar cartilage and underlying bone such that a low rate of loading generated more cell death while a high rate of loading created more matrix damage and subchondral bone thickening. Quinn et al. (2001) studied the effects of two strain rates and peak stress on adult bovine cartilage matrix and cell injury, and reported that a similar amount of cell death occurred for both strain rates, but the low rate created a greater distribution of cell death compared to the high rate of loading cell death being predominantly near fissures. Matrix damage as well as GAG release (up to 24 hours post-impact) was observed for the high rate of strain. Jeffrey et al. (2006) compared the effects of a single energy drop tower fast impact loading to a slower constant 40 mm/s crosshead speed loading up to the average strain observed during drop tower tests on articular cartilage. The slower rate of loading (30 times longer to reach peak stress and peak stress a factor of 20 lower than drop test) caused more rapid apoptosis although similar levels were reached after 3 days. Milentijevic et al. (2003) investigated the influence of impact load stress magnitude and stress rate (Milentijevic and Torzilli, 2005) on water loss, matrix deformation, and chondrocyte viability and reported that greater compressive strains were incurred in the superficial zone (as compared to the deep zone) and that cell death increased with increasing stress magnitude and decreasing stress rate.

Previous investigations have controlled and/or reported (Table 1): energy of impact, maximum stress, and maximum strain delivered along with corresponding rate of stress, rate of strain, velocity and/or duration of impact and constraint or not on lateral

expansion. Cartilage is a viscoelastic type material, and thus its resistance to load (stiffness) is velocity (strain rate) and time relaxation dependent, as well as being dependent upon its biomechanical material properties, thickness, cross section area of the impacted region and constraints placed on its lateral expansion during the traumatic event. Thickness of a cartilage explant with all physiologic layers of interest in a particular study is measurable, but it is not easy to obtain multiple samples of like thickness. Thus ideally the magnitude of the controlled impact parameter (energy, maximum stress, or maximum strain) should be normalized relative to cartilage thickness and set to this value before delivery. This is impossible to do with energy and maximum stress since these parameters are also dependent upon unknown cartilage material properties and time history of delivery. Jeffrey et al. (2006) reported that, "the peak stresses reached in the fast, drop tower impact loading were more than 20 times that of the slow velocity controlled, severe load suggesting that stress alone is not a good indicator of damage." Control of maximum strain and strain rate on the other hand are strictly thickness dependent, and thus are theoretically achievable to define a repeatable thickness normalized "severity of trauma." However, to achieve the same selected strain rate would require for the software available in the COL lab that the impact velocity be normalized and thus changed for each specimen of different thickness, which would require altering the control program's desired velocity and reloading the program after thickness measurement was made. We thus selected to use impact velocity and maximum strain as the two parameters to define repeatable "severity of trauma" catagories. Previous investigations using controlled impact velocity to different levels of maximum strain were at relatively slow rates (< 1 mm/sec) (Frank et al., 2000), compared

to estimated average *in vivo* joint trauma rates of 12.5 and 25 mm/sec (assuming 50% strain of 0.5 mm thick cartilage) corresponding to maximum force to the cartilage reported time for falling injury to occur within 20 ms (Robinovitch and Chiu, 1998) and for vehicular knee-dashboard injuries within 10 ms (King, 2001), respectively.

It was decided to investigate using the Comparative Orthopaedic Laboratory's (COL's) *Instron 8821s*, servo-hydraulic testing machine as shown in Figure 4 to achieve the objective(s) primarily due to: 1) minimal cost (since the machine was previously purchased and has been used for several other projects and the cost estimate of purchasing an servo-controlled electrodynamic machine (TestResources, 200LM25) with a force capability up to 740 N at a rate of 4600 mm/sec was approximately $50,000), and 2) the minimal effect the 4 mm diameter cartilage explant resistive force to impact would have on the controlled motion of the test machine's massive ram.

Therefore, the objective of this thesis work was to develop a clinically-relevant *ex vivo* PTOA model with repeatable severity of mechanical injury by delivering a single impact load with controlled combinations of velocity and maximum strain (i.e. severity of trauma categories) to a laterally-constrained articular cartilage explant to study their effect on articular cartilage's biomarkers: cell viability, extracellular matrix, and material properties. This is part of our broader goal of finding post trauma biomarkers that could clinically be measured to predict the likelihood of the onset of PTOA and its progression for purposes of selecting or determining optimum treatments.

Figure 4. Instron 8821s servo-hydraulic testing machine in the biomechanics lab of the Comparative Orthopaedic Laboratory (COL). For this project, the machine was equipped with a 1000 N load cell attached to the ram which has a maximum ram travel of 260 mm. A stainless steel impactor (tip diameter of 3.9 mm) attached to the end of the ram (below the load cell) and a stainless steel base (containing a stainless steel anvil with specimen-restraining well located in the center) was attached to the test table (See Appendix B for detailed fixture drawings).

CHAPTER 2

DEVELOPMENT OF AN *IN VITRO* MECHANICAL INJURY DEVICE AND PROTOCOL

The initial investigation of using the Instron 8821s, servo-hydraulic testing machine to approach constant velocity impact to desired maximum strain of canine cartilage for development of an *in vitro* post-traumatic osteoarthritis model is described fully in a final report for the graduate course, Biological Engineering (BE 7001): *Problems in Biological Engineering* completed by Nicole Poythress Waters on December 31, 2008. A hard copy is stored on file in the Department of Biological Engineering office at the University of Missouri-Columbia. The purpose of this chapter is to summarize and provide a working reference for future studies to the impact protocol developed and used to measure the thickness of and impact the specimens for the studies in Chapter 3 and 4 of this thesis.

The objectives of the work in the aforementioned final report were to: 1) determine whether the Instron 8821s servo-hydraulic testing machine was capable of impacting canine cartilage at a constant velocity to a specified maximum strain (compression divided by initial specimen thickness), 2) determine the maximum impact velocity capability of the Instron by tuning its proportional-integral-derivative (PID) values, 3) develop a method to measure specimen thickness and then use this thickness to impact the specimen to a desired maximum strain, and 4) determine if a cartilage specimen's impact resistance force (which is unknown and thus uncontrollable) would have a significant effect on the ram's impact position response (i.e. desired impact velocity and maximum strain).

The custom designed fixtures used to measure thickness and deliver impact load to a 4.0 mm diameter cartilage explant specimen is shown in Figure 5. Appendix B contains shop drawings for each component.

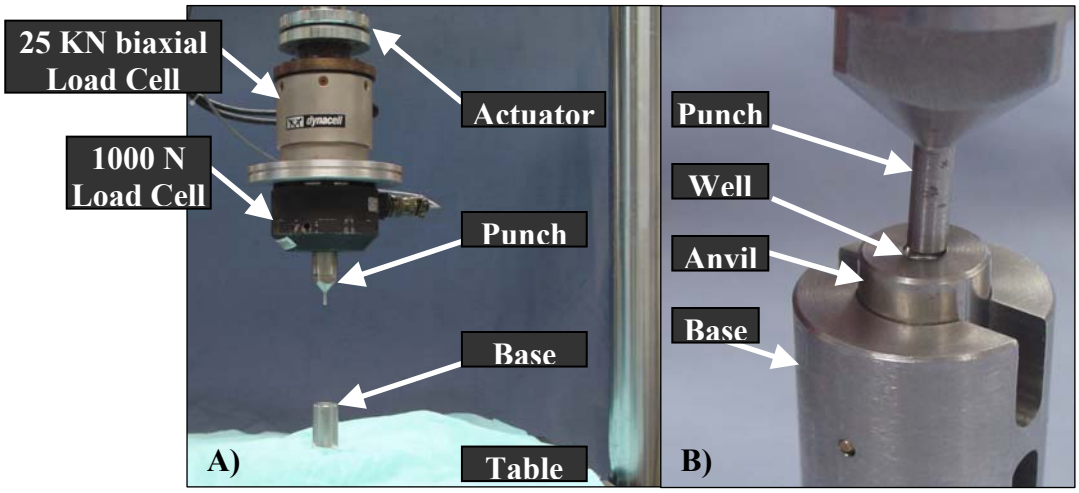

Figure 5. Custom designed stainless steel fixtures used to measure thickness and deliver impact load to ex vivo cartilage explants: A) Flat-tip punch (3.9-mm diameter) attached to load cell on test machine (Instron 8821S) actuator and fixture base attached to test machine table, and B) Removable anvil with 4.0 dia. by 2.54 mm deep well to laterally-constrain explant.

Optimal PID values were found to be 40, 0, 0. A relative ram displacement impact control program (see Section 2.1.1) was used to run impact tests with no cartilage specimen in the well (hereafter referred to as "no load") tests at programmed constant impact velocities v_1 of 125, 100, 50, 25, and 1 mm/sec to evaluate the ram's actual velocity, v_1, and its overshoot, T_o (see Section 2.1.2). The maximum ram velocity that the Instron could produce was found to be 100 mm/sec. Overshoot T_o was found to be dependent upon the selected input velocity, but repeatable for a selected velocity. The protocol and equations for measuring thickness of a specimen and thereafter determining the absolute initial ram position to use to impact the specimen at the selected velocity to the desired maximum level of compressive strain is contained in Section 2.1.3. The

resistance force of a rubber simulated specimen was found to have negligible effect on ram impact velocity and overshoot, and thus should have negligible effect when impacting cartilage specimens as discussed in Section 2.1.4. An attempt was made to use the force indicated by the 1000 N (Lebow model 3173 strain gauge, Eaton Corporation, Troy, MI) load cell attached between the ram and the punch (Figure 5) to determine impact stress delivered to (resisted by) the specimen, the specimen's material moduli (stiffness parameters), and the energy absorbed by the specimen during impact. The load cell was not an inertia force compensated model. As discussed in Section 2.2, attempts to compensate the indicated force to obtain reliable measurement of the resistance force during impact of the specimen failed, and thus corresponding stress, moduli and energy results are not available for the specimens tested for the studies presented in Chapter 3 and 4.

2.1 Impact Protocol with Controlled Maximum Strain and Velocity

2.1.1 Impact Program

The following position-control impact program with set maximum ram velocity, v_1, was generated using Instron's RS BasLab Scheduler Editor computer software to control the Instron 8821s ram position. An actual response for the numerical value of parameters given in the program listing, and definition of parameters is illustrated in Figure 6:

Step 1 (Hold)

Time duration (sec)	2

Step 2 (Trapezoid waveform)

End Point 1, EP_1 (mm)	-2.25
Rate 1, v_1 (mm/sec)	100
Dwell 1, D_1 (sec)	1.0
End Point 2, EP_2 (mm)	0
Rate 2, v_2 (mm/sec)	1.0
Dwell 2, D_2 (sec)	1.0
Reset after (cycles)	1.0

Step 3 (Hold)

Time duration (sec)	2

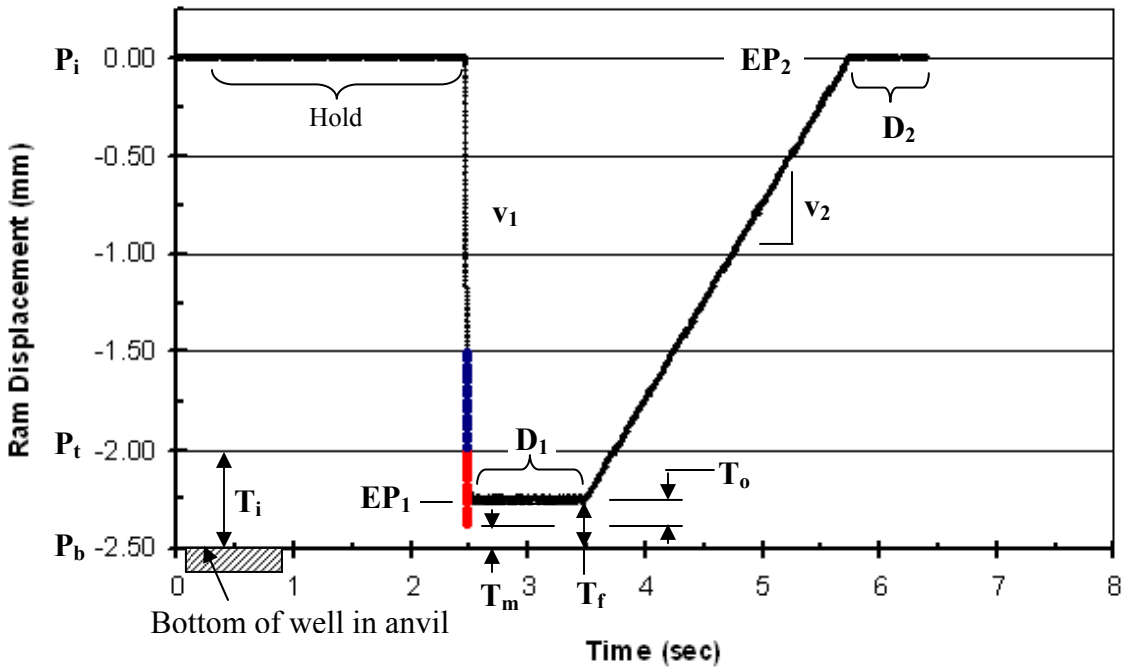

Figure 6. Impact parameter terminology and actual response generated using given parameter values for Instron computer software program and PID values 40, 0, 0. A specimen with assumed initial thickness T_i = 0.5 mm is used for illustrative purposes.

End point relative ram travel, EP_1, was selected to be -2.25 mm (for all tests) to assure that the ram has reached constant velocity prior to making contact with the specimen at displacement, P_t, that corresponds to the superior surface of a specimen with initial thickness, T_i, placed in the bottom of the well in the anvil. The final compressed thickness of the specimen is, T_f. The maximum compressed thickness of the specimen is T_m, which results from ram overshoot T_o beyond EP_1. The trapezoid waveform was used due to its intrinsic dwell time characteristics, thus minimizing additional hold steps. A nominal rate of v_2 = 1.00 mm/sec was arbitrarily selected to remove the ram from the specimen.

2.1.2 Controlling Maximum Specimen Compression for Various Impact Velocities

Overshoot, T_o, is a function of the selected desired "set" impact velocity v_1 as shown in the representative ram displacement versus time impact traces for the set velocities (100, 50, 25, 10, 1 mm/sec) in Figures 7-11, respectively, and as summarized in Table 2. The resolution of the numerical values for T_m, T_f and thus T_o are limited to that produced by the Instron's 16 bit data acquisition software in conjunction with the ram's 254 mm total possible range of travel, i.e. resolution = $254 / 2^{16}$ = 0.00388 mm. The effect of this resolution limitation can be observed in Figures 7-11 as 0.00388 mm step changes in indicated ram displacement. Suggestions to improve ram displacement resolution are summarized in Chapter 5.

The following are important observations relative to the characteristics of the Instron's ram displacement-time examples in Figures 7-11.

1. The velocity (slope of the ram displacement trace) during impact (red data points in the figures) is essentially constant (to within 0.05 mm of maximum travel for set velocity v_1 = 100 mm/sec with range of constant impact velocity improving with decreasing set velocity).
2. Final compressed thickness T_f was repeatable to within the resolution of the Instron for repeated test runs, and was not effected by the set velocity v_1.
3. Overshoot T_o was repeatable to within the resolution of the Instron for repeated runs with the same set velocity, but was a function of set velocity.

Table 2. Effect of set impact velocity v_1 on observed impact velocity v_1 and overshoot T_o. (n = 1 tested with no cartilage, thus no resistance force)

Figure	Set					Observed		Used in Chap. 3-4 tests
Number	**P** (dB)	**I** (I/sec)	**D** (msec)	**EP_1** (mm)	**v_1** (mm/sec)	**v_1** (mm/sec)	**T_o** (mm)	**T_o** (mm)
7	40	0	0	-2.25	100	103.33039	0.13178	0.13
8					50	49.75455	0.06976	
9					25	24.91149	0.03101	
10					10	9.98223	0.00775	
11					1	0.99951	0.00775	0.01

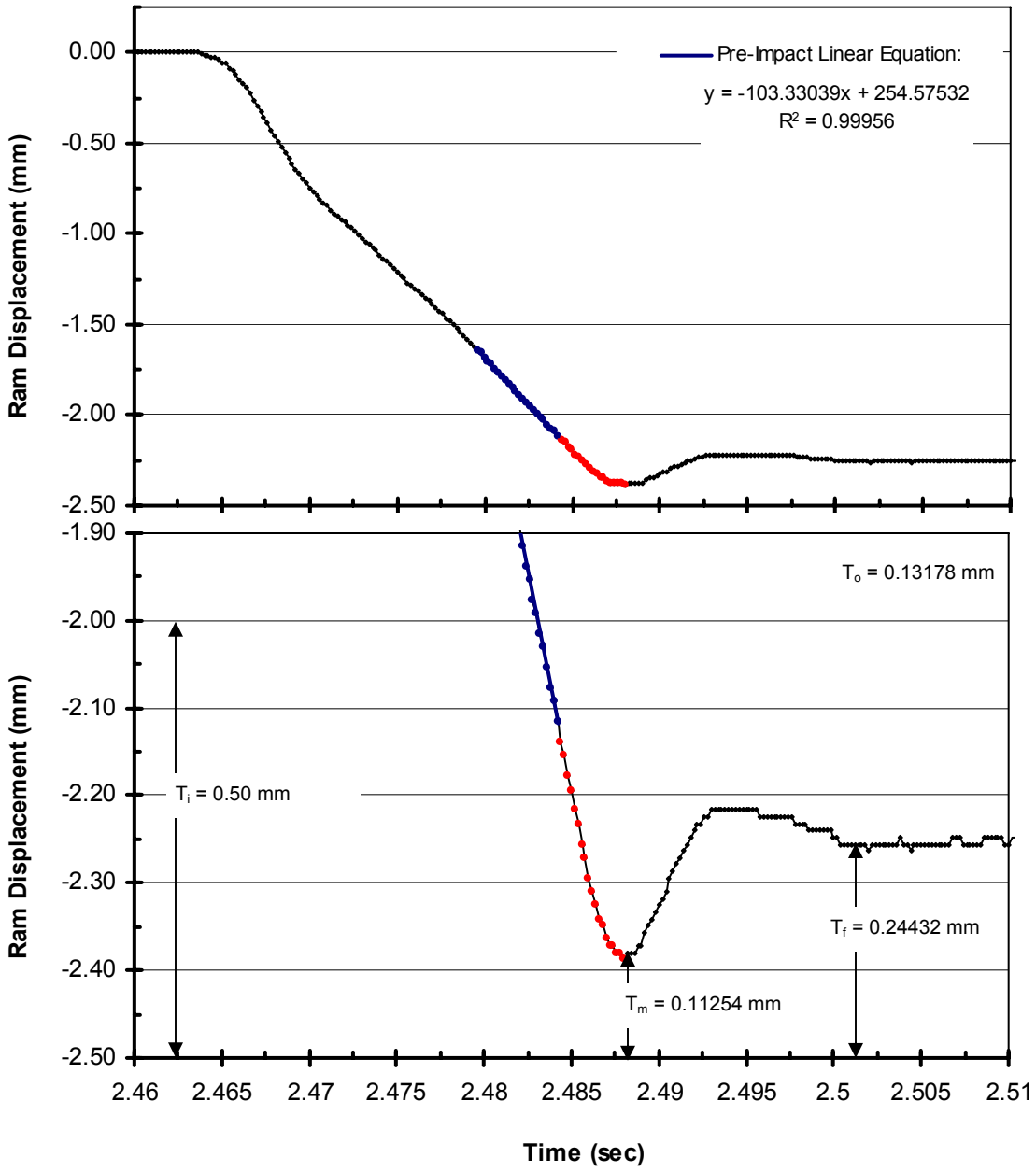

Figure 7. 100 mm/sec set velocity v_1 no load impact ram displacement (PID = 40, 0, 0; EP_1 = -2.25 mm). Red indicates data in impact region assuming cartilage initial thickness, T_i = 0.5 mm.

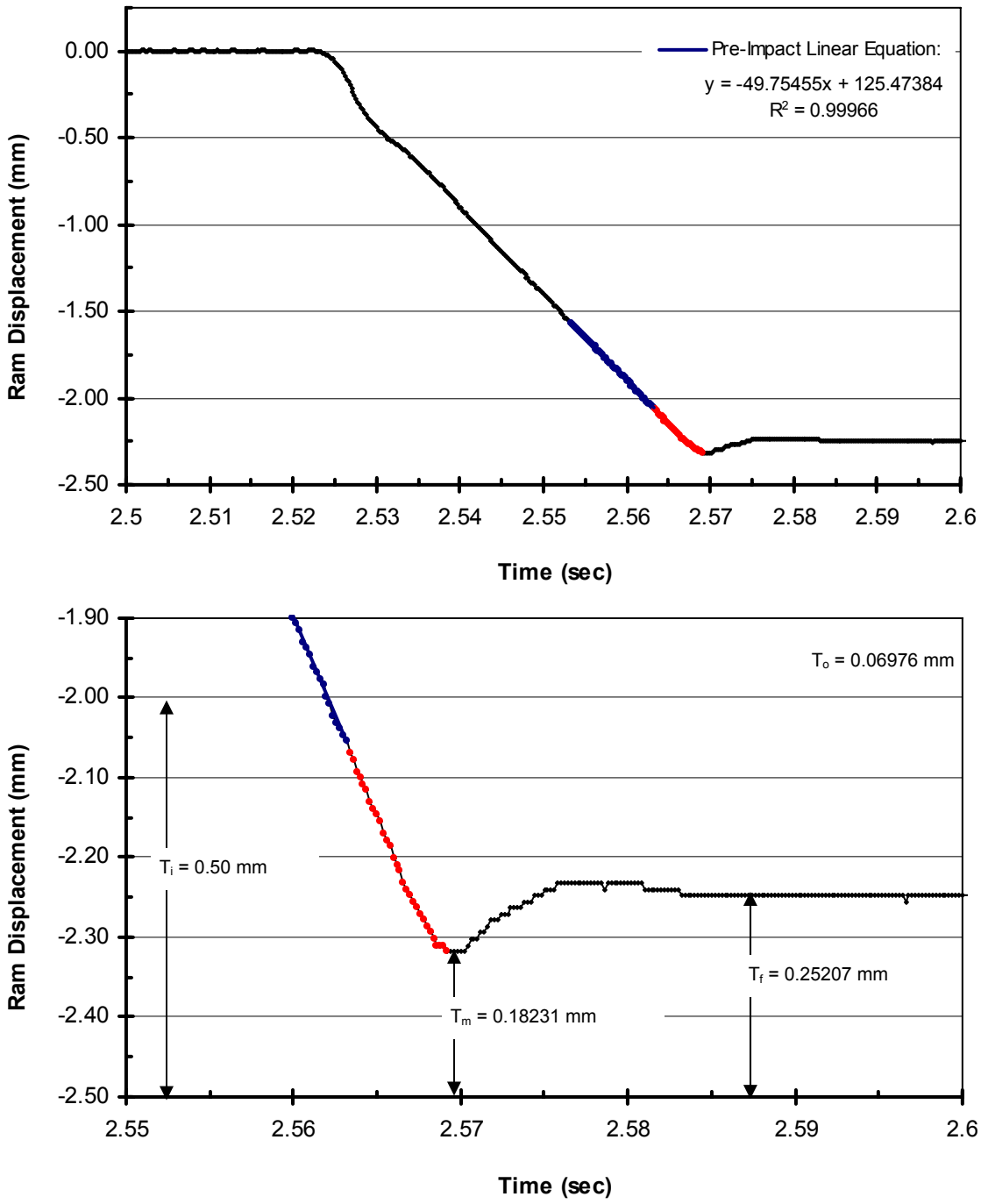

Figure 8. 50 mm/sec set velocity v_1 no load impact ram displacement (PID = 40, 0, 0; EP_1 = -2.25 mm). Red indicates data in impact region assuming cartilage initial thickness, T_i = 0.5 mm.

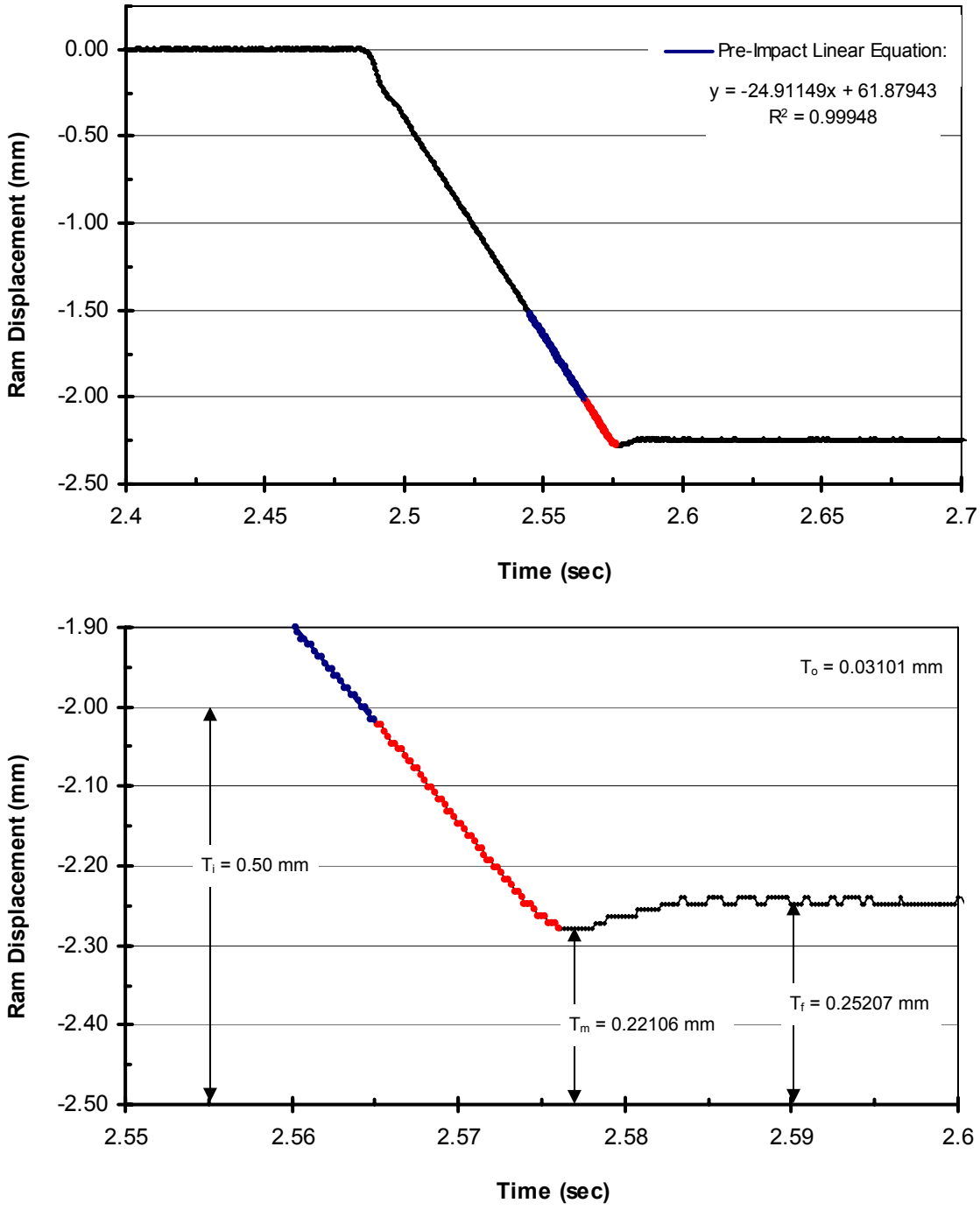

Figure 9. 25 mm/sec set velocity v_1 no load impact ram displacement (PID = 40, 0, 0; EP_1 = -2.25 mm). Red indicates data in impact region assuming cartilage initial thickness, T_i = 0.5 mm.

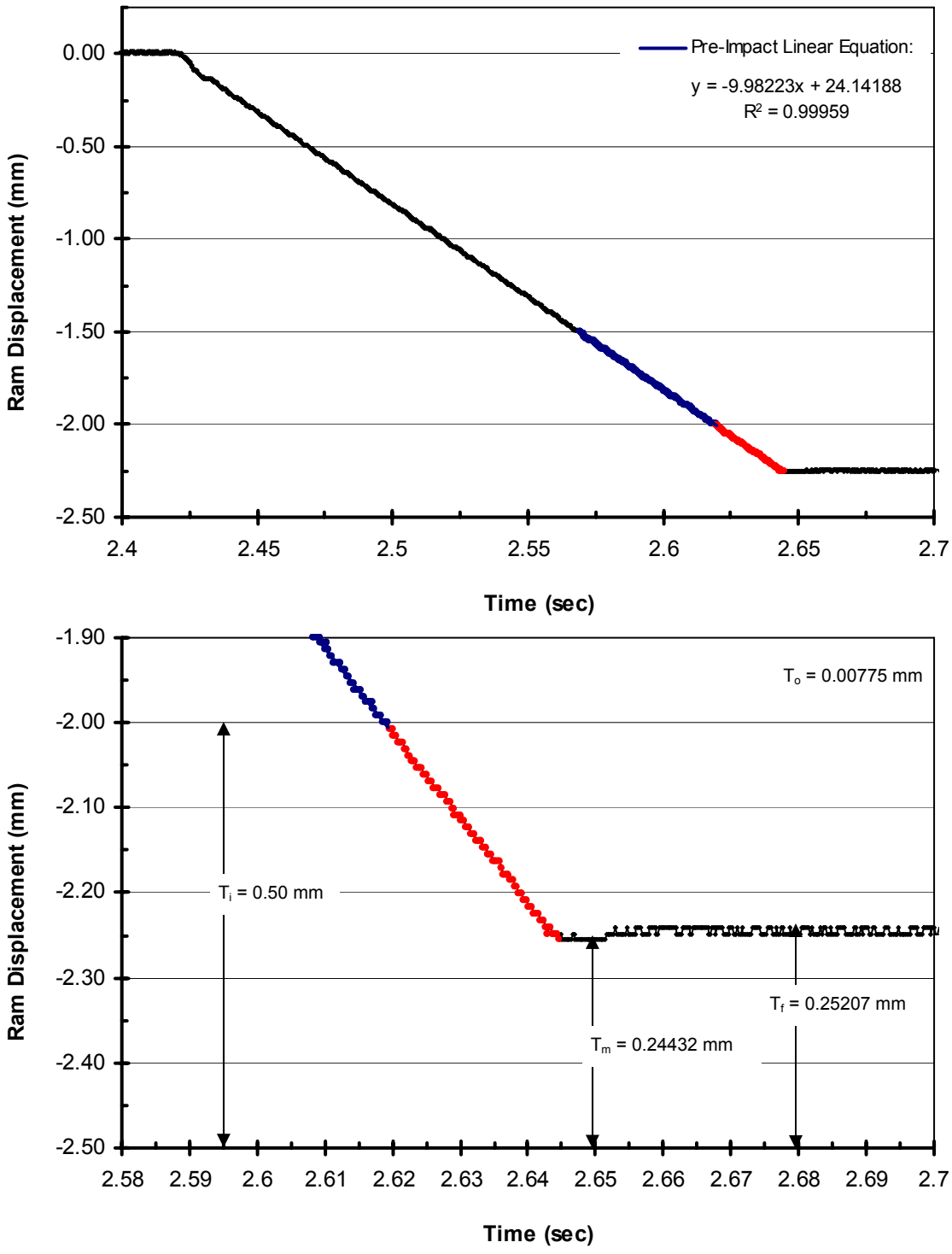

Figure 10. 10 mm/sec set velocity v_1 no load impact ram displacement (PID = 40, 0, 0; EP_1 = -2.25 mm). Red indicates data in impact region assuming cartilage initial thickness, T_i = 0.5 mm.

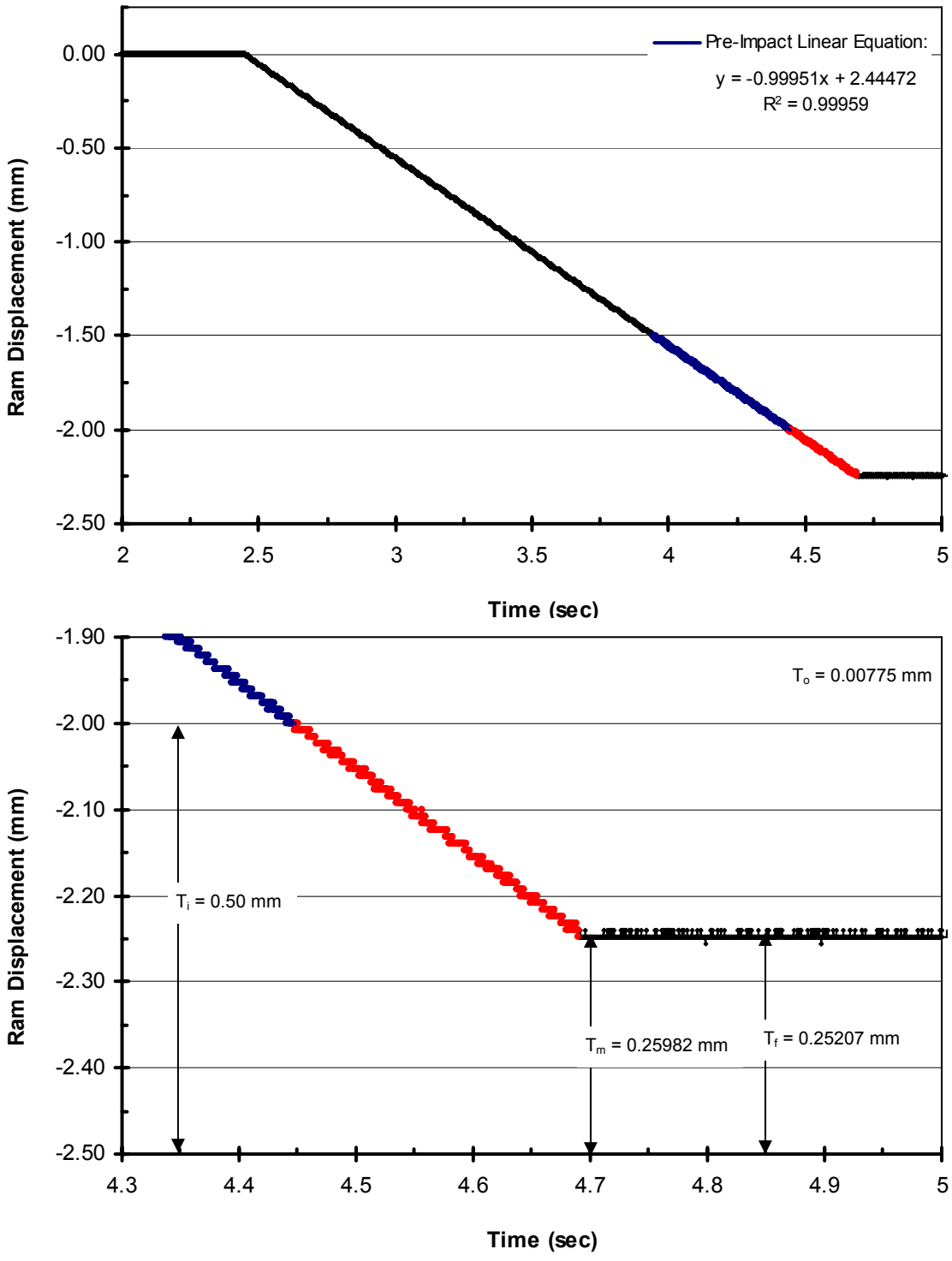

Figure 11. 1 mm/sec set velocity v_1 no load impact ram displacement (PID = 40, 0, 0; EP_1 = -2.25 mm). Red indicates data in impact region assuming cartilage initial thickness, T_i = 0.5 mm.

2.1.3 Setting Initial Absolute Ram Position to Achieve Desired Maximum Strain

The Instron's control panel displays absolute ram position, AP, and likewise the data acquisition software records absolute ram position. The relationship between absolute initial ram position, AP_i, and the impact displacement parameters illustrated in Figure 12 is

$$AP_i = AP_b + T_m + T_o + |EP_1| \quad (2\text{-}1)$$

AP_b is the absolute ram position with punch tip touching the bottom of the empty well (in anvil), which is a measurement made and recorded in the first step in measuring an explants thickness. T_m is the maximum compressed cartilage thickness. T_o is the compression overshoot. EP_1 is the set ram displacement at end point 1.

Maximum strain, ε, is defined as the change in explant thickness ($T_i - T_m$) divided by initial thickness, T_i. Solving this relationship for T_m and substituting it into equation 2-1 produces

$$AP_i = AP_b + (1-\varepsilon)T_i + T_o + |EP_1| \quad (2\text{-}2)$$

Overshoot, T_o, is dependent on impact velocity as was shown in Table 2.

Appendix A contains the step-by-step protocol to measure thickness T_i of an explant, use equation 2-2 to determine initial ram position, AP_i, and then impact cartilage to the desired strain.

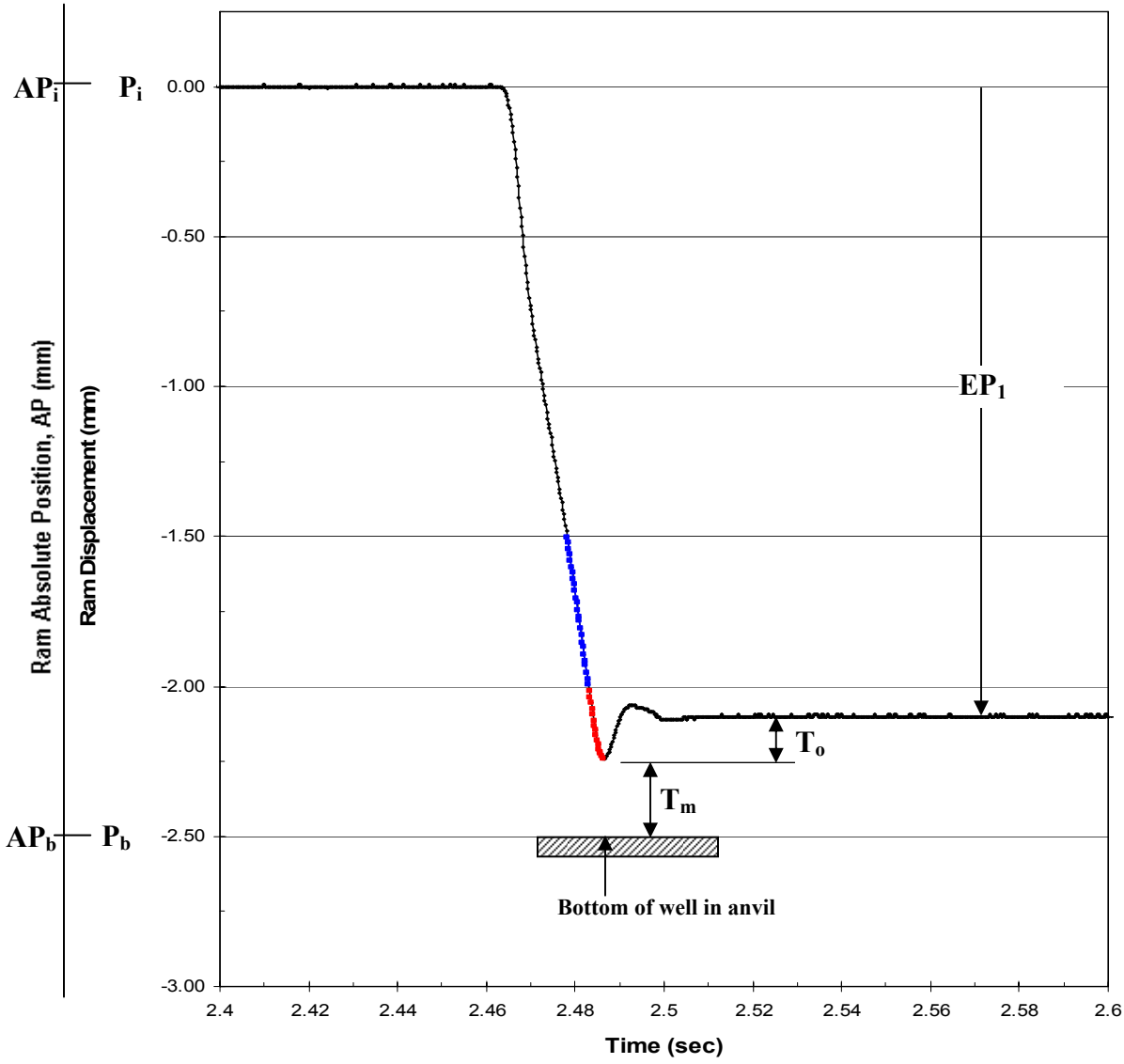

Figure 12. Visual representation of relationship between absolute ram position AP and ram displacement P, and parameters used in equation 2-2 to calculate the ram's absolute initial ram position AP_i that is set on the Instron to achieve desired maximum compression T_m (thus maximum strain ε) of cartilage that has a measured thickness T_i when using impact program with set endpoint EP_1 = -2.25 mm.

2.1.4 Effect of Specimen Impact Resistance Force

The impact program was used to impact a 4.0 mm diameter, $T_i = 0.73$ mm thick rubber cylinder simulated explant at a set velocity of 100 mm/sec and desired maximum 50% strain to investigate what effect an explants resistive force would have on the ram's impact motion. Of particular importance was to determine if the existence of an explant would affect the magnitude of ram overshoot T_o, and thus the ability to use no load determined values of overshoot T_o in Table 2 to calculate and set the ram's initial absolute position AP_i to achieve the desired maximum strain.

Figure 13A contains a trace of the indicated force (from the 1000N Lebow strain gauge load cell shown in Figure 5) with no explant (i.e. no resistive force applied to tip of the punch) during impact motion created with same set parameters used when impacting the rubber specimen. Figure 13B contains a trace of the indicated force during impact of the rubber specimen, with corresponding ram position trace shown in Figure 14.

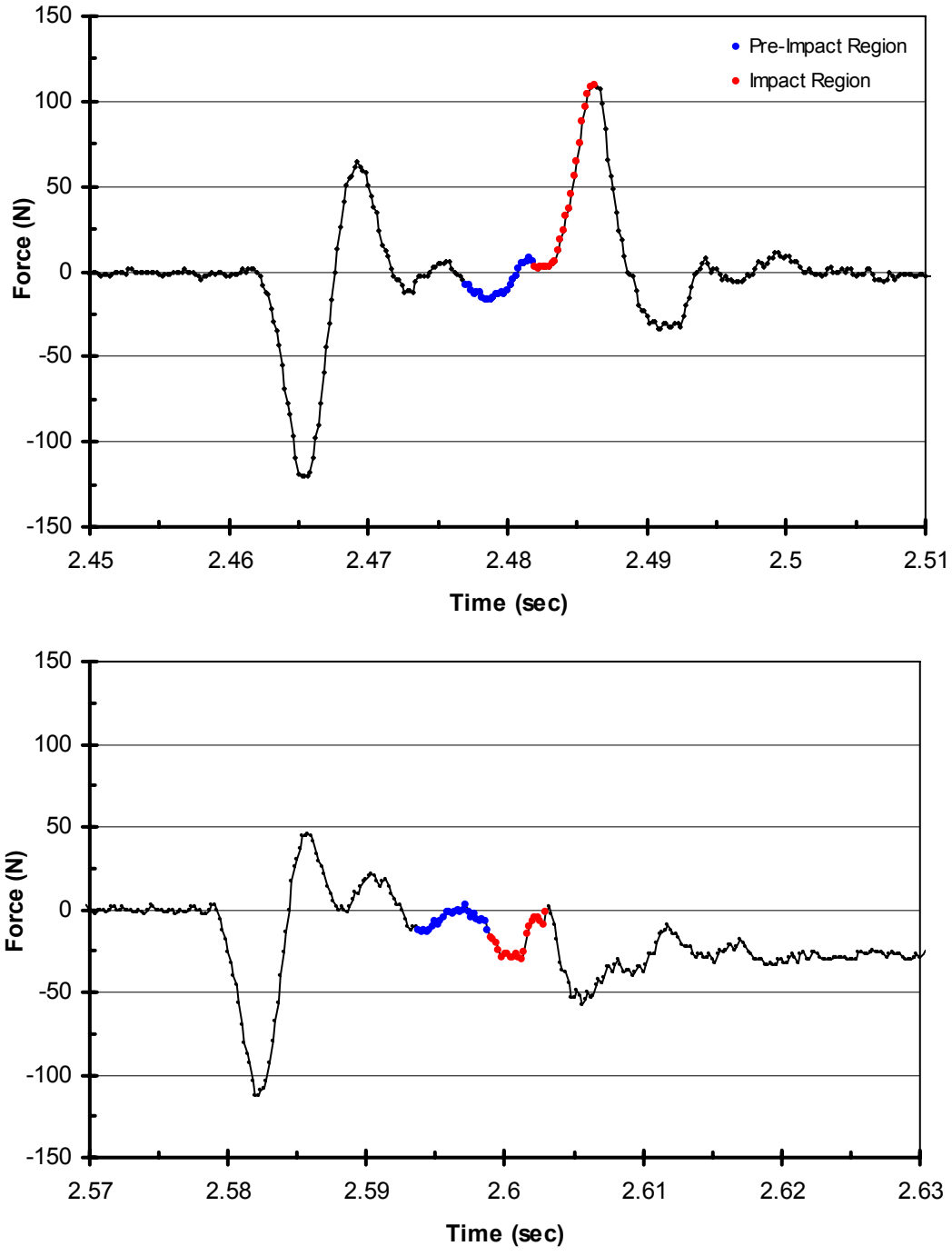

Figure 13. Indicated force, F, from impacting to 50%ε (PID = 40, 0, 0; EP_1 = -2.10 mm; v_1 = 100 mm/sec) for A) no specimen and B) rubber. Red indicates data in impact region of rubber initial thickness, T_i = 0.73 mm.

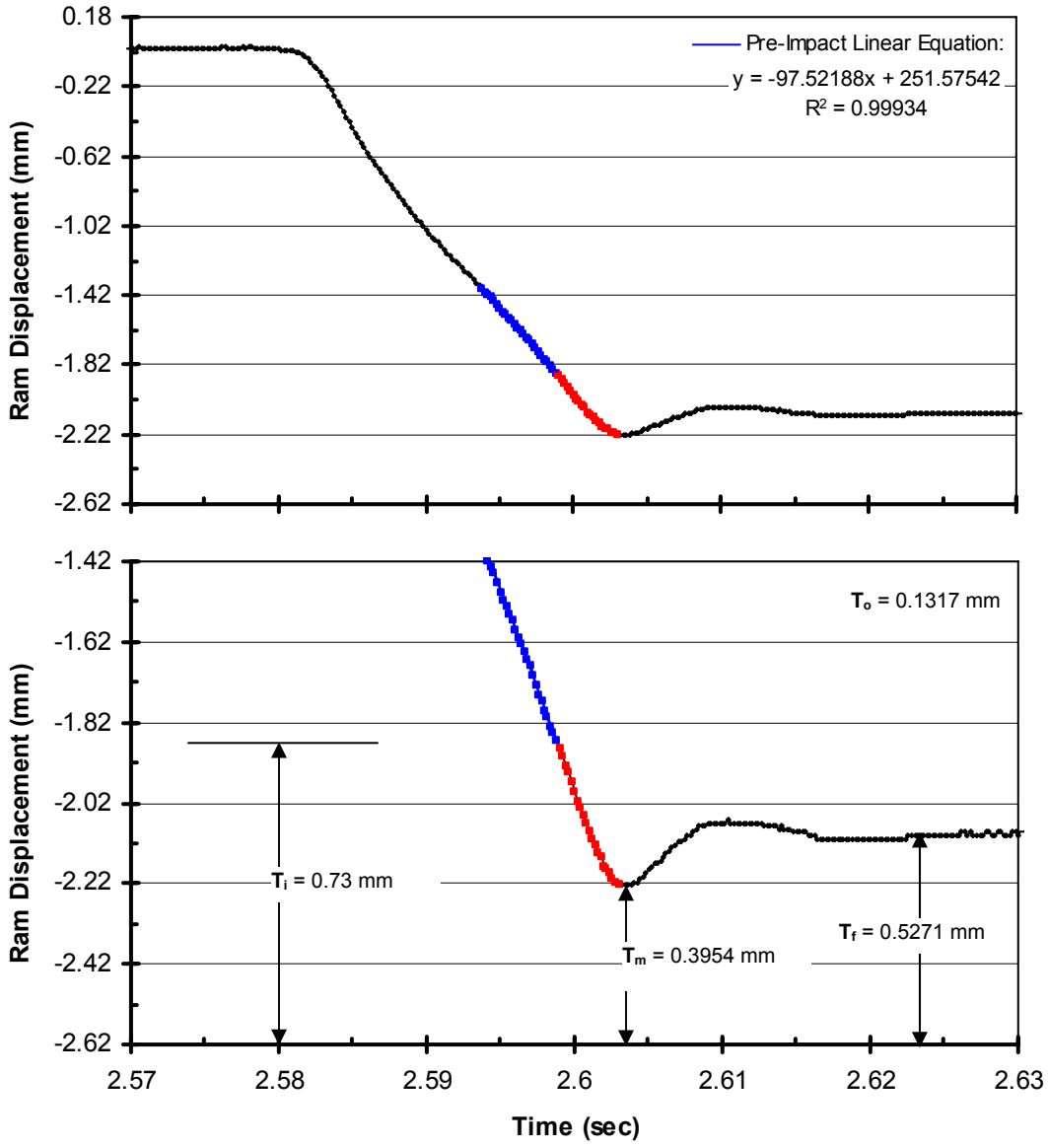

Figure 14. Ram displacement from impacting rubber to 50%ε (PID = 40, 0, 0; EP_1 = -2.10 mm; v_1 = 100 mm/sec) Red indicates data in impact region of rubber initial thickness, T_i = 0.73 mm.

If the load cell was an inertial force compensated model, theoretically the indicated force trace with no specimen would be zero during the entire impact motion, regardless of whether the ram-punch was accelerating or decelerating. The indicated force with no specimen present was zero during the zero acceleration initial and final hold periods, and nearly so during the nearly constant velocity v_1 (zero acceleration) portion of ram travel. This is an indication that the load cell had been properly zeroed. However, during the acceleration-deceleration from the initial hold to the constant velocity impact the indicated force ranged from a maximum compression (-120.94 N) to maximum tension force (+ 64.09 N), and during the deceleration to dwell 2 a maximum tension force (109.86 N), which is an indication that the 1000 N load cell with attached mass of punch is not inertial force compensated, and would need to be for accurate measurement of the dynamic resistance of an explant.

With the rubber explant in place, the load cell correctly indicated zero force during the initial ram position hold, which is proof that it was and remained correctly zeroed. Thus assuming it was correctly calibrated (which is required by the Instron controller upon start up) the constant indicated compressive force (-28.57 N) during the end of dwell 2 should be an accurate indication of the force on the specimen when compressed to its final compressed thickness T_f. The corresponding final compressive stress would be $\sigma_f = (-28.57)/ \pi(0.00195)^2 = 2.392$ MPa. One can obtain an indication of the maximum compressive force applied to the rubber explant if one assumes that it occurred at maximum compression T_m and that the indicated maximum force (-1.53 N and +109.86 N) during impact with and without the specimen present, respectively, occurred at the same maximum ram position. Subtracting the without specimen maximum

indicated force from the with specimen gives a predicted maximum compressive force of -111.39 N resisted by the rubber specimen, with corresponding stress of 9.32 MPa.

By comparing the ram displacement trace results in Figure 14 (with specimen) to Figure 7 (without specimen), overshoot (0.13 mm) was the same to within the resolution of the Instron ram position measurement capabilities. The maximum strain observed with the rubber specimen was 46.6 % compared to the desired 50%. The lower observed strain is likely the result of an accumulation of resolution errors in measuring thickness T_i, determination of T_o values in Table 2, measurement of AP_b to calculate the initial ram position AP_i and then the ability to set the ram to the exact AP_i position.

Thus, it was concluded that the rubber specimen impact resistance force had a negligible effect on the impact motion of the massive ram of the Instron 8821s. Cartilage specimens with maximum resistive stress of the order of 10 MPa or less should likewise have negligible effect. In the literature (see Table 1), the maximum resistive stress while impacting cartilage was reported to range from 3 to 60 MPa. If these higher maximum resistive stress values (> 10) are experienced while using the Instron 8821s, overshoot To actually achieved during these tests may be less than the "no load" values in Table 2, and thus the actual maximum strain (compression T_m) achieved may be less than the desired controlled value. Overshoot T_o can be checked for actual cartilage runs (particularly those that produce high stress values) to determine if higher explant resistive force is having a notable effect on T_o.

2.2 Attempt to Use Load Cell to Determine Impact Stress, Modulus, and Energy

2.2.1 Attempts to Compensate Load Cell Inertial Force

As shown in Figure 13A and discussed in Section 2.1.4, the 1000 N load cell being used to measure resistive force of the explant on the punch tip was not an inertial force compensated model. For example, the force generated during the impact region in Figure 13A was >0 N despite the fact that the punch never made contact with any specimen. Some force related parameters used to characterize cartilage that are typically reported in the literature are: maximum impact stress (maximum impact force/cross-sectional area of specimen), elastic modulus (slope of stress-strain curve during impact), and energy absorbed by the specimen during impact (area under the force-displacement curve during impact). To be able to determine these parameters, an attempt was made to correct the indicated force for the load cell's inertial force error.

Specifically, a 3rd-order polynomial ($P = c_3t^3 + c_2t^2 + c_1t + c_0$) was fit to the 100 mm/sec set velocity with no specimen present ram displacement-time data during the period of deceleration just before maximum displacement was reached, which corresponded to the period of time that the force-time appeared to have a straight line relationship (as can be observed in Figure 13A). The equation was differentiated twice to obtain the corresponding acceleration-time equation ($a = 6\ c_3t$). A linear force-time equation ($F = f_1t$) was fit to the force-time data over the same period of time used for determining the acceleration equation. To determine an effective mass m (of the load cell with punch attached), the equations for F and a were substituted into Newton's equation $F = ma$, and solved for $m = F/a = 6c_3/f_1$. Ideally, the effective mass value would be the same for repeated 100 mm/sec set velocity "no load" impact test runs in order to correct

for inertial forces by using it in the equation $F_{actual} = F_{indicated} - m*6c_3t$ where c3 would be determined by fitting a 3rd order polynomial to the displacement-time data for the actual test on the explant.

Three repeat 100 mm/sec set velocity "no load" test runs were conducted and the aforementioned technique used to determine an effective mass for each. The effective mass values so determined were 165.50, 196.87, and 225.18 g. Since these effective mass results were inconsistent and the magnitude of the inertial force was of the order of magnitude (max of 109 N in Figure 13A) or greater than the resistive force of the cartilage, the indicated force could not be accurately and reliably compensated for the load cell's inertial effect. Thus impact stress, modulus, and energy were not calculated for the tests in the studies reported in Chapter 3 and 4 of this thesis. However, using a slow 0.001 mm/sec and a 1 Hz sinusoidal 8 to 12 % strain protocol (due to the low acceleration/deceleration and corresponding inertial force error), material elastic, equilibrium and dynamic moduli were measured during and reported for the study in Chapter 4.

For future impact work with the Instron 8821s, I recommend that a miniature piezoelectric load cell be placed under the anvil, which will eliminate the effect of acceleration since the load cell itself would be stationary and the anvil in which the explant is placed would be nearly stationary during the impact test.

CHAPTER 3

EFFECTS OF IMPACT VELOCITY AND MAXIMUM STRAIN ON ARTICULAR CARTILAGE CELL VIABILITY, MATRIX COMPOSITION, AND METABOLISM

Post-traumatic osteoarthritis (PTOA) is often associated with a direct supraphysiologic impact load to articular cartilage; however the disease processes involved in conversion of insult to PTOA are ambiguous and warrant further investigation. The objective of this work was to study the effects of impact velocity and maximum strain on articular cartilage extracellular matrix, cell viability, and culture media composition. A servo-hydraulic materials testing machine was used to measure cartilage thickness (see Section 3.1.2) and subsequently impact cartilage explants at 1 mm/sec to 50% strain, 100 mm/sec to 10% strain, or 100 mm/sec to 50% strain (see Section 3.1.3). Thereafter, explants were cultured in supplemented media for twelve days. Cell viability was analyzed immediately post-injury and at day 12 as was cartilage matrix for collagen (hydroxyproline) and glycosaminoglycan (GAG) content (see Section 3.1.4). Media were tested for GAG content, collagen II synthesis (procollagen II C-propeptide), aggrecan synthesis (chondroitin sulfate-846), nitric oxide (NO), and prostaglandin E_2 (PGE_2) every three days during the culture period (see Section 3.1.5). Our results indicated that significant detrimental effects on cell viability, GAG, chondroitin sulfate-846, and PGE_2 were primarily strain dependent (see Section 3.2.2). There were no other significant differences noted among groups at the time points analyzed. This model allows for study of potential disease processes involved in PTOA and suggests that strain

has greater influence than velocity within the parameters studied. Media constituents assessed deserve consideration as potential biomarkers of disease in PTOA.

3.1 Methods

3.1.1 Tissue Harvest and Pre-Impact Culture

Using a scalpel blade, full thickness articular cartilage was aseptically harvested from the normal humeral heads of six adult canine cadavers euthanatized for reasons unrelated to this study. Cartilage explants (n = 48) were created using a 4 mm diameter biopsy punch (Fray Products, Buffalo, NY). Explants were placed in two 24-well plates (Becton Dickinson Labware, Franklin Lakes, NJ) and cultured in 1 ml Dulbecco's modified Eagle's medium high glucose (Gibco, Invitrogen, Carlsbad, CA) supplemented with 1X ITS (BD Biosciences, San Jose, CA), penicillin, streptomycin, amphotericin B, L-glutamine, sodium pyruvate, L-ascorbic acid, and non-essential amino acids and incubated at 37°C, 95% humidity, and 6% CO_2 for 48 hours prior to impact.

3.1.2 Explant Thickness Measurement

A servo-hydraulic materials test machine (model 8821s, Instron, Canton, MA) in conjunction with custom designed stainless steel fixtures (Figure 5) were used to measure the thickness and deliver the impact load to each explant at approximately 25°C (room temperature). The fixtures consisted of a flat-tip punch (3.9-mm diameter) attached to the load cell-ram of the test machine and a removable anvil containing a well (4.0-mm dia. by 2.54 mm deep to radially constrain the explant) that slip-fit within a tubular base attached to the test table. The anvil sat on a support cylinder secured to the

tubular base by an overload shear pin (with max force capacity of 630 N) to protect the punch and the 1000 N load cell (Lebow model 3173, Eaton Corporation, Troy, MI). To measure cartilage thickness, the punch was lowered in position-control at a rate of 0.01 mm/sec into the empty well and ram travel stopped by a load limit detect at 10 N compression. The corresponding absolute position AP_b of the ram was recorded. Next, the ram-punch was raised and explant inserted into well, followed by previous punch lowering protocol. The corresponding absolute position AP_t of the ram was recorded. Explant thickness, T_i, was calculated as the difference in ram position at 10 N with and without the explant, $T_i = AP_t - AP_b$.

3.1.3 Impact Injury and Post-Impact Culture

With explant still in well, the procedure described in Section 2.1.3 was used to impact the specimen. Briefly, the initial absolute position of the ram AP_i was calculated by substituting: the initial thickness measurement, T_i; desired strain, ε, (either 10% or 50%); EP_1 = - 2.25 mm, and ram overshoot T_o from Table 2 corresponding to the desired velocity (v = 1 mm/sec or 100 mm/sec). Next, the Instron controls were used to raise the ram to absolute position AP_i. The testing machine was then used in position-control to deliver the impact by starting the impact program. Six explants per group were used for day 0 analyses while the remaining six explants per group were cultured (similar to pre-impact conditions) for 12 days (Table 3). Media was changed at days 3, 6, 9, and 12 and stored at -20°C for further analysis.

Table 3. Test groups by nominal [velocity (mm/sec): max-strain (%)], and test result (mean ± standard deviation): specimen pre-impact thickness, impact velocity, max strain

	Test Groups			
Velocity: Max Strain (number of samples)	**0V:0S** (n =12)	**1V:50S** (n =12)	**100V:10S** (n =12)	**100V:50S** (n =12)
Initial thickness, T_i (mm)	0.51 ± 0.048	0.48 ± 0.079	0.58 ± 0.111	0.51 ± 0.092
Impact velocity, v (mm/sec)	0	1.00 ± 0.006	100.73 ± 0.330	99.55 ± 1.029
Max strain, ε (%)	0	48.9 ± 0.89	12.6 ± 0.89	45.1 ±2.12

3.1.4 Tissue Analysis

Cell viability of the cartilage explant was analyzed after impact on day 0 or after 12 days in culture by stereomicroscopy using a mixture of fluorescent live and dead cell stains (Invitrogen, Carlsbad, CA) in phosphate buffered saline (PBS) following manufacturer's guidelines. For this assay CellTracker™ Green CMFDA (5-chloromethylfluorescein diacetate) was used to stain live cells green and ethidium homodimer-1 to stain dead cells red. A cross-sectional piece (~1mm thick) of each cartilage explant was stained in 200 µl of the mixture for 30 minutes at room temperature. After staining, the samples were rinsed and stored in PBS. Fluorescence was captured at 5x magnification using a Leica MZFLIII stereo microscope. Image analysis was performed using the Fovea Pro plug-in for Adobe Photoshop (Adobe, San Jose, CA) to determine cell viability. After sectioning for viability testing, the remaining tissue of each cartilage explant was stored at -20°C until processed for biochemical analysis of tissue proteoglycan and collagen content. For biochemical analysis, tissues were dried by lyophilization, weighed to determine dry weight, and digested with papain. Total glycosaminoglycan (GAG) content of the tissue was determined using the 1,9-dimethylmethylene blue (DMMB) assay (Farndale et al., 1986) and total collagen content of the tissue was determined by measuring hydroxyproline (HP) as previously

reported (Reddy and Enwemeka, 1996). The results of the DMMB and HP assays were normalized to tissue dry weight and reported in units of μg/mg.

3.1.5 Media Analysis

Media GAG content was assessed using the DMMB assay used for tissue analysis. Type II collagen synthesis was determined by measuring the level of type II collagen carboxy-terminal propeptides (C-propeptide = CP II) during collagen synthesis using the CPII enzyme-linked immunosorbent assay (IBEX, Mont Royal, Quebec, CAN) according to manufacturer's protocol. Aggrecan synthesis was evaluated by measuring the release of chondroitin sulfate epitope 846 using the CS-846 assay (IBEX, Mont Royal, Quebec, CAN) according to manufacturer's protocol. Nitric oxide (NO) concentration was determined using the Griess assay (Promega, Madison, WI) according to the manufacturer's protocol. Prostaglandin E_2 (PGE_2) concentration was determined using an enzyme immunoassay kit (Cayman Chemical, Ann Arbor, MI) according to the manufacturer's protocol (Anz et al., 2009).

3.1.6 Statistical Analysis

Data were analyzed by one-way ANOVA using Tukey post-hoc group comparisons with significance set at $p<0.05$ using Sigma Stat® (San Rafael, CA).

3.2 Results

3.2.1 Tissue Analysis

The initial thickness, T_i, ranged from 0.36 to 0.75 mm with group average ranging from 0.48 to 0.58 mm thickness. The impact velocity and max strain observed for each

test group is summarized in Table 3. A representative motion profile for an impact velocity of 100 mm/sec to 50% strain given a cartilage explant 0.5 mm thick is shown in Figure 15.

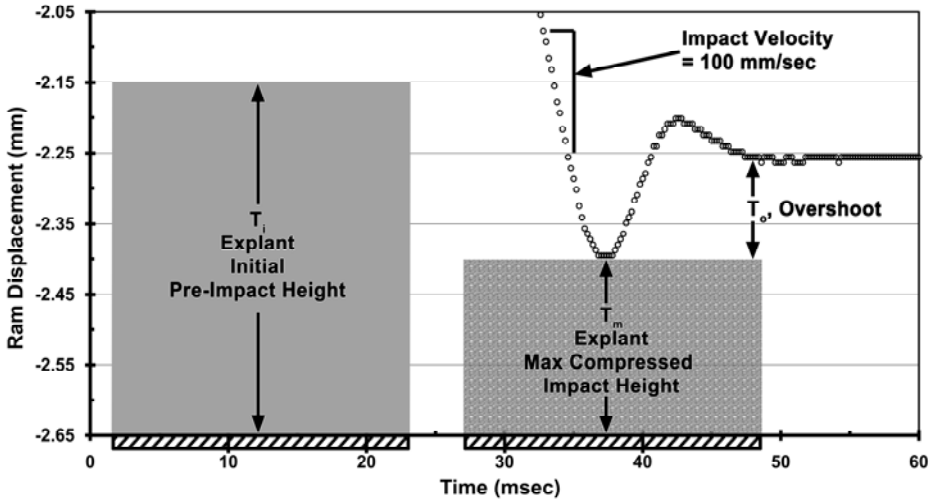

Figure 15. Representative motion profile generated by servo-hydraulic test machine (Instron 8821S) for a nominal impact velocity of 100 mm/sec and 50% max strain of a cartilage explant with an initial thickness, T_i = 0.5 mm.

The high strain groups (1V:50S and 100V:50S) experienced more cell death compared to the low/no strain groups (100V:10S and 0V:0S) at days 0 and 12 (Figure 16).

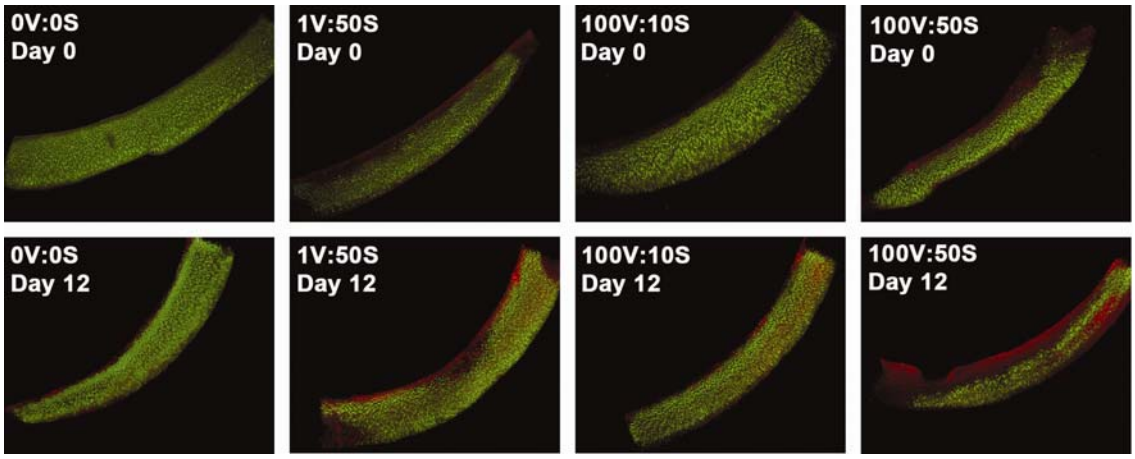

Figure 16. Effect of impact velocity and maximum strain on cell viability at day 0 and 12: red = dead cells, green = live cells.

Cell death was localized to the superficial zone of the cartilage at days 0 and 12 for both high strain groups, with a greater spatial distribution of cell death propagating from the superficial to deep zone of cartilage in the 100V:50S group compared to all other groups at day 12.

The total collagen (HP) and proteoglycan (GAG) content of the tissue are shown in Table 4. Tissue GAG content of all four groups were lower at day 12 compared to day 0 due to culture conditions (with only the no impact (0V:0S) group being statistically significant). There were no significant differences in GAG among groups at day 0 or day 12. There were no significant differences in HP content.

Table 4. Summary of tissue biomarker results (mean ± standard deviation)

Bio-marker	**0V: 0S**	**1V: 50S**	**100V: 10S**	**100V: 50S**	**0V: 0S**	**1V: 50S**	**100V: 10S**	**100V: 50S**
	Day 0				Day 12			
GAG (μg/mg)	194.6^{A} ± 21.61	175.3 ± 31.21	208.7 ± 69.33	177.8 ± 51.88	161.7^{A} ± 24.96	154.7 ± 38.83	141.7 ± 23.20	126.6 ± 38.86
HP (μg/mg)	14.21 ± 2.53	14.38 ± 6.45	12.58 ± 2.04	10.11 ± 1.80	14.31 ± 5.38	13.84 ± 5.21	12.52 ± 5.83	12.87 ± 4.16

GAG = glycosaminoglycan, HP = hydroxyproline.
Values sharing a similar letter are significantly different ($p < 0.05$)

3.2.2 Media Analysis

The results of all media biomarkers studied are shown in Table 5.

Table 5. Summary of media biomarker results (mean ± standard deviation)

Bio-marker	**0V: 0S**	**1V: 50S**	**100V: 10S**	**100V: 50S**	**0V: 0S**	**1V: 50S**	**100V: 10S**	**100V: 50S**
	Day 3				Day 6			
GAG (μg/ml)	27.9^{A} ± 2.36	77.2 ± 69.72	20.9^{A} ± 7.12	55.2 ± 49.13	16.7 ± 2.79	21.8 ± 11.23	16.1 ± 3.32	19 ± 10.19
CS-846 (μg/ml)	33.91^{A} ± 6.72	61.78^{A,B} ± 26.38	33.90^{B} ± 11.58	57.27 ± 28.22	40.27 ± 5.25	46.83 ± 6.07	40.27 ± 11.39	38.61 ± 14.85
PGE_2 (pg/ml)	50.39^{A,C} ± 21.43	970.10^{A,B} ± 276.88	144.49^{B,D} ± 176.13	779.35^{C,D} ± 156.22	1.25^{A,B} ± 0.99	201.19^{A} ± 97.87	16.26^{A,B} ± 21.79	296.32^{B} ± 147.24
NO (μM)	0.27 ± 0.66	0	0.92 ± 1.47	0.7 ± 1.73	0.41 ± 0.99	0	0.58 ± 1.43	2.04 ± 3.23
CPII (μg/ml)	0.38 ± 0.12	0.26 ± 0.81	0.36 ± 0.12	0.27 ± 0.97	0.24 ± 0.99	0.18 ± 0.11	0.24 ± 0.90	0.22 ± 0.11
	Day 9				Day 12			
GAG (μg/ml)	22.1 ± 5.60	23.1 ± 14.29	21.7 ± 4.67	20.8 ± 11.88	19.7 ± 3.75	17.7 ± 5.78	18 ± 2.54	17.4 ± 8.09
CS-846 (μg/ml)	49.61 ± 10.67	48.9 ± 9.80	54.22 ± 16.05	43.87 ± 14.52	46.39^{A} ± 11.03	36.84 ± 8.26	43.69 ± 12.72	31.77^{A} ± 7.65
PGE_2 (pg/ml)	0.67^{A,C} ± 1.54	75.16^{A,B} ± 42.64	2.71^{B,D} ± 2.36	95.24^{C,D} ± 103.48	20.89 ± 26.35	40.90^{A} ± 28.06	13.52^{A,B} ± 7.40	69.12^{B} ± 48.74
NO (μM)	2.4 ± 2.69	1.33 ± 2.07	2.45 ± 2.71	1.42 ± 2.20	0.60 ± 1.48	0	0.79 ± 1.92	0
CPII (μg/ml)	0.19 ± 0.14	0.15 ± 0.10	0.27 ± 0.18	0.20 ± 0.99	0.22 ± 0.16	0.16 ± 0.11	0.24 ± 0.22	0.14 ± 0.50

GAG = glycosaminoglycan, CS-846 = chondroitin sulfate 846, PGE_2 = prostaglandin E_2, NO = nitric oxide, CPII = procollagen II. Values sharing a similar letter are significantly different ($p < 0.05$)

On day 3, the low velocity: high strain (1V:50S) group released more GAG to the media compared to the high velocity: low strain (100V:10S) and no impact (0V:0S) groups, however these differences were not statistically significant ($p = 0.077$, 0.065 respectively). Likewise, on day 3 the high velocity: high strain (100V:50S) group released more GAG to the media compared to the high velocity: low strain (100V:10S) and no impact (0V:0S) groups, however these differences were not statistically

significant ($p = 0.132, 0.310$ respectively). The lack of statistical significance was more than likely due to variability within the high strain groups (Figure 17A).

On day 3, the media chondroitin sulfate-846 (CS-846) concentration appeared to be higher in the high strain groups (Figure 17B). The low velocity: high strain (1V:50S) group was significantly higher than the low and no strain (100V:10S, 0V:0S) groups, $p = 0.039, 0.031$, respectively. The high velocity: high strain (100V:50S) group only approached significance relative to the low strain group but was not significant relative to the no strain group, $p = 0.09, 0.24$, respectively.

The media PGE_2 concentration in both high strain (1V:50S, 100V:50S) groups at days 3, 6, and 9 were significantly higher ($p<0.01$) than the low/no strain groups, and only the low strain group ($p<0.05$) at day 12 (Figure 17C). There were no significant differences among groups for media CPII and NO content at days 3, 6, 9, and 12.

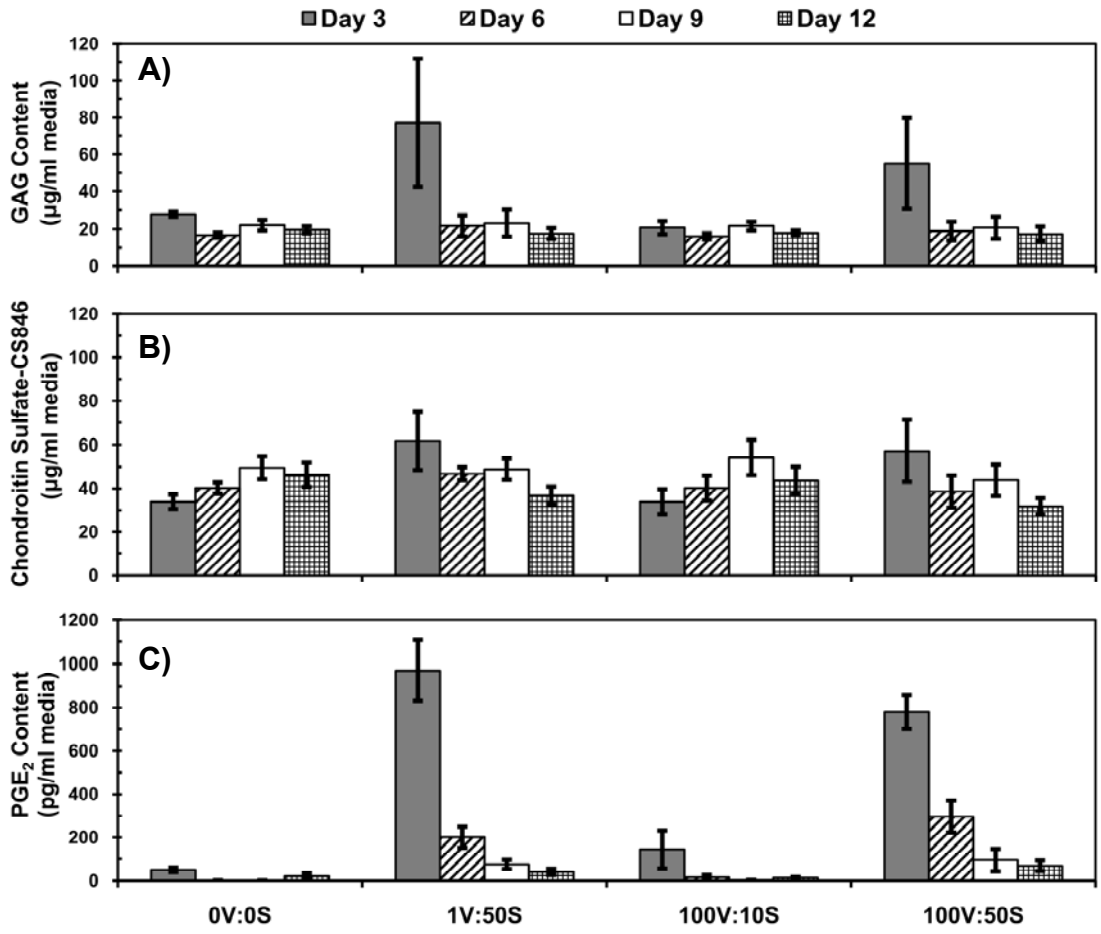

Figure 17. Effect of impact velocity and maximum strain on: A) Glycosaminoglycan, B) Chondroitin sulfate, and C) Prostaglandin E_2 content released from the articular cartilage explant into the culture media.

3.3 Discussion

In this study, degree of cell death due to a single impact injury to laterally constrained cartilage was primarily influenced by high strain. This finding is supported by previous work that indicated that strain (as compared to stress) is the major factor for cell death under static load (Shah et al., 2003). The mechanism by which cell death occurred was not specifically investigated in this study, however the effect of impact on cartilage

appeared to have a spatial (cell death located in the superficial zone of cartilage) as well as temporal (cell death in the high strain groups increasing with time) relationship with respect to cell death and it seems likely that both apoptosis and necrosis occurred. Torzilli et al. (2006) applied compressive loading to *immature* bovine cartilage explants at 0.5 MPa (ε = 10%), 1.0 MPa (20-40%), or 3.0 MPa (50-70%) and to *mature* bovine cartilage explants at 0.25-2.0 MPa (10-40%) or 2.5 MPa (50-70%). Similar to our findings, these investigators reported that cell death was initiated at the superficial zone and increased linearly in depth with increasing strain. Moreover, Torzilli et al. (2006) observed cell death within 24 hours post-injury to be localized within the superficial zone of cartilage that never exceeded 25% of the thickness of the specimen similar to our results for day 0 (post-impact) shown in Figure 16. However, we also analyzed cell death in cartilage explants after 12 days in culture and observed that cell death had migrated from the superficial to the middle/deep zones for the 100V:50S. This suggests that the rate of strain loading as well as maximum strain plays a role in cell death such that higher rates have a greater deleterious effect on cell viability for sustained periods of time as compared to lower rates (with equivalent maximum strain) that primarily affects cell death immediately following injury.

The absence of significant differences in the glycosaminoglycan (GAG) and total collagen content (hydroxyproline, HP) within the articular cartilage was anticipated since similar findings were reported in a comparable *ex vivo* cartilage impact model by Natoli et al. (2008). They reported no significant differences in GAG content (% wet wt.) and collagen content (% wet wt.) between impact groups at low energy (1.1J) or high energy (2.8 J) compared to the no impact control at either 1 week or 4 weeks post-injury (Natoli

et al., 2008). However, Natoli et al. (2008) did observe temporal effects of low and high impact with respect to a decline in GAG content for both groups at 4 weeks compared to the baseline as well as an increase in collagen content for the high impact group at 4 weeks compared to 1 week post-injury (Natoli et al., 2008). We saw a reduction in GAG content for all groups from day 0 to day 12 which was likely a result of *ex vivo* culture conditions.

The increased release of GAG to the media from the high strain groups on day 3 provides supporting evidence to that previously reported that single impact injury causes release of GAG due to physical insult to chondrocytes and disruption of the extracellular matrix (ECM) (DiMicco et al., 2004; Loening et al., 2000; Torzilli et al., 2006). Interestingly, there appeared to be an attempt at ECM repair via increased aggrecan production as indicated by the significant increase in media CS-846 observed in the 1V:50S group on day 3. However, this phenomenon appears to be transient in this PTOA model since differences among groups were not observed after day 3.

High strain (1V:50S, 100V:50S) impacts applied to cartilage resulted in significant increases in PGE_2 compared to the low/no strain groups on days 3, 6, and 9. This indicates that chondrocytes responded to injury in this impact model by synthesizing and releasing PGE_2. This study was designed to investigate the effects of impact velocity and maximum strain on articular cartilage only in our initial development of a PTOA model. Subsequent studies should assess the biochemical and biomechanical effects of each major joint tissue (cartilage, bone, synovium) and their relationships in PTOA. These studies will help to elucidate the roles that PGE_2 from each tissue source plays in physiologic responses associated with impact injury.

In contrast with previous experimental OA models established in our laboratory that consistently exhibit increased nitric oxide production, (Anz et al., 2009; Cook et al., 2007; Greenberg et al., 2006; Kuroki et al., 2005) we did not observe elevations in nitric oxide production after single impact injury to cartilage in this study. Loening et al. (2000) used a similar injury model of compressing juvenile bovine cartilage at a rate of 1 mm/sec to a maximum strain of 30-50% resulting in peak stresses of 4.5 to 25 MPa where they observed no significant differences in nitric oxide production until peak stress reached ≥20 MPa. They reported that the resulting peak stress achieved for a strain of 45% was 10.5 MPa, thus it is reasonable to infer that a strain >45% was needed to induce nitric oxide production in their model. Our model used adult canine articular cartilage with the assumption that most clinical patients affected by post-traumatic osteoarthritis are skeletally mature. It has been reported by others that juvenile cartilage responds more detrimentally to mechanical injury than adult cartilage, specifically with respect to cell death (Kurz et al., 2004; Torzilli et al., 2006). For adult cartilage, this implies that an even greater amount of peak stress (which is dependent on maximum strain) may be required for significant production of nitric oxide after impact injury. However, the use of excessively high stress and strain levels may not be clinically-relevant since articular cartilage is laterally constrained *in vivo*. A more suitable process for investigating the role of nitric oxide using this PTOA model may be to apply *in vitro* physiological loading to cartilage explants post-injury where the loading conditions would be analogous to normal daily living activities that a clinical PTOA patient may undergo.

In conclusion, severity of trauma to cartilage has been normalized relative to its thickness by quantitatively defining it in terms of (maximum strain delivered, and velocity) of a single impact to constrained cartilage explants. A large (25 kN actuator) servo-hydraulic test machine was capable of producing this model by measuring initial cartilage thickness (0.36 to 0.75 mm) followed by single impact having nearly constant impact velocity (1 up to 100 mm/sec used in this study) to controlled maximum strain levels (10 or 50% used in this study). Differences in biomarkers (cell viability, GAG, chondroitin sulfate-846, and PGE_2) were primarily maximum impact strain dependent.

CHAPTER 4

EFFECTS OF IMPACT VELOCITY AND MAXIMUM STRAIN ON ARTICULAR CARTILAGE BIOMARKERS AND MATERIAL MODULI

Mechanical injury to articular cartilage has been shown to elevate the risk of developing post-traumatic osteoarthritis (PTOA). However, the severity (rate and magnitude) of trauma needed to induce this process as well as the subsequent changes in extracellular matrix biomarkers and their relationship to material properties of cartilage is unknown. Thus, the objective of this work was to study the effects of impact velocity and maximum strain on articular cartilage extracellular matrix biomarkers and material moduli. A servo-hydraulic materials testing machine was used to measure cartilage thickness (see Section 4.1.2) and subsequently impact cartilage explants at 1 or 100 mm/sec to 10, 30, or 50% strain (see Section 4.1.4). Material testing was conducted to measure the elastic, equilibrium, and dynamic moduli at day 0 (pre-impact), day 6 (post-impact), and day 12 (post-impact) for all groups except the sham group which received this testing only at day 12 (post-impact) (see Section 4.1.3). Thereafter, explants were cultured in supplemented media for twelve days. The extracellular matrix of cartilage explants was analyzed for collagen (hydroxyproline) and glycosaminoglycan (GAG) content at day 12 (see Section 4.1.5). Media were tested for GAG content, nitric oxide (NO), and prostaglandin E_2 (PGE_2) at day 1, 2, 3, 6, 9, and 12 (see Section 4.1.6). Our results indicated that significant detrimental effects on GAG, PGE_2, and elastic modulus were primarily strain dependent (see Section 4.2). This work provides evidence that

there is a strong correlation between GAG release and the elastic/equilibrium modulus of articular cartilage following mechanical injury. There were no significant differences in nitric oxide production between groups for any time points analyzed in this study. However, PGE_2 appears to be a highly mechanosensitive (specifically strain-dependent) biomarker of disease in PTOA.

4.1 Methods

4.1.1 Tissue Harvest and Pre-Impact culture

Normal full-thickness articular cartilage explants (n = 32) were harvested from four adult canines euthanatized for reasons unrelated to this study using a 4 mm diameter biopsy punch. Explants were cultured in 1ml DMEM supplemented with 1X ITS (BD Biosciences), penicillin, streptomycin, amphotericin B, L-Glutamine, Sodium Pyruvate, L-Ascorbic Acid, and MEM Non-Essential amino acids at 37°C, 95% humidity, and 6% CO2 for 48 hours prior to impact.

4.1.2 Explant Thickness Measurement

Using the procedure described in Section 3.1.2, the thickness of each explant was measured at day 0, 6, 12 (Sham only at day 12). In comparison, the 0V:0S and Sham groups underwent identical culture conditions and did not receive any impact injury. In contrast, the thickness and material moduli of the 0V:0S group was measured at day 0, 6, and 12, whereas those parameters of the Sham group were measured only at day 12.

4.1.3 Material Moduli

While still in the well, the elastic and equilibrium moduli of each explant (Sham only on day 12) was measured by applying a compressive load at a rate of 0.001 mm/sec to 10% strain of explant thickness during static, stress-relaxation testing (Figure 18). The elastic modulus was calculated as the slope of a linear line fit though the stress-strain curve from 2 to 10% strain (Figure 19). The equilibrium modulus was calculated as the mean equilibrium stress from 298 to 300 seconds divided by 10% strain of explant.

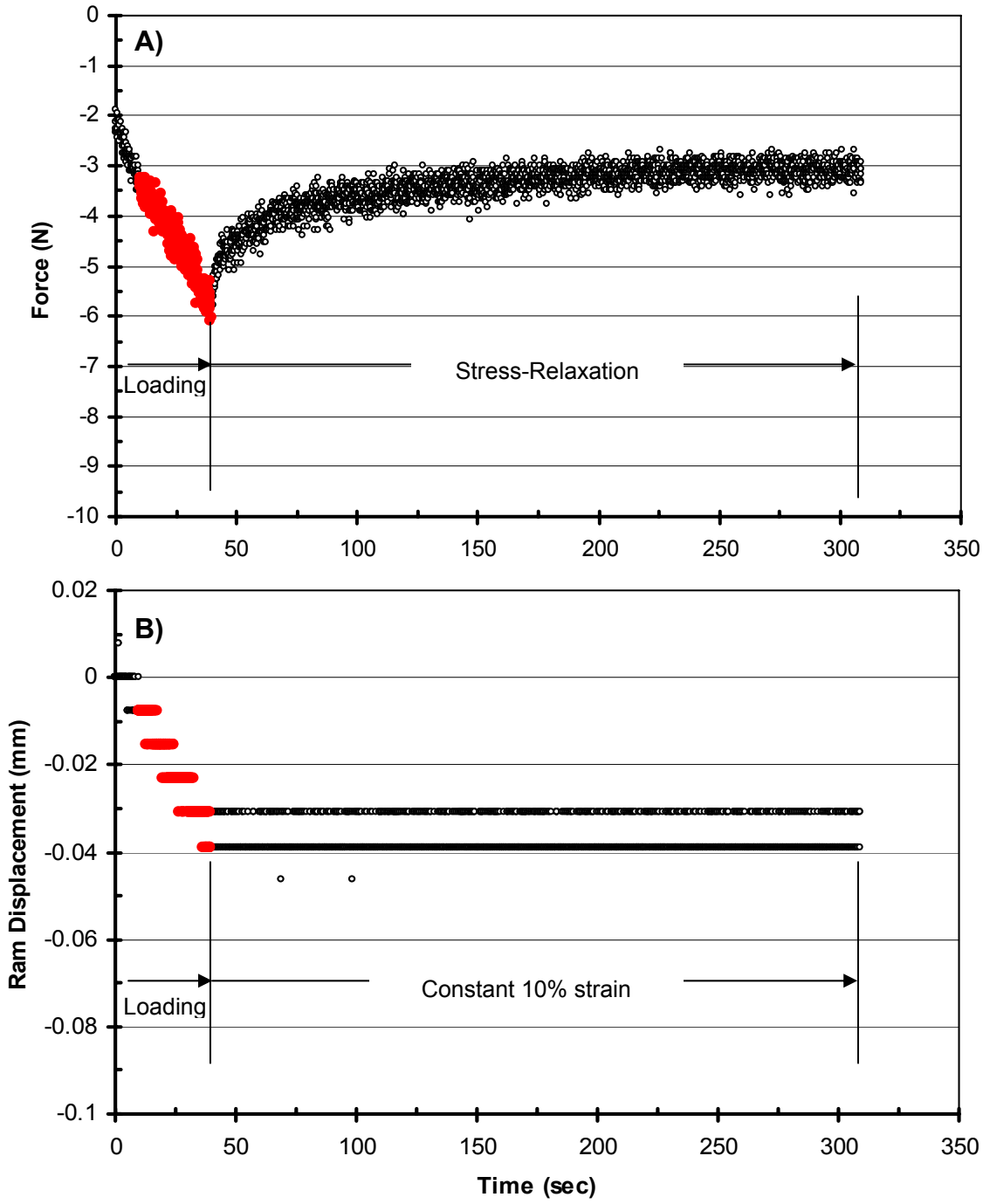

Figure 18. Example static, stress-relaxation testing of cartilage explant A) Force, and B) Ram displacement as a function of time. Red indicates data during 2 to 10% strain loading.

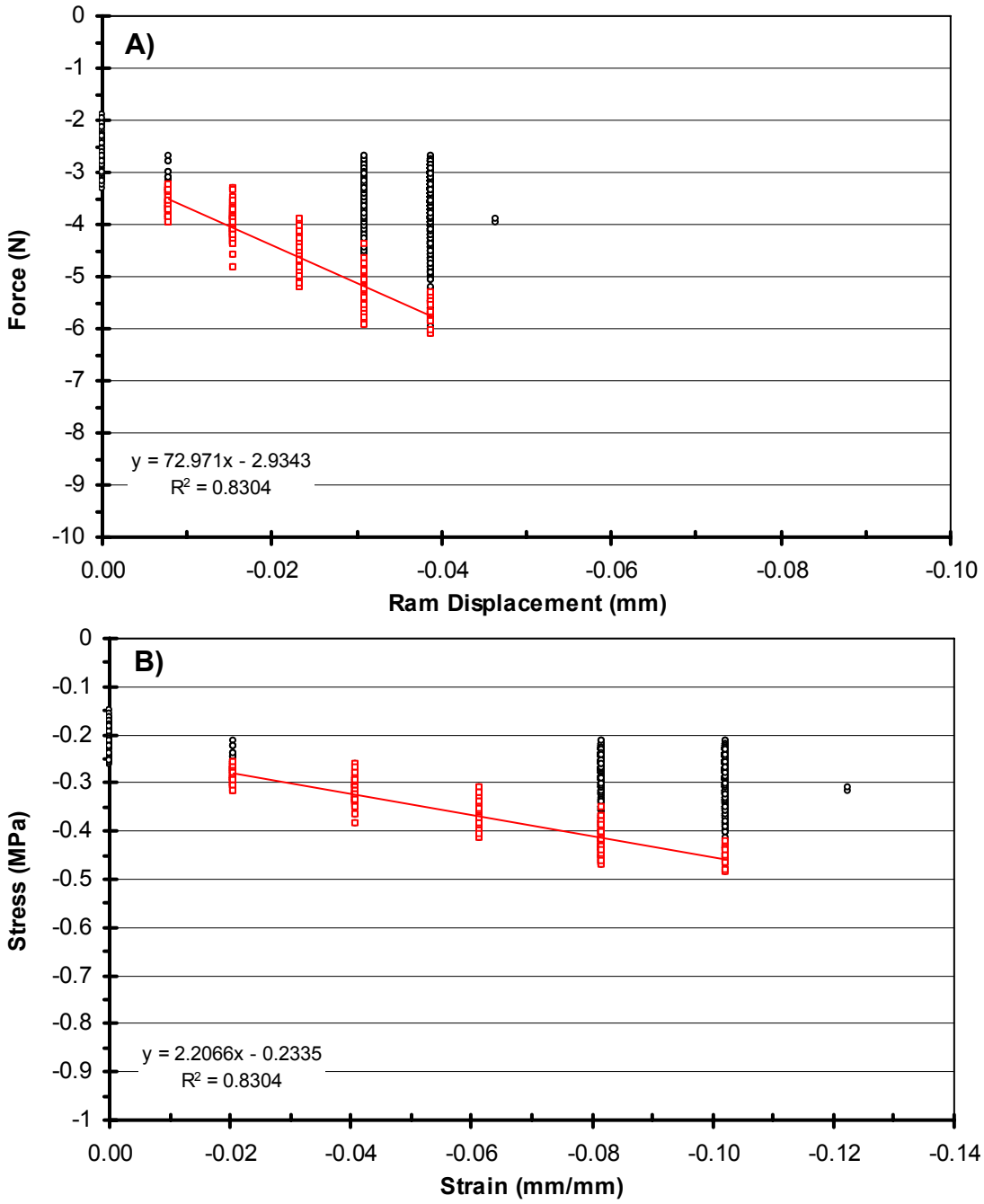

Figure 19. Example static, stress-relaxation testing of cartilage explant A) Force-Ram displacement curve, and B) Stress-strain curve. Red indicates data during 2 to 10% strain loading, which was used to calculate elastic modulus.

Immediately following stress-relaxation testing, the dynamic modulus was measured by applying a sinusoidal ram displacement that produced a 2% strain amplitude with 10% mean strain (i.e. 8 to 12% strain) at a frequency of 1.0 Hz for 10 cycles (Figure 20). The dynamic modulus was calculated as the slope of a linear line fit through the stress-strain curve from 8 to 12% strain on the 10^{th} cycle of loading (Figure 21).

.

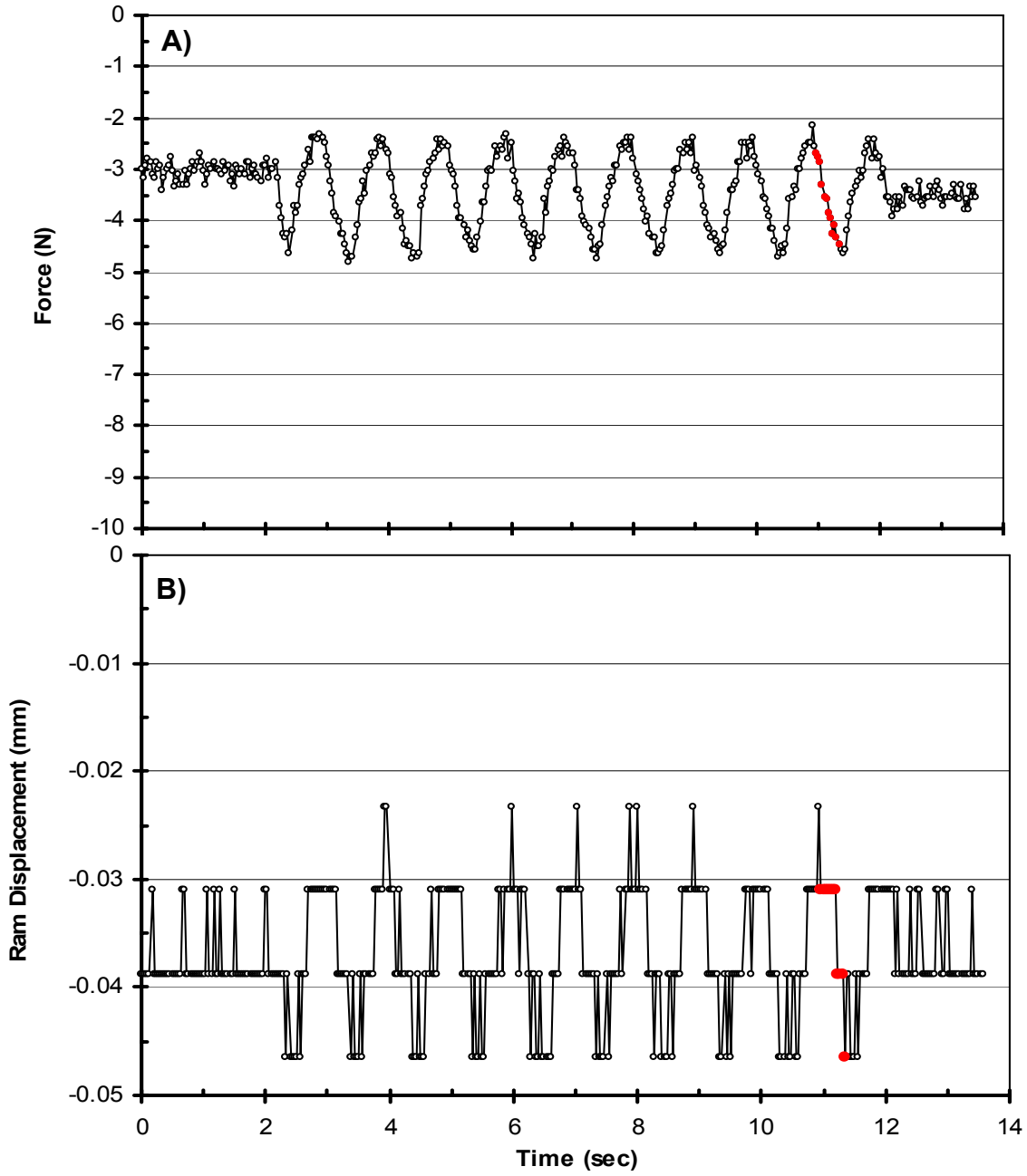

Figure 20. Example dynamic testing of cartilage explant A) Force, and B) Ram displacement as a function of time. Red indicates data during 8 to 12% strain on the 10th cycle of loading.

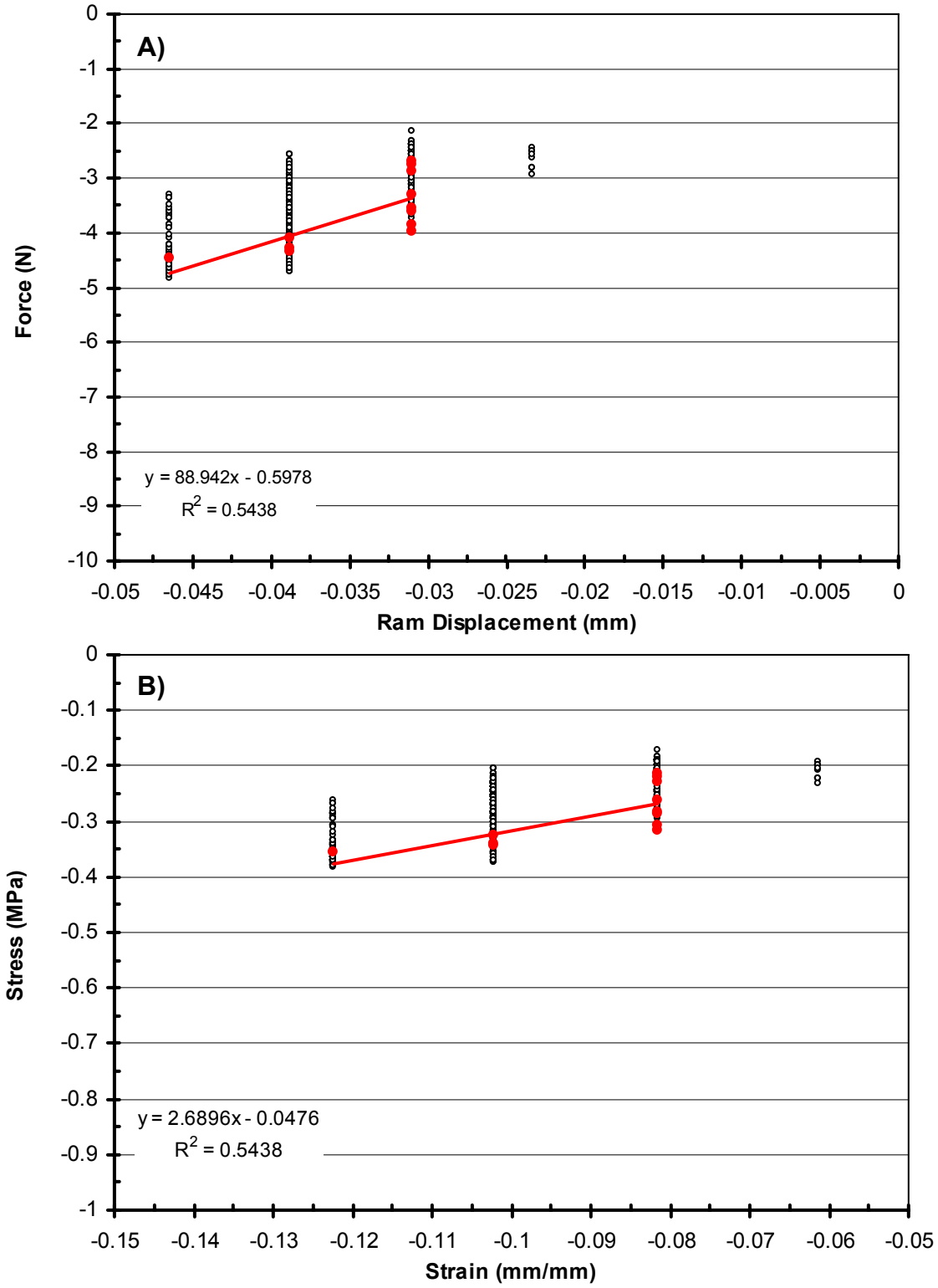

Figure 21. Example dynamic testing of cartilage explant A) Force-Ram displacement curve, and B) Stress-strain curve. Red indicates data during 8 to 12% strain on the 10th cycle of loading, which was used to calculate dynamic modulus.

4.1.4 Impact Injury and Post-Impact Culture

Using the procedure described in Section 3.1.3, at day 0 immediately following material testing, each explant was impacted (except for 0V:0S and Sham groups) with the desired nominal velocity (1 or 100 mm/sec, see groups in Table 6) with ram raised to an initial position that would result in the desired nominal strain (10, 30, or 50%, see groups in Table 6) on the explant at peak ram travel. Explants were cultured in 1ml of supplemented media as described above for 12 days. Media was changed at days 1, 2, 3, 6, 9, and 12 and stored at -20°C for further analysis.

4.1.5 Tissue Analysis

After twelve days of culture, all explants were assessed for total glycosaminoglycan (GAG) content using the 1,9-dimethylmethylene blue dye-binding (DMMB) assay and total collagen content by measuring hydroxyproline (HP) content.

4.1.6 Media Analysis

The following media analysis was performed at day 1, 2, 3, 6, 9, and 12. GAG content of the media was assessed using the DMMB assay. Nitric oxide (NO) concentration was determined using the Griess assay (Promega). Prostaglandin E_2 (PGE_2) concentration was determined using an EIA assay (Cayman Chemical). The day 6, 9, and 12 measured quantities were divided by 3 to produce results normalized to a per day basis. The cumulative mean values at each time point were also measured.

Table 6. Test groups by nominal [velocity (mm/sec) : max-strain (%)], and test result mean ± standard deviation: specimen initial thickness, impact velocity, max strain, elastic, equilibrium, and dynamic moduli.

Material Testing	Day	0V: 0S n = 4	1V: 10S n = 4	1V: 30S n = 4	1V: 50S n = 4	100V: 10S n = 4	100V: 30S n = 4	100V: 50S n = 4	Sham n = 4
Thickness (mm)	0	0.53 ± 0.102	0.57 ± 0.088	0.52 ± 0.099	0.53 ± 0.091	0.58 ± 0.064	0.58 ± 0.045	0.57 ± 0.054	
	6	0.35 ± 0.105	0.37 ± 0.079	0.26 ± 0.091	0.16 ± 0.049	0.38 ± 0.083	0.31 ± 0.030	0.21 ± 0.025	
	12	0.47 ± 0.104	0.46 ± 0.087	0.36 ± 0.075	0.26 ± 0.026	0.49 ± 0.050	0.43 ± 0.021	0.35 ± 0.059	0.41 ± 0.067
Elastic mod. (MPa)	0	3.62 ± 1.231	3.37 ± 0.789	5.04 ± 2.747	3.57 ± 1.833	5.19 ± 3.478	4.72 ± 1.935	5.36 ± 1.994	
	6	2.06^{A} ± 1.003	1.78 ± 0.756	0.85 ± 0.531	$0.42^{A,B}$ ± 0.339	1.89^{B} ± 0.585	1.32 ± 0.444	0.72 ± 0.277	
	12	2.87^{A} ± 1.302	2.51 ± 0.876	1.42 ± 0.191	$1.00^{A,B}$ ± 0.263	2.50 ± 1.519	1.73 ± 0.129	1.53 ± 0.115	2.93^{B} ± 0.629
Equil. mod. (MPa)	0	2.54 ± 0.878	2.42 ± 0.622	2.90 ± 0.791	2.11 ± 0.453	2.66 ± 1.793	1.97 ± 0.338	2.23 ± 0.492	
	6	1.21 ± 0.522	1.31 ± 0.151	1.32 ± 0.106	1.05 ± 0.102	1.38 ± 0.188	1.06 ± 0.595	0.87 ± 0.142	
	12	2.11 ± 0.248	1.62^{A} ± 0.173	1.48^{B} ± 0.213	1.54^{C} ± 0.235	1.40^{D} ± 0.825	1.36^{E} ± 0.329	1.30^{F} ± 0.267	2.76^{A-F} ± 0.531
Dyn. mod. (MPa)	0	5.23 ± 2.166	4.16 ± 0.514	3.66 ± 2.057	4.08 ± 1.628	5.06 ± 4.619	3.28 ± 0.672	4.23 1.118	
	6	1.73 ± 1.185	1.21 ± 0.690	1.35 ± 0.308	0.38^{A} ± 0.218	2.14^{A} ± 1.076	1.84 ± 0.134	0.84 ± 0.361	
	12	2.67 ± 1.175	2.05 ± 0.954	1.09 ± 0.578	0.94 ± 0.360	2.15 ± 1.117	1.88 ± 0.530	1.39 ± 0.579	2.69 ± 0.569

Values sharing the same letter are significantly different ($p<0.05$).

4.1.7 Statistical Analysis

Data were analyzed by one-way ANOVA using Tukey post-hoc group comparisons with significance set at $p<0.05$ using Sigma Stat® (San Rafael, CA).

4.2 Results

4.2.1 Material Moduli

There was a significant reduction in the elastic modulus for the low velocity: high strain group (1V:50S) compared to the no impact group (0V:0S) at day 6 and 12

(Table 6). There was a significant reduction in equilibrium modulus for all impacted groups (strain > 0%) compared to the sham group at day 12 (Table 6). There was a significant reduction in the dynamic modulus for the low velocity: high strain group (1V:50S) compared to the high velocity: low strain group (100V:10S) at day 6 (Table 6).

4.2.2 Tissue Analysis

There were no significant differences for any of the tissue biomarkers as shown in Table 7, except for amount of glycosaminoglycan (GAG) content in the high velocity: high strain (100V:50S) group compared to the low velocity: low strain (1V:10S) group with $p = 0.008$ at day 12.

Table 7. Summary of tissue biomarker results at day 12 (mean ± standard deviation)

Bio-marker	**0V:0S**	**1V:10S**	**1V:30S**	**1V:50S**	**100V:10S**	**100V:30S**	**100V:50S**	**Sham**
GAG (μg/mg)	143.39 ± 32.37	101.31^{A} ± 22.98	141.77 ± 33.37	138.06 ± 9.32	121.89 ± 15.31	158.01 ± 19.28	193.2^{A} ± 58.75	143.81 ± 32.80
HP (μg/mg)	40.04 ± 1.48	49.26 ± 23.46	49.50 ± 12.05	42.99 ± 5.20	39.70 ± 3.38	37.60 ± 6.36	46.72 ± 12.09	50.20 ± 4.16

GAG = glycosaminoglycan, HP = hydroxyproline.
Values sharing a similar letter are significantly different ($p < 0.05$)

4.2.3 Media Analysis

Table 8a contains media biomarker test results, with corresponding statistical significance values for GAG (Table 8b) and PGE_2 (Table 8c). Figure 22A and B respectively, contain bar graph representations of GAG and PGE_2 results.

On day 1, glycosaminoglycan (GAG) release was significantly higher for both high strain (1V:50S, 100V:50S) groups compared to sham, no impact (0V:0S), low strain (1V:10S, 100V:10S), and medium strain (1V:30S) with (100V:30S) approaching significance, $p< 0.07$. The three high velocity groups appeared to display (Figure 22A) a

trend of lower GAG with lower strain and likewise so did the three low velocity groups, however the medium strain (1V:30S, 100V:30S) groups were not different than the low strain (1V:10S, 100V:10S) groups or the no strain (0V:0S) and sham groups, $p > 0.90$. This implies that significant GAG release may be strain threshold dependent, $\geq 50\%$ based on results from this study. By day 2, the apparent trend was less pronounced with GAG release for the high strain groups being only significantly higher for the high velocity (100V:50S) and approaching significance, $p < 0.067$, for the low velocity (1V:50S) group compared to only the low strain (1V:10S) and Sham groups.

On days 1-3, prostaglandin E_2 (PGE_2) release was significantly higher for the high velocity-high strain (100V:50S) group compared to sham, no impact (0V:0S), low strain (1V:10S, 100V:10S), and medium strain (1V:30S, 100V:30S) groups. This was likewise true at day 6 with exception of the (100V:30S) group, and by day 9 with exception of three groups (100V:30S, 1V:30S, and 100V:10S only approaching significance $p = 0.905, 0.314, 0.086$, respectively), and by day 12 was only higher than one group (100V:10S). The three high velocity high strain groups appeared to display (Figure 22B) a trend of lower PGE_2 with lower strain, however the medium strain (1V:30S, 100V:30S) groups were not different than the low strain (1V:10S, 100V:10S) groups, and only at day 1 was different than the no strain (0V:0S) and sham groups. At day 1, the low velocity high strain group (1V:50S) group likewise had significantly higher PGE_2 with the low strain (1V:10S, 100V:10S) and no strain (0V:0S) and sham, but not significantly higher than the medium strain (1V:30S, 100V:30S) groups. The significant differences of the low velocity: high strain (1V:50S) group did not exist after day 1. These results imply that PGE_2 release is strain dependent as well as being impact velocity dependent, with

higher velocity impact prolonging the release up to 3 or possibly 6 days. The nitric oxide concentration values for most samples in all test groups were near or below the limit of detection of the assay (i.e. <1.5625), thus no further statistical analysis was performed.

Table 8a. Summary of media biomarker results (mean/day ± standard deviation, *cumulative mean*)

Bio-marker	Day	**0V: 0S** n = 4	**1V: 10S** n = 4	**1V: 30S** n = 4	**1V: 50S** n = 4	**100V: 10S** n = 4	**100V: 30S** n = 4	**100V: 50S** n = 4	**Sham** n = 4
GAG (μg/ml)	1	15.87 ± 4.36	13.81 ± 3.39	31.62 ± 23.32	109.29 ± 75.52	22.42 ± 6.90	39.7 ± 18.02	109.06 ± 32.51	13.62 ± 6.39
	2	12.9 ± 4.83 *28.77*	10.33 ± 2.15 *24.14*	18.18 ± 11.74 *49.80*	29.86 ± 17.57 *139.15*	17.78 ± 5.28 *40.20*	20.83 ± 7.98 *60.53*	31.80 ± 1.02 *140.85*	10.66 ± 4.24 *24.28*
	3	14.37 ± 4.01 *43.11*	12.57 ± 1.50 *36.71*	18.19 ± 8.56 *67.98*	19.7 ± 7.67 *158.85*	20.24 ± 3.77 *60.44*	20.27 ± 5.30 *80.80*	24.45 ± 2.49 *165.30*	13.88 ± 4.16 *38.17*
	6	15.33 ± 3.58 *89.13*	13.32 ± 2.07 *76.66*	17.1 ± 8.02 *119.27*	18.52 ± 8.55 *214.40*	20.41 ± 8.32 *121.66*	18.72 ± 1.91 *136.97*	19 ± 1.00 *222.31*	13.36 ± 5.12 *78.25*
	9	11.34 ± 2.24 *123.14*	9.78 ± 0.50 *105.99*	10.57 ± 3.98 *150.98*	10.38 ± 5.01 *245.55*	12.2 ± 2.60 *158.26*	12.1 ± 1.86 *173.28*	12.03 ± 1.07 *258.38*	9.39 ± 3.34 *106.41*
	12	11.87 ± 3.00 *158.75*	10.95 ± 1.45 *138.85*	9.58 ± 2.14 *179.73*	9.76 ± 4.93 *274.83*	12.78 ± 2.57 *196.59*	12.9 ± 2.16 *212.00*	11 ± 0.70 *291.38*	10.3 ± 3.19 *137.31*
PGE_2 (pg/ml)	1	38.75 ± 24.00	136.24 ± 57.24	362.62 ± 60.18	531.49 ± 242.19	155.79 ± 63.96	343.53 ± 145.21	706.37 ± 88.90	1.78 ± 3.56
	2	3.98 ± 3.38 *42.73*	14.26 ± 6.12 *150.50*	36.55 ± 12.43 *399.17*	81.85 ± 36.87 *613.35*	9.03 ± 8.61 *164.82*	49.04 ± 29.27 *392.57*	146.63 ± 83.82 *853.00*	1.07 ± 2.14 *2.85*
	3	0.00 ± 0.00 *42.73*	3.18 ± 4.40 *153.68*	11.81 ± 7.03 *410.98*	19.74 ± 14.19 *633.09*	2.20 ± 4.40 *167.02*	25.73 ± 21.84 *418.30*	100.78 ± 69.97 *953.78*	0.00 ± 0.00 *2.85*
	6	5.95 ± 5.40 *60.57*	7.65 ± 3.45 *176.63*	12.87 ± 8.38 *449.61*	20.98 ± 8.09 *696.02*	6.95 ± 4.21 *187.88*	26.83 ± 17.79 *498.78*	50.03 ± 24.75 *1103.87*	0.00 ± 0.00 *2.85*
	9	0.52 ± 1.04 *62.13*	0.36 ± 0.73 *177.72*	5.81 ± 7.25 *467.03*	5.82 ± 2.98 *713.47*	3.4 ± 2.28 *198.07*	9.47 ± 6.66 *527.18*	13.73 ± 8.39 *1145.07*	0.85 ± 0.76 *5.39*
	12	5.68 ± 5.64 *79.16*	3.31 ± 3.09 *187.65*	6.37 ± 4.65 *486.14*	5.36 ± 5.63 *729.55*	2.3 ± 2.66 *204.96*	15.45 ± 8.46 *573.52*	18.41 ± 13.95 *1200.30*	7.75 ± 3.11 *28.64*
NO (μM)	1-12	<1.5625 (concentration values were near/below lowest detection value)							

GAG = glycosaminoglycan, PGE_2 = prostaglandin E_2, NO = nitric oxide.

Table 8b. Statistical p-value comparisons for media GAG

	Statistical p-value comparisons							
Groups	**0V:0S**	**1V:10S**	**1V:30S**	**1V:50S**	**100V:10S**	**100V:30S**	**100V:50S**	**Sham**
Day 1								
0V:0S		1.000	0.996	0.006	1.000	0.954	0.006	1.000
1V:10S	1.000		0.991	0.005	1.000	0.931	0.005	1.000
1V:30S	0.996	0.991		0.031	1.000	1.000	0.032	0.990
1V:50S	0.006	0.005	0.031		0.012	0.069	1.000	0.005
100V:10S	1.000	1.000	1.000	0.012		0.992	0.012	1.000
100V:30S	0.954	0.931	1.000	0.069	0.992		0.070	0.929
100V:50S	0.006	0.005	0.032	1.000	0.012	0.070		0.005
Sham	1.000	1.000	0.990	0.005	1.000	0.929	0.005	
Day 2								
0V:0S		1.000	0.986	0.141	0.991	0.886	0.074	1.000
1V:10S	1.000		0.891	0.060	0.914	0.665	0.030	1.000
1V:30S	0.986	0.891		0.544	1.000	1.000	0.358	0.910
1V:50S	0.141	0.060	0.544		0.504	0.804	1.000	0.067
100V:10S	0.991	0.914	1.000	0.504		1.000	0.325	0.931
100V:30S	0.886	0.665	1.000	0.804	1.000		0.618	0.698
100V:50S	0.074	0.030	0.358	1.000	0.325	0.618		0.034
Sham	1.000	1.000	0.910	0.067	0.931	0.698	0.034	
Day 3, 6, 9, 12 (there was not a statistically significant difference in mean values among treatment groups, P = 0.051, 0.251, 0.777, 0.563)								

Table 8c. Statistical p-value comparisons for media PGE_2

	Statistical p-value comparisons							
Groups	**0V:0S**	**1V:10S**	**1V:30S**	**1V:50S**	**100V:10S**	**100V:30S**	**100V:50S**	**Sham**
Day 1								
0V:0S		0.912	0.008	<0.001	0.807	0.014	<0.001	1.000
1V:10S	0.912		0.123	<0.001	1.000	0.193	<0.001	0.683
1V:30S	0.008	0.123		0.417	0.195	1.000	0.004	0.003
1V:50S	<0.001	<0.001	0.417		0.002	0.292	0.375	<0.001
100V:10S	0.807	1.000	0.195	0.002		0.293	<0.001	0.529
100V:30S	0.014	0.193	1.000	0.292	0.293		0.003	0.005
100V:50S	<0.001	<0.001	0.004	0.375	<0.001	0.003		<0.001
Sham	1.000	0.683	0.003	<0.001	0.529	0.005	<0.001	
Day 2								
0V:0S		1.000	0.876	0.065	1.000	0.597	<0.001	1.000
1V:10S	1.000		0.982	0.150	1.000	0.837	<0.001	0.999
1V:30S	0.876	0.982		0.591	0.944	0.999	0.003	0.823
1V:50S	0.065	0.150	0.591		0.099	0.872	0.185	0.050
100V:10S	1.000	1.000	0.944	0.099		0.723	<0.001	1.000
100V:30S	0.597	0.837	0.999	0.872	0.723		0.001	0.523
100V:50S	<0.001	<0.001	0.003	0.185	<0.001	0.011		<0.001
Sham	1.000	0.999	0.823	0.050	1.000	0.523	<0.001	
Day 3								
0V:0S		1.000	0.998	0.961	1.000	0.863	<0.001	1.000
1V:10S	1.000		1.000	0.985	1.000	0.925	<0.001	1.000
1V:30S	0.998	1.000		1.000	1.000	0.995	0.002	0.998
1V:50S	0.961	0.985	1.000		0.980	1.000	0.005	0.961
100V:10S	1.000	1.000	1.000	0.980		0.908	<0.001	1.000
100V:30S	0.863	0.925	0.995	1.000	0.908		0.011	0.863
100V:50S	<0.001	<0.001	0.002	0.005	<0.001	0.011		<0.001
Sham	1.000	1.000	0.998	0.961	1.000	0.863	<0.001	
Day 6								
0V:0S		1.000	0.990	0.630	1.000	0.246	<0.001	0.996
1V:10S	1.000		0.998	0.751	1.000	0.339	<0.001	0.982
1V:30S	0.990	0.998		0.975	0.996	0.708	0.004	0.781
1V:50S	0.630	0.750	0.975		0.703	0.996	0.036	0.241
100V:10S	1.000	1.000	0.996	0.703		0.299	<0.001	0.990
100V:30S	0.246	0.339	0.708	0.996	0.299		0.150	0.063
100V:50S	<0.001	<0.001	0.004	0.036	<0.001	0.150		<0.001
Sham	0.996	0.982	0.781	0.241	0.990	0.063	<0.001	

Table 8c. Statistical p-value comparisons for media PGE_2 (continued)

	Statistical p-value comparisons							
Groups	**0V:0S**	**1V:10S**	**1V:30S**	**1V:50S**	**100V:10S**	**100V:30S**	**100V:50S**	**Sham**
Day 9								
0V:0S		1.000	0.767	0.766	0.988	0.190	0.013	1.000
1V:10S	1.000		0.741	0.740	0.984	0.175	0.012	1.000
1V:30S	0.767	0.741		1.000	0.996	0.955	0.314	0.818
1V:50S	0.766	0.740	1.000		0.996	0.955	0.315	0.817
100V:10S	0.988	0.984	0.996	0.996		0.631	0.086	0.994
100V:30S	0.190	0.175	0.955	0.955	0.631		0.905	0.225
100V:50S	0.013	0.012	0.314	0.315	0.086	0.905		0.017
Sham	1.000	1.000	0.818	0.817	0.994	0.225	0.017	
Day 12								
0V:0S		1.000	1.000	1.000	0.996	0.496	0.197	1.000
1V:10S	1.000		0.998	1.000	1.000	0.243	0.077	0.982
1V:30S	1.000	0.998		1.000	0.989	0.584	0.251	1.000
1V:50S	1.000	1.000	1.000		0.998	0.457	0.175	1.000
100V:10S	0.996	1.000	0.989	0.998		0.169	0.050	0.945
100V:30S	0.496	0.243	0.584	0.457	0.169		0.998	0.755
100V:50S	0.197	0.077	0.251	0.175	0.050	0.998		0.389
Sham	1.000	0.982	1.000	1.000	0.945	0.755	0.389	

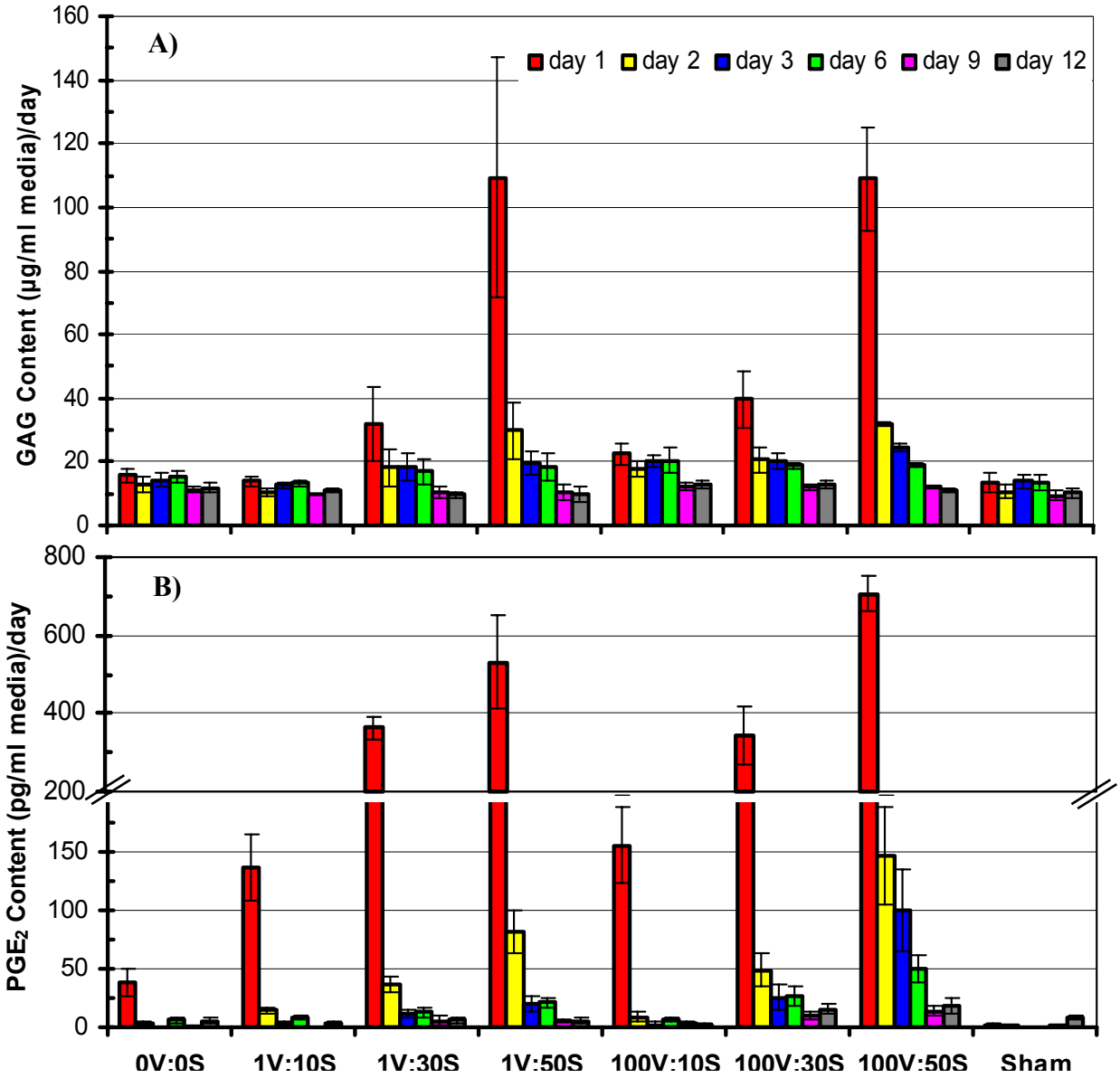

Figure 22. Effect of impact velocity and maximum strain on: A) Glycosaminoglycan, B) Prostaglandin E_2 content released from the articular cartilage explant into the culture media.

4.2.4 Correlation of Material Moduli to Glycosaminoglycan Release

There was a strong correlation between the mean (3 day release) values of GAG released from the cartilage into the media and the confined compression elastic modulus (Table 9, Figure 23, R = 0.94-0.98) and equilibrium modulus (Table 9, Figure 24, R = 0.87-1.00).

Table 9. Summary of media 3 day GAG release from cartilage, elastic, and equilibrium moduli values (mean ± standard deviation)

Bio-marker	Day	**0V: 0S** n = 4	**1V: 10S** n = 4	**1V: 30S** n = 4	**1V: 50S** n = 4	**100V: 10S** n = 4	**100V: 30S** n = 4	**100V: 50S** n = 4	**Sham** n = 4
GAG (μg/ml) 3 day release	0	0	0	0	0	0	0	0	0
	6	45.98 ± 10.74	39.95 ± 6.20	51.29 ± 24.05	55.55 ± 25.64	61.22 ± 24.95	56.17 ± 5.73	57.01 ± 3.00	40.08 ± 15.36
	12	35.61 ± 8.99	32.86 ± 4.36	28.75 ± 6.41	29.27 ± 14.78	38.33 ± 7.71	38.71 ± 6.47	33.00 ± 2.10	30.90 ± 9.57
Elastic Mod (MPa)	0	3.62 ± 1.231	3.37 ± 0.789	5.04 ± 2.747	3.57 ± 1.833	5.19 ± 3.478	4.72 ± 1.935	5.36 ± 1.994	
	6	2.06 ± 1.003	1.78 ± 0.756	0.85 ± 0.531	0.42 ± 0.339	1.89 ± 0.585	1.32 ± 0.444	0.72 ± 0.277	
	12	2.87 ± 1.302	2.51 ± 0.876	1.42 ± 0.191	1.00 ± 0.263	2.50 ± 1.519	1.73 ± 0.129	1.53 ± 0.115	2.93 ± 0.629
Equil. Mod (MPa)	0	2.54 ± 0.878	2.42 ± 0.622	2.90 ± 0.791	2.11 ± 0.453	2.66 ± 1.793	1.97 ± 0.338	2.23 ± 0.492	
	6	1.21 ± 0.522	1.31 ± 0.151	1.32 ± 0.106	1.05 ± 0.102	1.38 ± 0.188	1.06 ± 0.595	0.87 ± 0.142	
	12	2.11 ± 0.248	1.62 ± 0.173	1.48 ± 0.213	1.54 ± 0.235	1.40 ± 0.825	1.36 ± 0.329	1.30 ± 0.267	2.76 ± 0.531

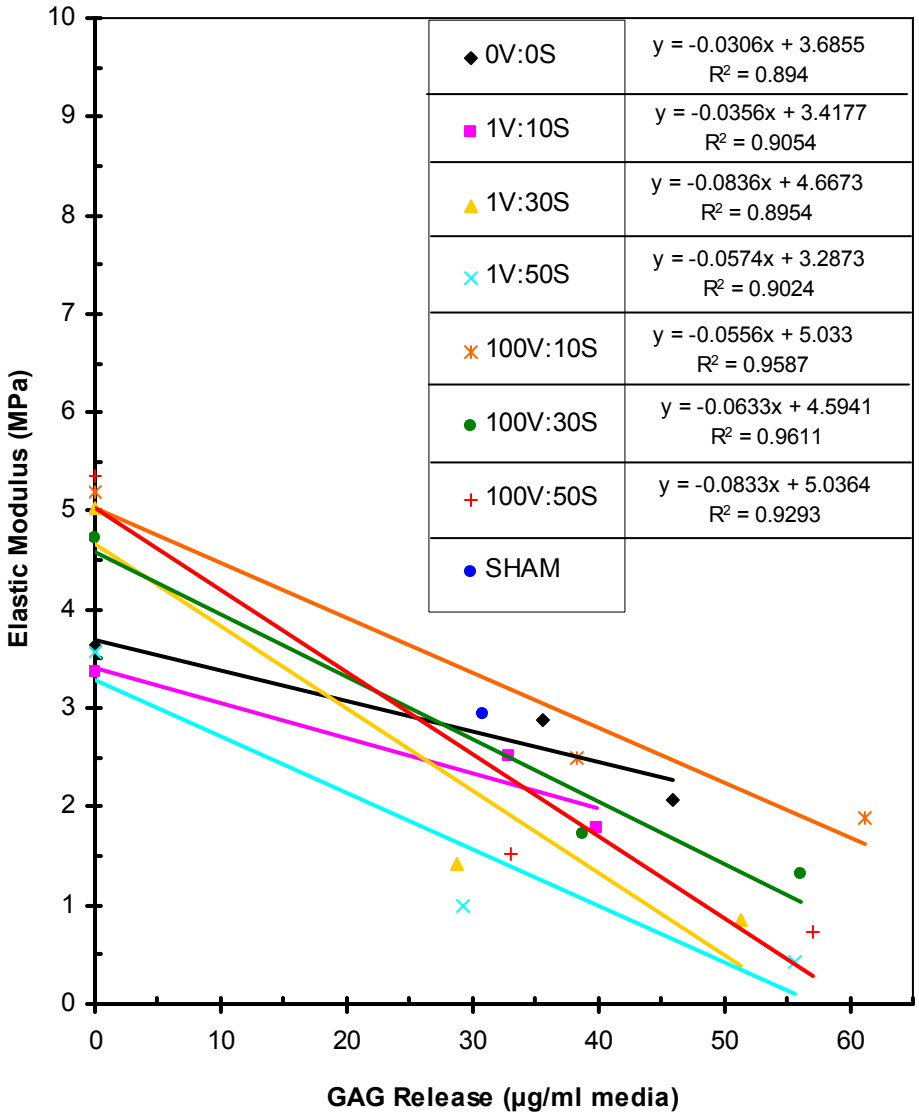

Figure 23. Correlation of the confined compression elastic modulus to 3 day GAG release from cartilage into the culture media post-impact.

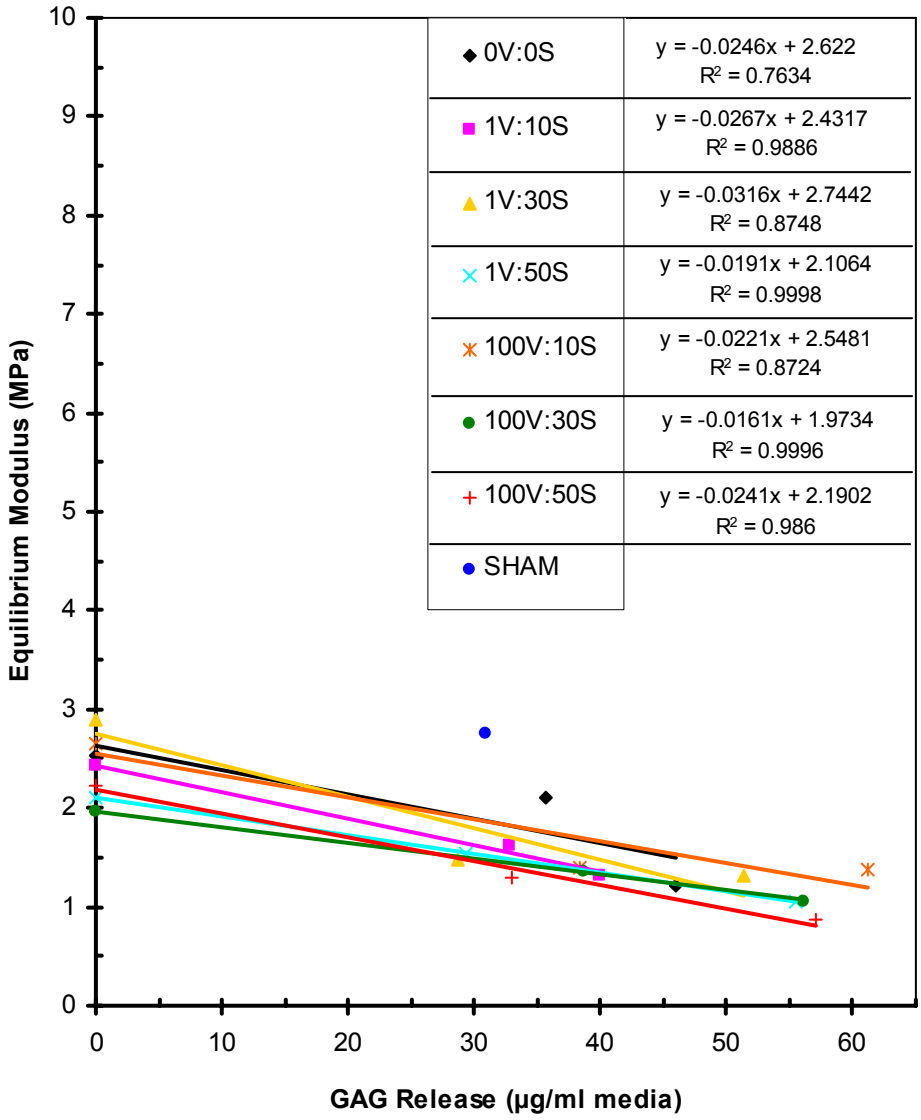

Figure 24. Correlation of the confined compression equilibrium modulus to 3 day GAG release from cartilage into the culture media post-impact.

4.3 Discussion

Material testing was conducted using test fixtures (Figure 5) fabricated to deliver impact loads to cartilage explants. Thus, the experimental set-up was similar to previously described uniaxial confined compressive stress-relaxation tests (Ateshian et al., 1997) with the exception that a non-porous, flat 3.9 mm diameter stainless steel tip was used as the loading platen. To determine material moduli in this study, the tissue was compressed at a constant rate (i.e. 0.001 mm/sec) followed by relaxation at a constant 10% strain, allowing decay of forces with time as fluid flowed within the cartilage's matrix (Figure 18A). The characteristic shape of the force-time graph suggests that fluid was exuded, but it is unknown (since a porous platen was not incorporated to allow free escape of the interstitial fluid across the surface) how much fluid exudation occurred across the surface or sides of the tissue. Cartilage is a nonhomogenous material, thus the state of compressive strain in the solid matrix will likely vary during *in vivo* loading such that the surface region (superficial zone) may experience more severe compaction as compared to the bottom region (deep zone). However, we did not attempt to measure the strain within each zone of cartilage. Our primary purpose for conducting the material testing in this study was to measure *relative* moduli values between test groups for correlation to the amount of matrix biomarkers that were present following mechanical injury with controlled impact velocity and maximum strain of articular cartilage.

The equilibrium modulus for human articular cartilage correlates in a positive manner ($r = 0.69$) with proteoglycan content (Roth et al., 1981). Moreover, it has been shown that more highly loaded regions of articular cartilage exhibit greater proteoglycan content

(Akizuki et al., 1986) and *in vitro* removal of proteoglycans from cartilage with trypsin digestion has been shown to result in a tenfold decrease of compressive modulus (Stahurski et al., 1981). This suggests that proteoglycans are responsible for providing compressive stiffness of the articular cartilage. Indeed, our data supports this concept with even stronger correlations (R = 0.87–1.00 as shown in Figures 23-24) between the equilibrium modulus and the cumulative amount of glycosaminoglycan (GAG) released from the cartilage into the media following impact injury.

The majority of GAG released was detected at the earliest time point post-injury (day 1) and occurred primarily in a strain-dependent manner. This is consistent with the findings of DiMicco et al. (2004) that provided evidence that initial (within 4 hours post-injury) GAG release of cartilage explants compressed to 50% thickness at a strain rate 100%/sec (comparable to the 1V:50S group in this study) can not be mitigated with inhibitors of biosynthesis (cycloheximide) nor MMP activity (CGS 27023A or GM 6001). This suggests that initial release of GAG is due to mechanical damage.

The cumulative mean value of GAG released for days 1-3 varied in Chapter 4 as compared to the respective group in Chapter 3. For example, the mean values of the 1V:50S and 100V:50S groups were greater in Chapter 4 (158.85 and 165.30 μg/ml media, respectively shown in Table 8) as compared to Chapter 3 (77.2 and 55.2 μg/ml media, respectively shown in Table 5). One possible explanation for this phenomenon may be that different volumes of tissue were used in the two studies. Assuming that the cartilage explants have a purely cylindrical shape, the volume, V, of an explant is dependent upon its initial thickness according to $V = \pi r^2 h$, where r is the radius (1/2 diameter) and h is the height or thickness of the explant. Because all of the explants had

a 4 mm diameter, then the initial thickness of the explant may be used to approximate volume. The mean initial thickness of explants in the 1V:50S and 100V:50S groups in Chapter 4 (0.53 and 0.57 mm, respectively shown in Table 6) were greater than the values reported in Chapter 3 (0.48 and 0.51 mm, respectively shown in Table 3). Thus, it may be plausible that an explant with a greater initial volume may release higher amounts of GAG as compared to a similarly treated smaller volume explant. Thickness of explants was only measured at day 0 (pre-impact), and day 6 and 12 (post-impact) for most groups. In order to correct for volume at all time points analyzed in future work, the amount of DNA content will be quantified so GAG released can be normalized to the amount of DNA present.

There were no differences in collagen content within the tissue for any group. Yet there may be differences in type II collagen content (quantity) and/or organization (quality) which was not tested but may exist that may correlate to trends in the dynamic modulus that were measured. Recently, Park et al. (2008) demonstrated that the unconfined compressive equilibrium and dynamic moduli were reduced in cartilage explants following various concentrations (0, 2, and 10 U/ml) of collagenase digestion. Specifically, the equilibrium modulus was reduced by 49% with 2 U/ml and 61% with 10 U/ml, whereas the dynamic modulus at 40 Hz was in the range of 13-20% with 2 U/ml and 24-33% with 10U/ml. Park et al. (2008) anticipated that collagenase digestion would more significantly affect the dynamic modulus as compared to the equilibrium modulus, but the opposite result occurred. Although our material testing was performed on confined (radially-constrained) cartilage, our results are similar to Park et al. (2008) such that we found a significant reduction in elastic modulus of cartilage explants in the

1V:50S group at day 6 and 12 following impact injury as compared to the no impact 0V:0S group, whereas no significant differences were observed in dynamic modulus for these groups. Park et al. (2008) provided evidence through collagen II histological staining that there were differences between the control and collaganase-treated groups, yet there were no statistical differences in biochemical characterization of collagen content of the cartilage explants. Likewise, there were no statistical differences in the collagen content of our cartilage explants following impact injury. Park et al. (2008) suggested that "…observed changes in mechanical properties, without dramatic changes in biochemical composition may point to the fact that the mechanical integrity of collagen is impaired, without it being removed from the explants." Collagen II forms a tight, interwoven matrix with proteoglycan within articular cartilage, so it may be plausible that these collagen fibrils are damaged following impact injury since an initial release of glycosaminoglycan was shown in this study as well as in Chapter 3. Another explanation for the lack of significant changes in the dynamic modulus in this present study may be due to increases of collagen I (attempt of cartilage to maintain its mechanical properties) that were not evaluated. For example, Natoli et al. (2008) evaluated the effects of low (1.1 J) and high (2.8 J) impact on articular cartilage explants at 24 hours, 1 week, and 4 weeks with respect to cell death gene expression, matrix biochemistry, and biomechanics. Interestingly, Natoli et al. (2008) reported that collagen I gene expression was upregulated from 1 to 4 weeks. The hydroxyproline assay used to measure collagen content of cartilage explants in this present study is not specific to types of collagen. Further studies are needed to evaluate whether decreases in collagen II with increases in collagen I attribute to minimal changes in dynamic modulus of cartilage

following impact injury. Thus, the question of what is the short- and long-term relationship between collagen I and II with respect to the material properties of articular cartilage following impact injury needs to be addressed in future work.

Similar to the findings in Chapter 3, there were no significant differences in nitric oxide produced in this present study. It remains to be seen whether the presence of additional joint tissues (i.e. synovium) placed with injured cartilage within the culture media and/or whether physiological loading of cartilage post-injury initiates nitric oxide production.

Prostaglandin E_2 (PGE_2) release was primarily strain-dependent in this study as was shown in Chapter 3. Similarly, Jeffrey and Aspden (2007) reported increase release of PGE_2, GAG, and cell death in *ex vivo* cartilage explants following impact load (0.13 J). The authors report that the release of PGE_2 and cell death was mitigated by the presence of celecoxib (selective cyclooxygenase-2, COX-2 inhibitor) and indomethacin (non-selective COX inhibitor), but the release of GAG remained unaffected (Jeffrey and Aspden, 2007). Despite the low sample size ($n = 4$), it appears that PGE_2 is a mechanosensitive biomarker which has been recently reported by others (Gosset et al., 2008). Gosset et al. (2006, 2008) attribute this to the upstream enzyme microsomal prostaglandin E synthase type 1 (mPGES-1) which is highly sensitive to dynamic compressive loading in cartilage explants. However, mPGES-1 was unaffected by dynamic compressive loading in osteoblasts embedded within a synthetic extracellular matrix despite the fact that increased levels of cyclooxygenase-2 (COX-2) mRNA levels and PGE_2 production were reported (Sanchez et al., 2009). The authors concluded that increases in PGE_2 and the mechanosensitive cytokine, interleukin-6 (IL-6), were

responsible for the decrease in the osteoprotegrin (OPG)/ receptor activator of nuclear factor ligand (RANKL) ratio and play a key role in bone remodeling in osteoarthritis (Sanchez et al., 2009). Post-traumatic osteoarthritis involves multiple joint tissues, thus future work is needed to evaluate the combined effects of each tissue on relevant biomarkers of PTOA.

CHAPTER 5

CONCLUSION & RECOMMENDATIONS

5.1 Conclusion

The large (25 kN actuator) Instron 8821s servo-hydraulic test machine may be used to measure the thickness of cartilage explants that are of the order of 0.5 mm thick, and then to deliver supraphysiologic impact loads with constant velocity up to 100 mm/sec to a desired maximum strain of cartilage. Release of GAG and PGE_2 biomarkers into the media were found to be strain sensitive with an indication that a strain threshold (in the order of 50%) may exist for significant release to occur. Significant differences in GAG release were observed 1 day post impact for both the high strain (50%) groups (low velocity (1 mm/sec) and high velocity (100 mm/sec)) relative to the lower strain impact groups, with relatively few if any statistically significant differences occurring thereafter at days 2, 3, 6, 9 and 12. Significant differences in PGE_2 release were consistently observed 1, 2, 3 and 6 days post impact for the high velocity: high strain group (100V:50S), which only appeared at day 1 for the low velocity: high strain group (1V:50S); which implies that higher velocity impact prolongs the release of PGE_2. Release of detectable levels of nitric oxide was not observed. Cartilage explant's radially confined compression elastic modulus and equilibrium modulus were found to correlate to GAG release from the explant.

Because both inflammatory mediators (nitric oxide and prostaglandin E_2) are indicated in the pathogenesis of osteoarthritis it remains to be seen whether physiological loading subsequent to cartilage injury triggers nitric oxide production and/or whether this is dependent upon other factors. Future doctorate work will be continued with this PTOA model by incorporating subchondral bone and synovium and post-impact physiologic loading while assessing relevant gene expression, additional biomarkers, and tissue material properties. This model appears to be an appropriate *ex vivo* model for investigating the relationship between severity of trauma and PTOA biomarkers for discovery of ways to predict the likelihood of PTOA onset and to identify effective treatments.

5.2 Recommendations

One of the limitations in this thesis work was the resolution (0.003876 mm) of the test machine's ram position, where resolution is the length of stroke, 254 mm divided by the number of digital increments this range is divided into (2^{16}) where 16 = bit capacity of the computer and/or software being used. A recommendation for improving the resolution would be to update the Instron test software from utilizing 16-bit to the 32-bit capacity of the Instron controller. This would increase the resolution to 5.91×10^{-8} mm.

The absolute initial ram position AP_i (which affects the accuracy of the desired maximum impact strain achieved) was calculated based upon two decimal places past zero. Recently, it was discovered that the Instron software has a Live Display feature (click on yellow 141 icon located in the RS Console) that displays the real-time values

for linear position and load as well as rotational position and torque. The number of decimal places may be increased to 10, although four decimal places past zero should be sufficient for calculating a more accurate absolute initial ram position for future work. It will be important to re-evaluate the overshoot, T_o, to obtain more accurate values after improving resolution.

To be able to determine impact stress, material moduli, and impact energy absorbed, the load cell's inertial force effect must be eliminated or accurately compensated for. One possible recommendation discussed in Section 2.1.4 is to use a piezoelectric load cell placed under the cartilage support anvil instead of having it attached to and move with the impact punch. Also, the electromagnetic noise should be less than experienced with the existing strain gauge load cell.

APPENDIX

A. Thickness Measurement and Impact Protocol

The protocol for sequentially measuring thickness and impacting several specimens of cartilage with varying thicknesses, T_i, under laterally constrained conditions is as follows:

1. Load Instron 8821s BasLab software program for a desired velocity
   i.e. v_1 = 0.1 to 100 mm/sec. (Version containing thickness measurement)
2. Place empty specimen anvil (with well facing upwards) into base support located on the test table of the Instron 8821.
3. Activate (by selecting "continue") the first thickness measurement portion of the program to lower ram into bottom of anvil well until -10 N is detected and record this absolute ram base position, AP_b.
4. Manually raise ram to arbitrary position and place cartilage into well of anvil.
5. Activate the second thickness measurement portion of the program to lower ram towards cartilage surface until -10 N is detected and record this absolute ram position, AP_t.
6. Calculate cartilage thickness by using: $T_i = AP_t - AP_b$.
7. Determine the initial ram position, AP_i, by using equation 2-2 (EP_1 = -2.25 mm), overshoot T_o from Table 2, and the desired maximum strain ε:

$$AP_i = AP_b + (1-\varepsilon)T_i + T_o + |EP_1| \qquad (2\text{-}2)$$

8. Use the Instron set point control or manually move ram to position, AP_i.

Note: If using the Instron set point control then the value of 0.02 should be added to APi to obtain the set point value, SAP_i to get Instron indicated ram position.

9. Run impact program.

B. Fixture Drawings

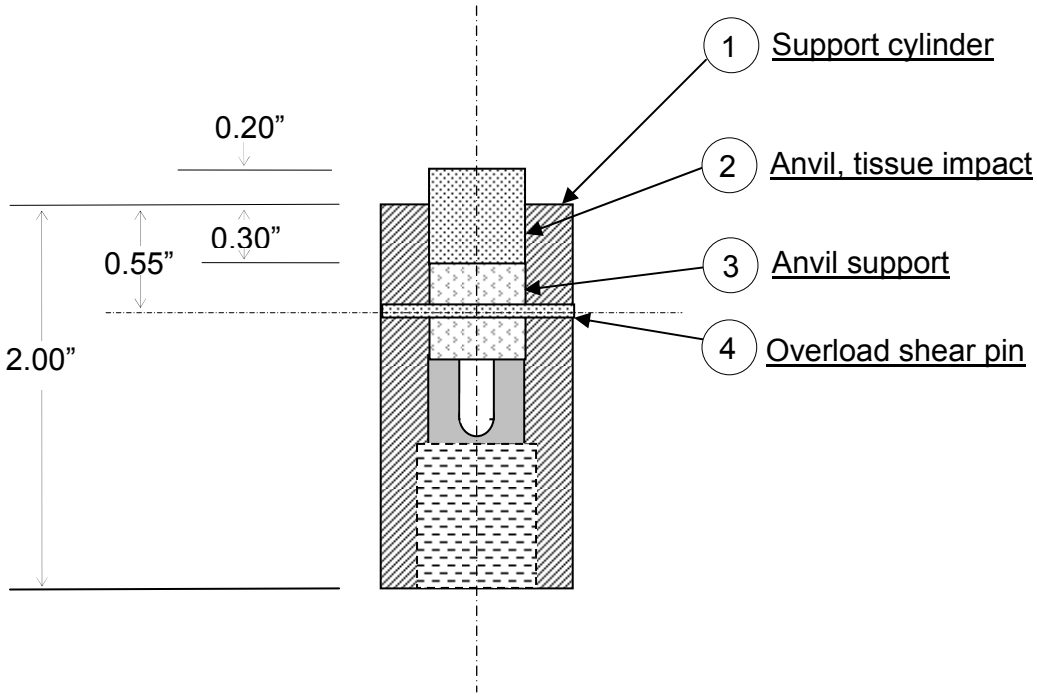

Anvil Support Assembly

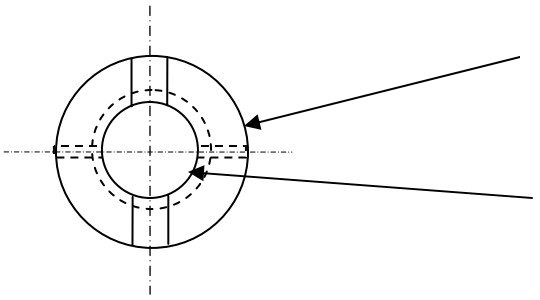

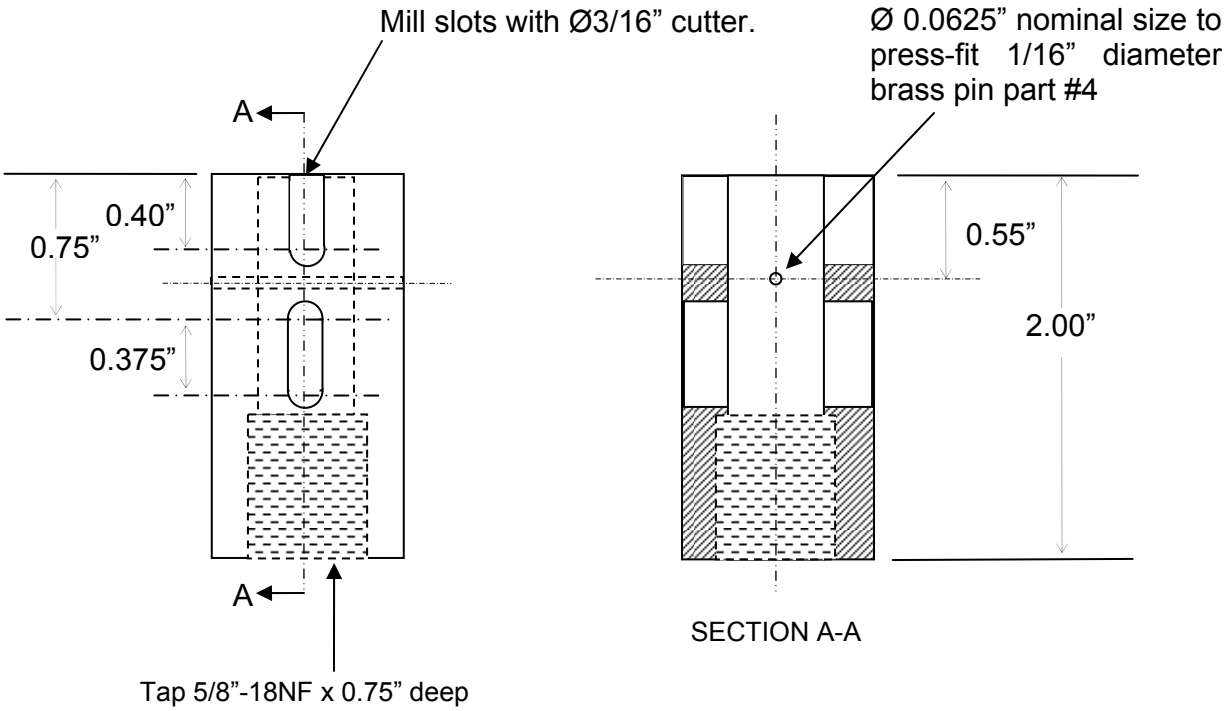

Material: 1” diameter stainless steel x 2” long.

Quantity: 1

Part 1: Support Cylinder

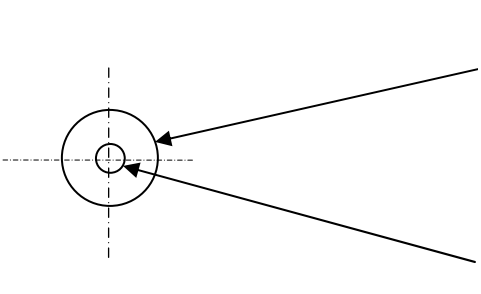

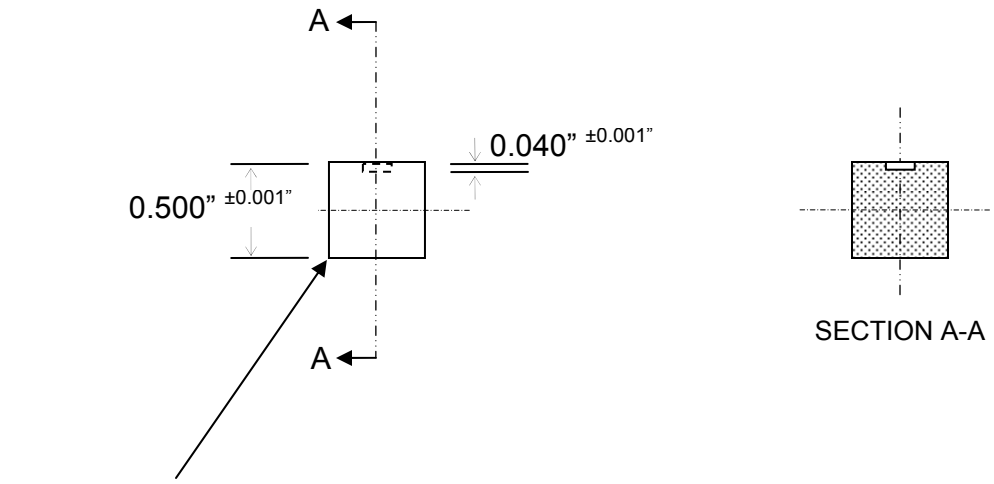

Material: 0.5” diameter stainless steel x 0.5” long.
Quantity: 1

Part 2: Anvil, tissue impact

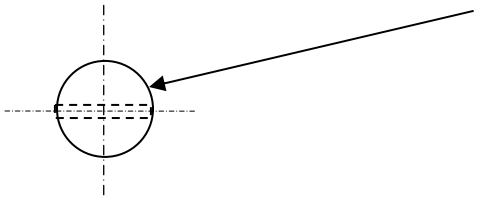

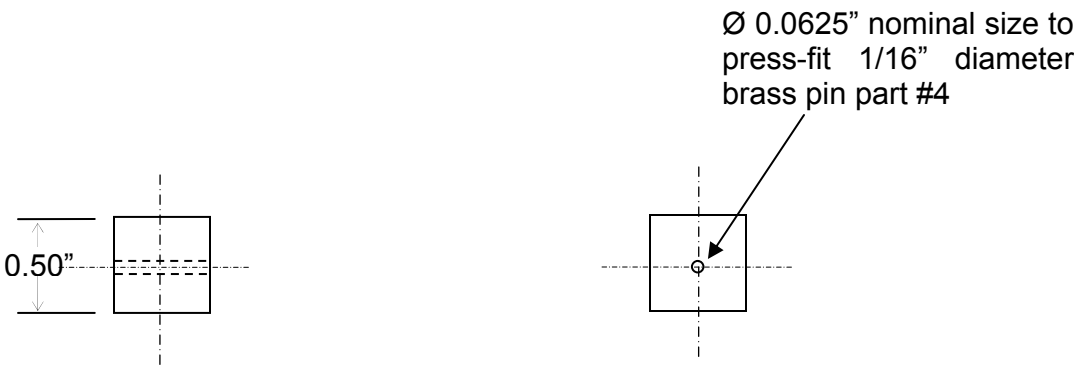

Material: 0.5” diameter stainless steel x 0.5” long.
Quantity: 1

Part 3: Anvil support

Material: MacMaster Carr #97325A110 1/16” diameter brass pin x 1/2” long.
Quantity: Minimum of 25

Part 4: Overload shear pin

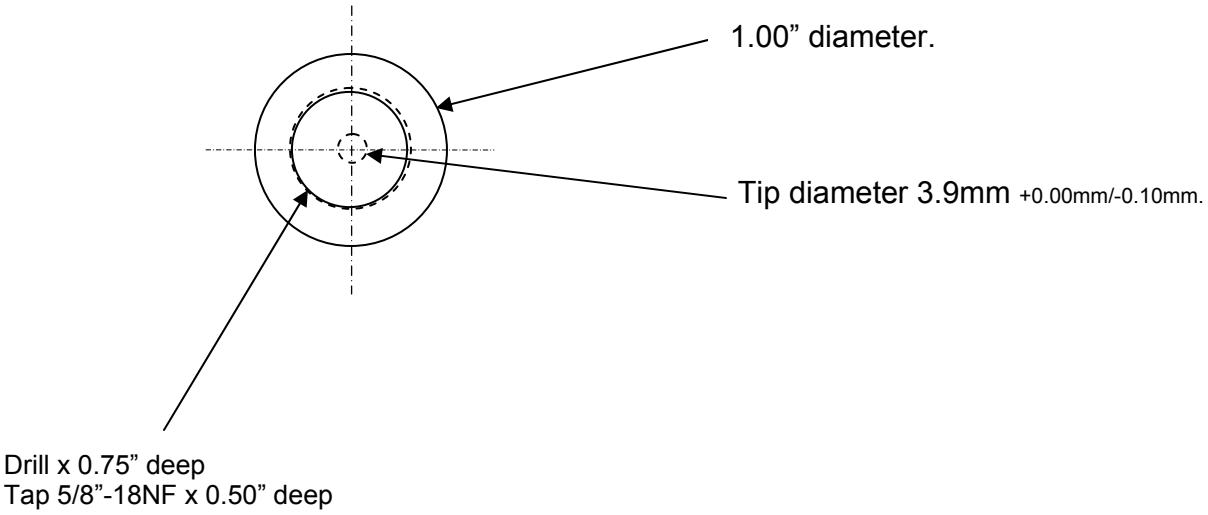

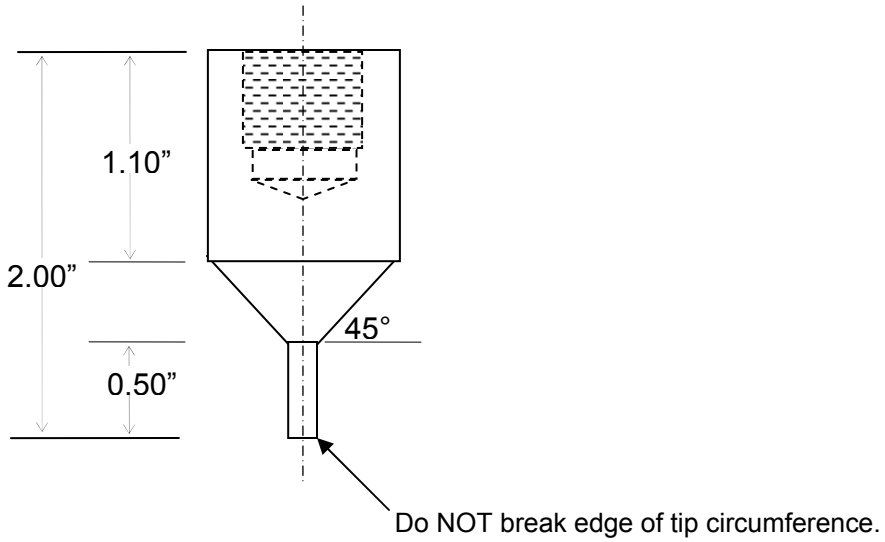

Material: 1” diameter stainless steel x 2” long.
Quantity: 1

Part 5: Impactor

REFERENCES

Abramson SB. 2008. Osteoarthritis and nitric oxide. Osteoarthritis Cartilage 16 Suppl 2: S15-20.

Akizuki S, Mow VC, Muller F, Pita JC, Howell DS and Manicourt DH. 1986. Tensile properties of human knee joint cartilage: I. Influence of ionic conditions, weight bearing, and fibrillation on the tensile modulus. J Orthop Res 4: 379-92.

Anz A, Smith MJ, Stoker A, Linville C, Markway H, Branson K and Cook JL. 2009. The effect of bupivacaine and morphine in a coculture model of diarthrodial joints. Arthroscopy 25: 225-31.

Armstrong CG and Mow VC. 1982. Variations in the intrinsic mechanical properties of human articular cartilage with age, degeneration, and water content. J Bone Joint Surg Am 64: 88-94.

Ashwell MS, O'Nan AT, Gonda MG and Mente PL. 2008. Gene expression profiling of chondrocytes from a porcine impact injury model. Osteoarthritis Cartilage 16: 936-46.

Ateshian GA, Warden WH, Kim JJ, Grelsamer RP and Mow VC. 1997. Finite deformation biphasic material properties of bovine articular cartilage from confined compression experiments. J Biomech 30: 1157-64.

Athanasiou KA, Rosenwasser MP, Buckwalter JA, Malinin TI and Mow VC. 1991. Interspecies comparisons of in situ intrinsic mechanical properties of distal femoral cartilage. J Orthop Res 9: 330-40.

Athanasiou KA, Agarwal A, Muffoletto A, Dzida FJ, Constantinides G and Clem M. 1995. Biomechanical properties of hip cartilage in experimental animal models. Clin Orthop Relat Res 254-66.

Bollet AJ and Nance JL. 1966. Biochemical Findings in Normal and Osteoarthritic Articular Cartilage. II. Chondroitin Sulfate Concentration and Chain Length, Water, and Ash Content. J Clin Invest 45: 1170-1177.

Borrelli J, Jr. 2006. Chondrocyte apoptosis and posttraumatic arthrosis. J Orthop Trauma 20: 726-31.

Borrelli J, Jr., Torzilli PA, Grigiene R and Helfet DL. 1997. Effect of impact load on articular cartilage: development of an intra-articular fracture model. J Orthop Trauma 11: 319-26.

Borrelli J, Jr., Burns ME, Ricci WM and Silva MJ. 2002. A method for delivering variable impact stresses to the articular cartilage of rabbit knees. J Orthop Trauma 16: 182-8.

Borrelli J, Jr., Zhu Y, Burns M, Sandell L and Silva MJ. 2004. Cartilage tolerates single impact loads of as much as half the joint fracture threshold. Clin Orthop Relat Res 266-73.

Borrelli J, Jr., Silva MJ, Zaegel MA, Franz C and Sandell LJ. 2009. Single high-energy impact load causes posttraumatic OA in young rabbits via a decrease in cellular metabolism. J Orthop Res 27: 347-52.

Borrelli J, Jr., Tinsley K, Ricci WM, Burns M, Karl IE and Hotchkiss R. 2003. Induction of chondrocyte apoptosis following impact load. J Orthop Trauma 17: 635-41.

Brown TD, Johnston RC, Saltzman CL, Marsh JL and Buckwalter JA. 2006. Posttraumatic osteoarthritis: a first estimate of incidence, prevalence, and burden of disease. J Orthop Trauma 20: 739-44.

Buckwalter JA and Brown TD. 2004. Joint injury, repair, and remodeling: roles in post-traumatic osteoarthritis. Clin Orthop Relat Res 7-16.

Burgin LV and Aspden RM. 2007. A drop tower for controlled impact testing of biological tissues. Med Eng Phys 29: 525-30.

Chrisman OD, Ladenbauer-Bellis IM, Panjabi M and Goeltz S. 1981. 1981 Nicolas Andry Award. The relationship of mechanical trauma and the early biochemical reactions of osteoarthritic cartilage. Clin Orthop Relat Res 275-84.

Cook JL, Kuroki K, Stoker A, Streppa H and Fox DB. 2007. Review of in vitro models and development and initial validation of a novel co-culture model for the study of osteoarthritis. Current Rheumatology Reviews 3: 172-82.

D'Lima DD, Hashimoto S, Chen PC, Colwell CW, Jr. and Lotz MK. 2001a. Human chondrocyte apoptosis in response to mechanical injury. Osteoarthritis Cartilage 9: 712-9.

D'Lima DD, Hashimoto S, Chen PC, Colwell CW, Jr. and Lotz MK. 2001b. Impact of mechanical trauma on matrix and cells. Clin Orthop Relat Res S90-9.

D'Lima DD, Hashimoto S, Chen PC, Lotz MK and Colwell CW, Jr. 2001c. Prevention of chondrocyte apoptosis. J Bone Joint Surg Am 83-A Suppl 2: 25-6.

DiMicco MA, Patwari P, Siparsky PN, Kumar S, Pratta MA, Lark MW, Kim YJ and Grodzinsky AJ. 2004. Mechanisms and kinetics of glycosaminoglycan release following in vitro cartilage injury. Arthritis Rheum 50: 840-8.

Duda GN, Eilers M, Loh L, Hoffman JE, Kaab M and Schaser K. 2001. Chondrocyte death precedes structural damage in blunt impact trauma. Clin Orthop Relat Res 302-9.

Ewers BJ, Jayaraman VM, Banglmaier RF and Haut RC. 2000. The effect of loading rate on the degree of acute injury and chronic conditions in the knee after blunt impact. Stapp Car Crash J 44: 299-313.

Ewers BJ, Dvoracek-Driksna D, Orth MW and Haut RC. 2001. The extent of matrix damage and chondrocyte death in mechanically traumatized articular cartilage explants depends on rate of loading. J Orthop Res 19: 779-84.

Ewers BJ, Jayaraman VM, Banglmaier RF and Haut RC. 2002. Rate of blunt impact loading affects changes in retropatellar cartilage and underlying bone in the rabbit patella. J Biomech 35: 747-55.

Farndale RW, Buttle DJ and Barrett AJ. 1986. Improved quantitation and discrimination of sulphated glycosaminoglycans by use of dimethylmethylene blue. Biochim Biophys Acta 883: 173-7.

Fermor B, Weinberg JB, Pisetsky DS, Misukonis MA, Fink C and Guilak F. 2002. Induction of cyclooxygenase-2 by mechanical stress through a nitric oxide-regulated pathway. Osteoarthritis Cartilage 10: 792-8.

Frank EH, Jin M, Loening AM, Levenston ME and Grodzinsky AJ. 2000. A versatile shear and compression apparatus for mechanical stimulation of tissue culture explants. J Biomech 33: 1523-7.

Froimson MI, Ratcliffe A, Gardner TR and Mow VC. 1997. Differences in patellofemoral joint cartilage material properties and their significance to the etiology of cartilage surface fibrillation. Osteoarthritis Cartilage 5: 377-86.

Furman BD, Strand J, Hembree WC, Ward BD, Guilak F and Olson SA. 2007. Joint degeneration following closed intraarticular fracture in the mouse knee: a model of posttraumatic arthritis. J Orthop Res 25: 578-92.

Gosset M, Berenbaum F, Levy A, Pigenet A, Thirion S, Saffar JL and Jacques C. 2006. Prostaglandin E2 synthesis in cartilage explants under compression: mPGES-1 is a mechanosensitive gene. Arthritis Res Ther 8: R135.

Gosset M, Berenbaum F, Levy A, Pigenet A, Thirion S, Cavadias S and Jacques C. 2008. Mechanical stress and prostaglandin E2 synthesis in cartilage. Biorheology 45: 301-20.

Grabowski PS, Wright PK, Van 't Hof RJ, Helfrich MH, Ohshima H and Ralston SH. 1997. Immunolocalization of inducible nitric oxide synthase in synovium and cartilage in rheumatoid arthritis and osteoarthritis. Br J Rheumatol 36: 651-5.

Green DM, Noble PC, Bocell JR, Jr., Ahuero JS, Poteet BA and Birdsall HH. 2006. Effect of early full weight-bearing after joint injury on inflammation and cartilage degradation. J Bone Joint Surg Am 88: 2201-9.

Greenberg DD, Stoker A, Kane S, Cockrell M and Cook JL. 2006. Biochemical effects of two different hyaluronic acid products in a co-culture model of osteoarthritis. Osteoarthritis Cartilage 14: 814-22.

Guilak F, Fermor B, Keefe FJ, Kraus VB, Olson SA, Pisetsky DS, Setton LA and Weinberg JB. 2004. The role of biomechanics and inflammation in cartilage injury and repair. Clin Orthop Relat Res 17-26.

Haut RC, Ide TM and De Camp CE. 1995. Mechanical responses of the rabbit patello-femoral joint to blunt impact. J Biomech Eng 117: 402-8.

Holmes MH and Mow VC. 1990. The nonlinear characteristics of soft gels and hydrated connective tissues in ultrafiltration. J Biomech 23: 1145-56.

Huser CA and Davies ME. 2006. Validation of an in vitro single-impact load model of the initiation of osteoarthritis-like changes in articular cartilage. J Orthop Res 24: 725-32.

Huser CA and Davies ME. 2007. Calcium signaling leads to mitochondrial depolarization in impact-induced chondrocyte death in equine articular cartilage explants. Arthritis Rheum 56: 2322-34.

Huser CA and Davies ME. 2008. Effect of a glucosamine derivative on impact-induced chondrocyte apoptosis in vitro. A preliminary report. Osteoarthritis Cartilage 16: 125-8.

Huser CA, Peacock M and Davies ME. 2006. Inhibition of caspase-9 reduces chondrocyte apoptosis and proteoglycan loss following mechanical trauma. Osteoarthritis Cartilage 14: 1002-10.

Jeffrey JE and Aspden RM. 2006. The biophysical effects of a single impact load on human and bovine articular cartilage. Proc Inst Mech Eng [H] 220: 677-86.

Jeffrey JE and Aspden RM. 2007. Cyclooxygenase inhibition lowers prostaglandin E2 release from articular cartilage and reduces apoptosis but not proteoglycan degradation following an impact load in vitro. Arthritis Res Ther 9: R129.

Jeffrey JE, Gregory DW and Aspden RM. 1995. Matrix damage and chondrocyte viability following a single impact load on articular cartilage. Arch Biochem Biophys 322: 87-96.

Jeffrey JE, Thomson LA and Aspden RM. 1997. Matrix loss and synthesis following a single impact load on articular cartilage in vitro. Biochim Biophys Acta 1334: 223-32.

Jeffrey JE, Brodie JP and Aspden RM. 2006. The effects of a single fast impact load compared with slow severe loading on articular cartilage in vitro. Osteoarthritis Cartilage 14: S81-S82.

King AI. 2001. Fundamentals of impact biomechanics: Part 2--Biomechanics of the abdomen, pelvis, and lower extremities. Annu Rev Biomed Eng 3: 27-55.

Krueger JA, Thisse P, Ewers BJ, Dvoracek-Driksna D, Orth MW and Haut RC. 2003. The extent and distribution of cell death and matrix damage in impacted chondral explants varies with the presence of underlying bone. J Biomech Eng 125: 114-9.

Kuroki K, Stoker AM and Cook JL. 2005. Effects of proinflammatory cytokines on canine articular chondrocytes in a three-dimensional culture. Am J Vet Res 66: 1187-96.

Kurz B, Jin M, Patwari P, Cheng DM, Lark MW and Grodzinsky AJ. 2001. Biosynthetic response and mechanical properties of articular cartilage after injurious compression. J Orthop Res 19: 1140-6.

Kurz B, Lemke A, Kehn M, Domm C, Patwari P, Frank EH, Grodzinsky AJ and Schunke M. 2004. Influence of tissue maturation and antioxidants on the apoptotic response of articular cartilage after injurious compression. Arthritis Rheum 50: 123-30.

Lahm A, Uhl M, Erggelet C, Haberstroh J and Mrosek E. 2004. Articular cartilage degeneration after acute subchondral bone damage: an experimental study in dogs with histopathological grading. Acta Orthop Scand 75: 762-7.

Lai WM, Hou JS and Mow VC. 1991. A triphasic theory for the swelling and deformation behaviors of articular cartilage. J Biomech Eng 113: 245-58.

Lai WM, Mow VC, Sun DD and Ateshian GA. 2000. On the electric potentials inside a charged soft hydrated biological tissue: streaming potential versus diffusion potential. J Biomech Eng 122: 336-46.

Lawrence RC, Helmick CG, Arnett FC, Deyo RA, Felson DT, Giannini EH, Heyse SP, Hirsch R, Hochberg MC, Hunder GG, Liang MH, Pillemer SR, Steen VD and Wolfe F. 1998. Estimates of the prevalence of arthritis and selected musculoskeletal disorders in the United States. Arthritis and Rheumatism 41: 778-799.

Lewis JL, Deloria LB, Oyen-Tiesma M, Thompson RC, Jr., Ericson M and Oegema TR, Jr. 2003. Cell death after cartilage impact occurs around matrix cracks. J Orthop Res 21: 881-7.

Li C, Pruitt LA and King KB. 2006. Nanoindentation differentiates tissue-scale functional properties of native articular cartilage. J Biomed Mater Res A 78: 729-38.

Loening AM, James IE, Levenston ME, Badger AM, Frank EH, Kurz B, Nuttall ME, Hung HH, Blake SM, Grodzinsky AJ and Lark MW. 2000. Injurious mechanical compression of bovine articular cartilage induces chondrocyte apoptosis. Arch Biochem Biophys 381: 205-12.

Lu XL, Sun DD, Guo XE, Chen FH, Lai WM and Mow VC. 2004. Indentation determined mechanoelectrochemical properties and fixed charge density of articular cartilage. Ann Biomed Eng 32: 370-9.

Mankin HJ and Thrasher AZ. 1975. Water content and binding in normal and osteoarthritic human cartilage. J Bone Joint Surg Am 57: 76-80.

Maroudas A and Venn M. 1977. Chemical composition and swelling of normal and osteoarthrotic femoral head cartilage. II. Swelling. Ann Rheum Dis 36: 399-406.

Milentijevic D and Torzilli PA. 2005. Influence of stress rate on water loss, matrix deformation and chondrocyte viability in impacted articular cartilage. J Biomech 38: 493-502.

Milentijevic D, Helfet DL and Torzilli PA. 2003. Influence of stress magnitude on water loss and chondrocyte viability in impacted articular cartilage. J Biomech Eng 125: 594-601.

Milentijevic D, Rubel IF, Liew AS, Helfet DL and Torzilli PA. 2005. An in vivo rabbit model for cartilage trauma: a preliminary study of the influence of impact stress magnitude on chondrocyte death and matrix damage. J Orthop Trauma 19: 466-73.

Mitrovic D, Quintero M, Stankovic A and Ryckewaert A. 1983. Cell density of adult human femoral condylar articular cartilage. Joints with normal and fibrillated surfaces. Lab Invest 49: 309-16.

Morel V and Quinn TM. 2004. Short-term changes in cell and matrix damage following mechanical injury of articular cartilage explants and modelling of microphysical mediators. Biorheology 41: 509-19.

Morel V, Berutto C and Quinn TM. 2006. Effects of damage in the articular surface on the cartilage response to injurious compression in vitro. J Biomech 39: 924-30.

Mow VC and Huiskes R. 2005. Basic orthopaedic biomechanics & mechano-biology. 3rd ed. Philadelphia, PA: Lippincott Williams & Wilkins. 720 p.

Mow VC, Holmes MH and Lai WM. 1984. Fluid transport and mechanical properties of articular cartilage: a review. J Biomech 17: 377-94.

Mow VC, Ratcliffe A and Poole AR. 1992. Cartilage and diarthrodial joints as paradigms for hierarchical materials and structures. Biomaterials 13: 67-97.

Mow VC, Kuei SC, Lai WM and Armstrong CG. 1980. Biphasic creep and stress relaxation of articular cartilage in compression? Theory and experiments. J Biomech Eng 102: 73-84.

Mrosek EH, Lahm A, Erggelet C, Uhl M, Kurz H, Eissner B and Schagemann JC. 2006. Subchondral bone trauma causes cartilage matrix degeneration: an immunohistochemical analysis in a canine model. Osteoarthritis Cartilage 14: 171-8.

Natoli RM and Athanasiou KA. 2008. P188 reduces cell death and IGF-I reduces GAG release following single-impact loading of articular cartilage. J Biomech Eng 130: art. no. 041012.

Natoli RM, Scott CC and Athanasiou KA. 2008. Temporal effects of impact on articular cartilage cell death, gene expression, matrix biochemistry, and biomechanics. Ann Biomed Eng 36: 780-92.

Otsuki S, Brinson DC, Creighton L, Kinoshita M, Sah RL, D'Lima D and Lotz M. 2008. The effect of glycosaminoglycan loss on chondrocyte viability: a study on porcine cartilage explants. Arthritis Rheum 58: 1076-85.

Park S, Nicoll SB, Mauck RL and Ateshian GA. 2008. Cartilage mechanical response under dynamic compression at physiological stress levels following collagenase digestion. Ann Biomed Eng 36: 425-34.

Parratte S and Pagnano MW. 2008. Instability after total knee arthroplasty. Instr Course Lect 57: 295-304.

Patwari P, Cheng DM, Cole AA, Kuettner KE and Grodzinsky AJ. 2007. Analysis of the relationship between peak stress and proteoglycan loss following injurious compression of human post-mortem knee and ankle cartilage. Biomech Model Mechanobiol 6: 83-9.

Patwari P, Gaschen V, James IE, Berger E, Blake SM, Lark MW, Grodzinsky AJ and Hunziker EB. 2004. Ultrastructural quantification of cell death after injurious compression of bovine calf articular cartilage. Osteoarthritis Cartilage 12: 245-52.

Patwari P, Cook MN, DiMicco MA, Blake SM, James IE, Kumar S, Cole AA, Lark MW and Grodzinsky AJ. 2003. Proteoglycan degradation after injurious compression of bovine and human articular cartilage in vitro: interaction with exogenous cytokines. Arthritis Rheum 48: 1292-301.

Quinn TM, Allen RG, Schalet BJ, Perumbuli P and Hunziker EB. 2001. Matrix and cell injury due to sub-impact loading of adult bovine articular cartilage explants: effects of strain rate and peak stress. J Orthop Res 19: 242-9.

Radin EL, Paul IL and Lowy M. 1970. A comparison of the dynamic force transmitting properties of subchondral bone and articular cartilage. J Bone Joint Surg Am 52: 444-56.

Reddy GK and Enwemeka CS. 1996. A simplified method for the analysis of hydroxyproline in biological tissues. Clin Biochem 29: 225-9.

Repo RU and Finlay JB. 1977. Survival of articular cartilage after controlled impact. J Bone Joint Surg Am 59: 1068-76.

Robinovitch SN and Chiu J. 1998. Surface stiffness affects impact force during a fall on the outstretched hand. J Orthop Res 16: 309-13.

Roth V, Mow VC, Lai WM and Eyre DR. 1981. Correlation of intrinsic compressive properties of bovine articular cartilage with its uronic acid and water content. Trans. Orthop. Res. Soc. 6: 49.

Sanchez C, Gabay O, Salvat C, Henrotin YE and Berenbaum F. 2009. Mechanical loading highly increases IL-6 production and decreases OPG expression by osteoblasts. Osteoarthritis Cartilage 17: 473-81.

Scott CC and Athanasiou KA. 2006. Design, validation, and utilization of an articular cartilage impact instrument. Proc Inst Mech Eng [H] 220: 845-55.

Setton LA, Mow VC, Muller FJ, Pita JC and Howell DS. 1993. Altered structure-function relationships for articular cartilage in human osteoarthritis and an experimental canine model. Agents Actions Suppl 39: 27-48.

Setton LA, Mow VC, Muller FJ, Pita JC and Howell DS. 1994. Mechanical properties of canine articular cartilage are significantly altered following transection of the anterior cruciate ligament. J Orthop Res 12: 451-63.

Shah AK, Yuan LJ, Torzilli PA and Chen CTC. 2003. Strain is the major factor for chondrocyte death in articular cartilage under static load. American Society of Mechanical Engineers, Bioengineering Division (Publication) BED 55: 331-32.

Stahurski TM, Armstrong CG and Mow VC. 1981. Variation of the intrinsic aggregate modulus and permeability of articular cartilage with trypsin digestion. Proc. Biomech. Symp. Trans. ASME 43: 137-140.

Thompson RC, Jr., Oegema TR, Jr., Lewis JL and Wallace L. 1991. Osteoarthrotic changes after acute transarticular load. An animal model. J Bone Joint Surg Am 73: 990-1001.

Thompson RC, Jr., Vener MJ, Griffiths HJ, Lewis JL, Oegema TR, Jr. and Wallace L. 1993. Scanning electron-microscopic and magnetic resonance-imaging studies of injuries to the patellofemoral joint after acute transarticular loading. J Bone Joint Surg Am 75: 704-13.

Torzilli PA, Deng XH and Ramcharan M. 2006. Effect of compressive strain on cell viability in statically loaded articular cartilage. Biomech Model Mechanobiol 5: 123-32.

Torzilli PA, Grigiene R, Borrelli J, Jr. and Helfet DL. 1999. Effect of impact load on articular cartilage: cell metabolism and viability, and matrix water content. J Biomech Eng 121: 433-41.

Vrahas MS, Smith GA, Rosler DM and Baratta RV. 1997. Method to impact in vivo rabbit femoral cartilage with blows of quantifiable stress. J Orthop Res 15: 314-7.

Wan LQ, Miller C, Guo XE and Mow VC. 2004. Fixed electrical charges and mobile ions affect the measurable mechano-electrochemical properties of charged-hydrated biological tissues: the articular cartilage paradigm. Mech Chem Biosyst 1: 81-99.

Ward BD, Furman BD, Huebner JL, Kraus VB, Guilak F and Olson SA. 2008. Absence of posttraumatic arthritis following intraarticular fracture in the MRL/MpJ mouse. Arthritis Rheum 58: 744-53.

Wylde V, Dieppe P, Hewlett S and Learmonth ID. 2007. Total knee replacement: is it really an effective procedure for all? Knee 14: 417-23.